VOLUME-1

European Centre

for

Medium Range Weather Forecasts

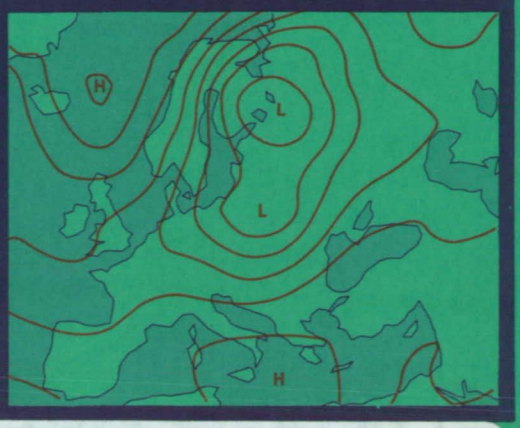

ECMWF CONTRACT REPORT TO ESA

ESA REPORT REFERENCE
CR (P) 2604

A STUDY OF THE FEASIBILITY OF USING SEA AND WIND INFORMATION FROM THE ERS-1 SATELLITE

Part 1: Wind Scatterometer Data

AUTHORS
D. Anderson
A. Hollingsworth
S. Uppala
P. Woiceshyn

ESRIN CONTRACT NO:
6297/86/HGE-I(SC)

ESRIN STUDY MANAGER
E. ORIOL

The work described in this report was carried out under ESA Contract.
Responsibility for the contents resides with the authors who prepared it

Centre Européen pour les Prévisions Météorologiques à Moyen Terme

Europäisches Zentrum für mittelfristige Wettervorhersage

European Centre for Medium Range Weather Forecasts (ECMWF)
Shinfield Park, Reading, Berkshire, RG2 9AX, England

European Centre for Medium-Range Forecasts
Shinfield Park, Reading, Berkshire, U.K.

European Space Agency Contract Report

A STUDY OF THE FEASIBILITY OF USING SEA AND WIND INFORMATION FROM THE ERS-1 SATELLITE

Part 1: Wind Scatterometer Data

AUTHORS
D. Anderson
A. Hollingsworth
S. Uppala
P. Woiceshyn*

ESRIN CONTRACT NO:
6297/86/HGE-I(SC)

ESRIN STUDY MANAGER
E. ORIOL

*Permanent Affiliation
Jet Propulsion Lab.
Pasadena, Ca.

June 1987

CONTENTS

ABSTRACT

This study is concerned with the feasibility of using wind scatterometer data from the ERS-1 satellite in a real time data assimilation system. The main topics are the potential this offers for quality assurance and validation of the ERS-1 scatterometer data, and secondly the question of how best to assimilate scatterometer data. It is difficult to achieve reliable simulations for new systems. It was therefore decided to experiment with assimilations of SeaSat-A Scatterometer System (SASS) data in order to explore these main topics.

The results of passive assimilations of scatterometer data (where the SASS data are not used but all other data are), and of active assimilations of scatterometer data (where all data including SASS data are used), show that the use of wind scatterometer data in an assimilation enables one to make a penetrating and comprehensive validation and quality assurance of the scatterometer data, through comparisons with collocated ship data and through comparison with the wind fields generated by the assimilation. Several important but unpublished defects in the SASS wind speed and direction determinations were documented in this way, together with confirmations of the results of earlier studies. Comprehensive quality assurance and validation of the ERS-1 wind scatterometer data is therefore possible in near real time.

The impact of the SASS data on analyses and forecasts was large in the Southern Hemisphere, generally small in the Northern Hemisphere, and occasionally large in the Tropics. The relative lack of impact in the Northern Hemisphere could be attributed to several causes. The speed and directional problems with the data meant that it could not be given sufficient weight to make a large impact. Moreover when the SASS data quality was good, much of the new information was on small scales where the ECMWF analysis algorithm imposed a rather heavy filter on the data. The filter properties of the assimilation will need revisions permitting higher resolution analyses in order to fully exploit ERS-1 data. A special study of the QEII storm and the Ark Royal storm illustrated these points. Short range forecasts with the ECMWF forecast system for the QE-II storm without SASS data were distinctly better than the best forecasts in earlier studies by others; the addition of SASS data had a small beneficial impact. Similar results were found for the Ark Royal storm.

A study was made of the performance of several ambiguity removal algorithms. Real and simulated dual-pol data were used to determine a ranking of the directional ambiguities for SASS, while simulated data were used for ERS-1 and NSCAT. The SASS real data calculations provide a worst-case estimate of the performance of ERS-1, while the simulated ERS-1 data (and NSCAT data) provide a best case estimate. It is shown for the SASS data that tests with simulated data give more optimistic results than tests with real data. The errors in the ambiguity removal results occurred in 'clusters'. It was demonstrated that the probabilities which can be calculated for the ambiguous wind directions on ERS-1 contain more information than is given by a simple ranking of the directions. Suggestions are made on how to use this information.

The report concludes with a number of recommendations based on the results of the study.

Preface

The purpose of this study is to assess the feasibility of

(1) using an operational weather forecasting model to assist in the validation and quality assurance of ERS-1 scatterometer winds

(2) assimilating ERS-1 data in an operational data assimilation to improve the analyses, especially of the surface wind field, and to improve forecasts made from those analyses

(3) preliminary testing of objective dealiasing methods for the ERS-1 data.

Since ERS-1 data does not yet exist, one is forced to use simulated data or real data from another scatterometer. Simulated data usually gives overly optimistic results, so we have chosen where appropriate to use real data from the SASS scatterometer on SeaSat. However, because the SASS scatterometer had only two beams with single and dual pol capabilities and future scatterometers will have 3 beams operating in single and dual polarisation mixes there is no close analogue between dealiasing SASS 2-beam data and ERS-1 3-beam single polarisation data, so simulated data are used for part of the work on objective ambiguity removal. (Section 5.2).

Even when real data from SASS is used in topics 1, 2 and 3 there is no exact correspondence between ERS-1 and SASS scatterometers. But the experience with SASS should give a good indication of what could be done with ERS-1 data as illustrated by the following.

1. Quality Assurance and Validation

In section 2, a comparison is made between SASS data and collocated ship data. The results highlight a speed dependent bias in the data, which suggests that SASS data is in error at low wind speeds. A large discrepancy is also noted at high wind speeds, both when the SASS is compared with ship speeds, and when it is compared with the short range forecasts used in the assimilation, suggesting that the SASS model function is inadequate. The quoted accuracy of SASS of 1.3 m/s (e.g. Lame and Born 1982) is shown to be misleading, as is the rms direction accuracy of 17° over the range of 360°.

Comparison of SASS directions with Ship and short range forecast directions reveal that when SASS angles are measured relative to the space craft they are not uniformly distributed with respect to direction. Further, the nature of the angular irregularity is shown to be a function of incidence angle. The cause of this angular error is under study, but is unlikely to be a result of dealiasing alone. Rather it is indicative of errors in the measurement of σ° in the upwind/downwind/crosswind specification of σ° with direction, or in the procedure relating collocated σ° measurements to winds and directions.

Some synoptic examples of the quality of the dealiased winds are given in section 4, where SASS data is overlaid on the analysis. This illustrates features which the scatterometer data identifies well e.g. sharp fronts, as well as features which appear inconsistent with meteorological expectation. The errors noted here are likely to be a combination of dealiasing errors and the angular irregularities noted above.

Similar comparisons and quality control can be readily carried out for ERS-1 data, but only if sufficient information is available. For example, to identify the angular errors, it was necessary to work with the comprehensive SASS data set including all aliases and azimuth and incidence angle information as well as ship and model data. Even so, not all relevant information, such as precipitation, was available. A truly comprehensive quality control requires the availability of all relevant information in a manageable form.

2. Assimilation

Scatterometer data is single-level boundary layer data. It has long been recognised that single-level data is difficult to assimilate to maximum effect in forecast models, and boundary layer data is especially difficult to use.

It is shown in section 3, that in the northern hemisphere, SASS has relatively little impact on the analyses or forecasts. This results partly from data redundancy with other observing systems and partly from the fact that the best way of using single-level high resolution planetary boundary layer data has not yet been determined. The small impact in the northern hemisphere may also arise from problems with the SASS data as illustrated in sections 2 and 4.2.

It is to be hoped that ERS-1 data will have less speed bias and angular uncertainty than SASS and so greater weight may be ascribed to the ERS-1 data. This in turn will allow it to influence the analysis to a greater extent.

Scatterometers can see to higher resolution than most other instruments, so it will be necessary to adjust assimilation procedures to deal with high resolution data. Further, it is envisaged that in the next few years, more research on the use of single-level data, will allow it to have greater impact on analyses than is presently achieved. Thus not all results of this study will necessarily hold for ERS-1 data.

3. Dealiasing

From the point of view of objective dealiasing, the differences between ERS-1 and SASS are quite large: SASS was normally operated as a pair of two-antennae instruments (one pair on each side of the space craft). Normally, this gives up to 4 possible solutions with little skill expected in the first-ranked solution. ERS-1 will have three antennae with substantial skill in the first-ranked solution. For these reasons, the preliminary dealiasing work reported in this study uses simulated data. However, for brief periods, SASS was operated in dual pol mode and this does result in some skill in the first-ranked solution. So tests on objective ambiguity removal have also been made for this dual pol data. This should be considered as a worst case for ERS-1 under normal operation, i.e. excluding the 10% of time when ERS-1 will be effectively a two antennae instrument.

1. INTRODUCTION

The SASS (SeaSat A Scatterometer System) instrument on SeaSat was a 14.6 GHz active microwave instrument, designed to permit inference of the ocean surface wind vector (speed and direction) from precise measurements of the pulsed radiation back-scattered by gravity-capillary waves riding on the sea surface. The radar received-power return expressed as the normalised radar cross section (σ^o) is not related theoretically to any geophysical parameter such as the surface wind vector, but via an empirical model function. In the course of processing SASS data, a number of empirical model functions have been proposed. The relationship embodied in the empirical model is between σ^o and the wind at 19.5 m in neutral conditions. The neutral wind is uniquely related to friction velocity V* but would differ from the real (observed) wind at 19.5 m. This difference is probably small, but could be significant under very stable boundary layer conditions.

Four dual polarised antennas were aligned so that they pointed at 45° and 135° relative to the subsatellite track to produce an X shaped pattern of illumination on the earth. So, a given surface location was first viewed by the forward beam and then, between 1 and 4 mins later by the rear beam, the time lag depending on where the chosen location was within the swath.

The empirical relationship relating σ^o to wind speed used to produce the SASS data for this study is known as SASS-1. It emerged from a series of studies involving aircraft measurements as well as comparisons of the SASS derived wind fields with in situ measurements, notably those taken in the GOASEX and JASIN experiments. It had been intended that JASIN would be for validation only, but the final SASS1 function used for data production was tuned by some data from JASIN (Woiceshyn et al., 1986).

It has been reported (Lame and Born 1982, Jones et al. 1982) that the scatterometer had a demonstrated accuracy of 1.3 m/s rms for wind speed and 17° for direction. One should note, however, that these numbers are derived from fits to the JASIN data set, over the entire range of 4 to 16 m/s and 360°, which was partly used to fine tune the model function. One would like to verify these fits by comparisons with other data encompassing larger geographical and environmental variation.

To infer a wind speed and direction from σ^o values it is necessary to view the same (or almost the same) patch of ocean twice. Using at least two measurements of σ^o, one can invert the $\sigma^o=f(v, \phi)$ model function to retrieve speed and direction. Although there are two equations (one for each σ^o) for two unknowns (speed v and direction ϕ) the solution is not unique: Up to 4 solutions (occasionally more) are possible. The speed does not vary much between the solutions, but the directions (called aliases) do. The numerical technique used to find the solutions, called SOS (Sum of Squares), is described in Appendix B. Note only that the data we will use is for 100 km boxes, usually containing several σ^o measurements from both forward and aft beams. The SOS technique has some undesirable artefacts which will be discussed later.

The most frequent mode of operation was for single polarisation, usually V (vertical) but sometimes H (horizontal) on all 4 beams. The instrument was also operated for limited periods in dual polarisation mode on one side of the spacecraft. This latter mode of operation is of interest for testing ambiguity removal techniques in that it increases the over-determinism of the measurements, leading to a modest increase in the skill of the ranking.

The rms error for direction quoted earlier (17°), is a comparison of the difference between the SASS direction closest to the comparison direction and the comparison direction. One normally does not know the best solution, and has to dealias i.e. pick a direction by some other means. The rms error of 17° is therefore a minimum: if one first dealiased the data and then calculated an rms fit, 17° over 360° could only be achieved if all the dealiases were chosen correctly. The estimated accuracy of 17° is therefore likely to be overoptimistic, firstly by the definition of angular difference, and secondly by the fact that the JASIN data set was used for both tuning and validation.

In this report we will try to extend the comparison of SASS data with other instruments, and apply the comparisons over a wider geographical area. One of the principal comparisons will be with ship data. This data is archived at all major weather centres, so the collocation of SASS data is best done using the met-service archives. The period which will be considered is confined to the interval 6-17 September 1978.

A further advantage of doing validation at a weather centre is that the forecast model, used in analysis-assimilation mode can also be considered as a calibration instrument, which incorporates data from many observing systems into a coherent analysis.

In Section 2 we compare the SASS data with ships and in Section 3 with the model. A further objective of this report is to determine if the SASS data can be assimilated beneficially into an analysis-assimilation cycle, to improve the analyses and subsequently the forecast. This is considered in Section 4. In Section 5, a report is given of some preliminary work on objective ambiguity removal using SASS dual-pol data and simulated ERS-1 and NSCAT data. Section 6 contains a summary and discussion of results, while Section 7 presents some recommendations to ESA.

2. QUALITY ASSURANCE OF SASS DATA BY COLLOCATING WITH SHIP REPORTS

At an operational weather centre, a large number of ship reports are received each day. So it is possible to compare the scatterometer measurements with neighbouring ship reports over a much larger geographical area and range of environmental conditions than is possible with an organised campaign which is perforce for a limited area and duration. Even so, voluntary observing ships do not sample all the world's ocean equally. Fig. A1 shows that the North Atlantic and Pacific are moderately well covered but the tropics and southern ocean are more sparsely sampled. Originally, SASS data from the dealiased data set (see App. A) was collocated with ships. This dealiased record contains only information on speed and direction: it does not contain information on incidence angle or azimuth to which the quality of the measurements is shown to be sensitive. Collocation was repeated using data from the more comprehensive record. Even this however does not permit a truly comprehensive quality assessment. For example, V pole and H pole measurements cannot always be separated nor can one always identify those observations influenced by precipitation. One cannot do all the quality assessment one would like because of lack of information in the SASS data record. The supply of only one speed and direction, as has been proposed for ERS-1, would not allow a comprehensive quality control.

For technical reasons (see Section 3) data is blocked into 6 hour periods. Only ship and SASS occurring in the same time block and within 100 km of each other are collocated. The period of collocation is from 6-17 September 1978 inclusive.

2.1 Comparison of collocated speeds

The rms difference between ship and SASS speeds varies a little from one 6 hour block to the next but is usually about 4.5 m/s, seldom below 3 m/s or above 6 m/s. The value of 4.5 m/s is none-the-less considerably higher than the value of 1.3 m/s quoted by Jones et al (1982). The present collocation is with winds from merchant ships which are themselves likely to be quite noisy and so some increase in rms error from this source is to be expected. In Section 3.1, a value of 3.6 m/s is assumed for the ship rms error. On this assumption the rms error for SASS might be estimated at ~ 3 m/s. The bias averaged over all collocations is usually ~ 1 m/s with the SASS speeds larger than ship speeds. This bias is an average over all speeds; more relevant is whether there is a speed dependent bias.

Fig. 2.1a is a plot of the difference between SASS speed and ship speed as a function of ship wind speed. All collocations of SASS with ships are included in this figure for the period 6-17 September. Shading represents the square root of the number of collocations. (2.5 on the axis corresponds to 156 collocations, 5 to 625 etc). The statistics of the speed differences are not Gaussian, as may be seen on Fig. 2.1f, which shows a contour plot of SASS speed against ship speed. Figure 2.1a suggests strongly that SASS speed is biased high with respect to ship speed at low ship speeds, but low with respect to ship speeds at high speeds. In the mid-speed range the agreement is reasonable. Since SASS-1 was tuned by fitting to ship data in the JASIN area in the speed range 4 to 16 m/s this mid-speed-range agreement is perhaps to be expected. None-the-less, the speed at which SASS is perceived to read low relative to ship (10 m/s) is much lower than has been found in other collocations (Jones et al. 1982, Pierson 1981, Ernst 1981).

One should note however that since the distribution function illustrated on Fig. 2.1f is not Gaussian especially at higher speeds, other interpretations are possible. The line of maximum probability lies above the line of perfect agreement until speeds of approximately 14 m/s, implying SASS speeds are higher than ship speeds in the range 0-14 m/s. Fig. 2.1a is based on plotting the speed differences versus ship speed. If a similar plot was made versus SASS speed, one can see from Fig. 2.1f that it is possible to conclude that SASS was higher than ship speed at the high wind speed end.

Wentz et al. (1984) and Woiceshyn et al. (1986) have noted that there is a marked difference between the speed returned from Vpol or Hpol σ^{o}s at high wind speed (approximately 5 m/s difference at wind speeds of 25 m/s in a statistical sense) and this difference can be 8m/s in at least one specific synoptic situation, the Ark Royal Storm. The data set used in the present study does not separate V-pol and H-pol measurements. The bulk of the σ^{o}s used to derive the 100 km average wind speeds are V-pol, but when both V-pol and H-pol exist they are combined.

In high winds the speeds estimated from V-pol measurements are lower than those estimated from H-pol. An intercomparison of H-pol and V-pol can show internal discrepancies, but not which is to be preferred. Woiceshyn et al. (1986) compare V-pol and H-pol with a subset of the JASIN data set. There is

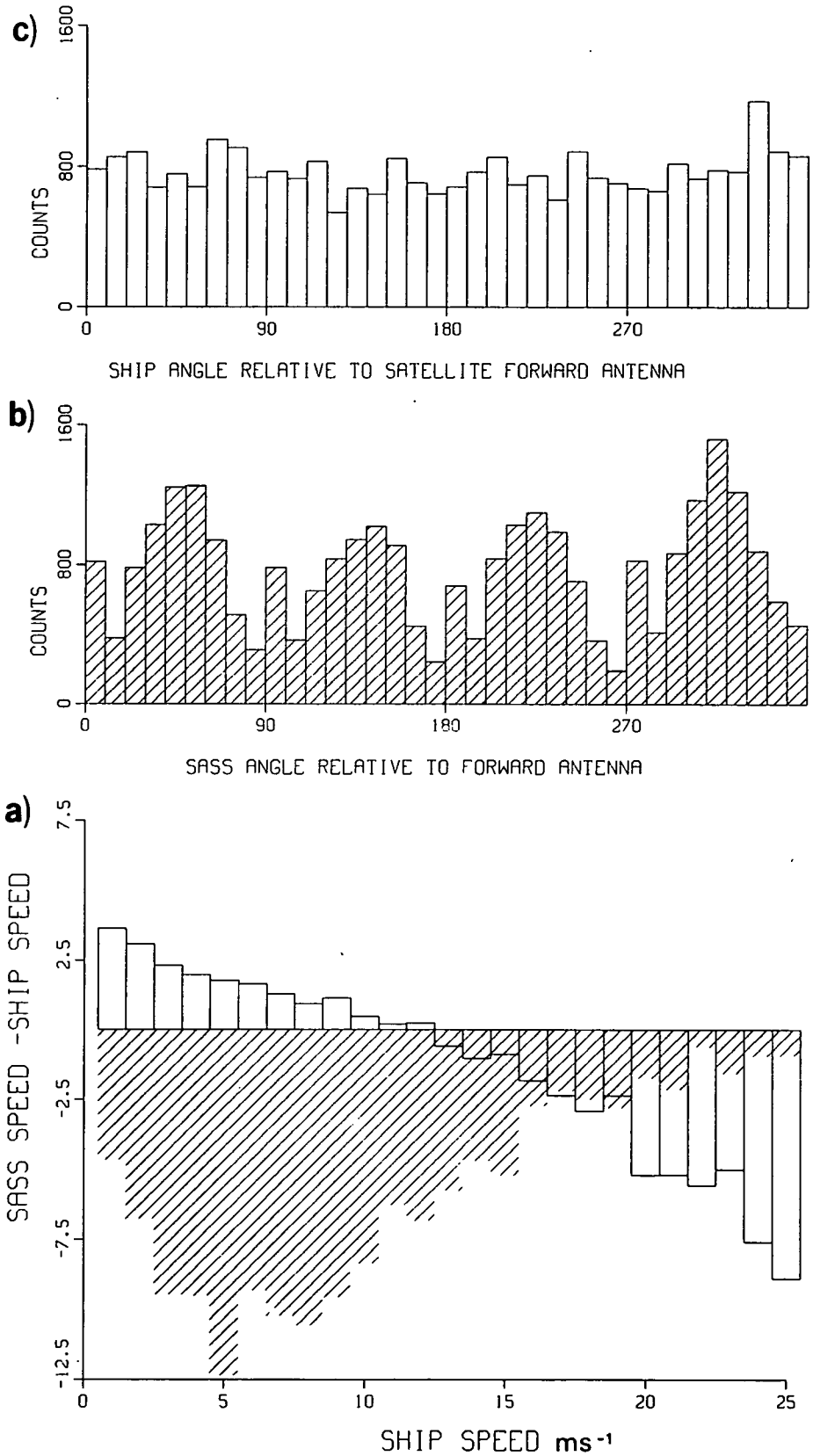

Fig. 2.1a The mean speed difference between SASS speed and collocated ship speed plotted as a function of ship speed. The SASS speed is higher than ship speed at low ship speeds but substantially low compared with ship speeds at high ship speeds. The shading indicates the square root of the number of collocations. (-2.5 corresponds to 156, -5 to 625). Collocations are over the period from 3Z on the 6th September to 21Z on the 17th September 1978.

b) No. of occurrences of a given SASS angle relative to the forward antenna.

c) No. of occurrences of a given SHIP angle with the angular direction measured relative to the forward antenna of the spacecraft.

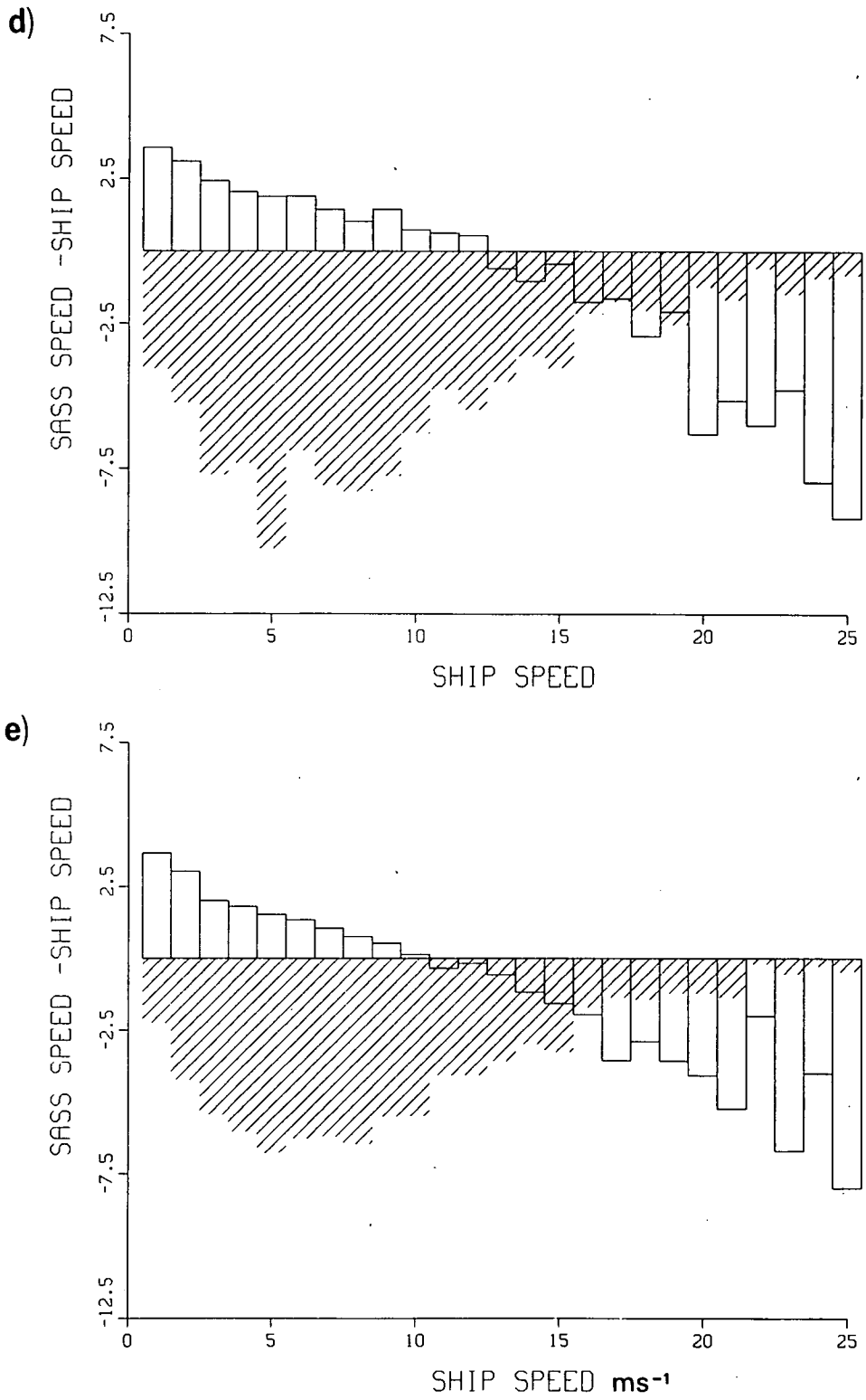

Fig. 2.1 d) As for 2.1a but when the ship reports are from Beaufort estimates.
e) As for 2.1a but when ship reports are from anemometer readings.
The speed bias does not seem to depend strongly on whether it is measured by Beaufort or anemometer. The magnitude of the differences at speeds above 15 m/s seem to be greater than those noted in earlier, less comprehensive comparisons, notably those in the limited but more accurate JASIN experiment (e.g. Jones et al 1982).

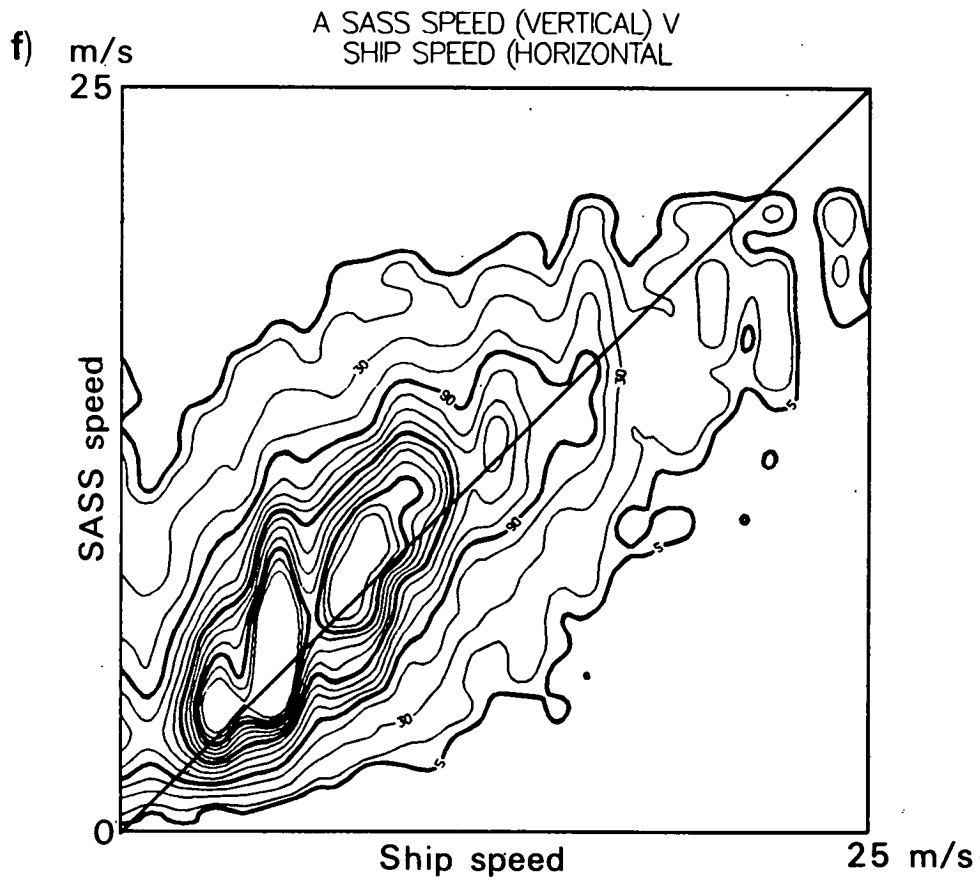

Fig. 2.1f Contour plot of the number of collocations of SASS speeds with ship speeds.

one data point (see their Fig. 8) which suggests V-pol is low compared with JASIN in-situ speeds at 17 m/s. (There are no higher speed collocations). This result is consistent with the results of Fig. 2.1, but 2.1 suggests a much larger discrepancy between SASS and ship.

There are indications that a power law relating σ^o to wind as used for SASS is not appropriate. For example, Duncan et al. (1974), Woiceshyn et al. (1986), indicate a change in the functional relationship between σ^o and wind speed at approximately 10 m/s. Pierson and Donelan (1986) show the speed bias to be expected if the relationship between σ^o and wind is actually as they propose, but is interpreted to be a power law. SASS would give high readings between 4 m/s and 18 m/s, but be biased low at speeds above 18 m/s. The bias is predicted to be a function of incidence angle. At 25 m/s, the bias is $\sim$ 5 m/s. The cross over points of 4 m/s and 18 m/s have been selected: different imposed cross over points would give different biases. The bias at low wind speeds noted in Fig. 2.1 is discussed further in Section 2.1.2.

2.1.1 Comparison of SASS with anemometer and Beaufort measurements

To discuss the results more fully it is helpful to consider the two methods used to report wind strength at sea. Ship measurements are made by two means - anemometer measurements and visual Beaufort estimates. The former is objective, but suffers from the fact that it is almost a spot measurement (from one to ten minute average) by an instrument at a variety of heights and often not ideally located on the ship. The latter is a subjective measurement but may be more of a spatial and temporal average.

Figs. 2.1d and 2.1e show the differences between SASS speed and ship speed plotted against ship speed when the ship speed is obtained by (d) Beaufort and (e) Anemometer respectively. There is little distinction; in fact given the different geographical distribution of anemometer ships and Beaufort ships (with anemometer reports mainly in the Pacific) the agreement is remarkably good. [By using the SASS data for intercalibration, this figure can also be used to judge the accuracy of the calibration of the Beaufort Scale against anemometer].

2.1.2 Comparison of SASS and SHIP as a function of latitude

The tuning of SASS-1 was confined to a small area in the North Atlantic. Not only was the speed range restrictive (speeds were almost all less than 16 m/s), but so also was the range of environmental conditions. It has long been felt that σ^o should be a function of temperature, since viscosity varies from 1.79 x 10^{-6} m^2/s at 0°C to .84 x10^{-6} m^2/s at 25°C. If the spectrum of short waves is as proposed by Lleonart and Blackman (1980), then the spectral energy density of short waves should vary as the square root of viscosity, and the radar cross section by 1.6 dB. This could give rise to wind errors of several meters/second (Stewart 1984). It must be noted that controversy still exists as to whether the energy density of short waves is proportional to viscosity as in Lleonart and Blackman (1980) and Stewart (1984), or is inversely proportional to viscosity as in Donelan and Pierson (1986).

It has also been found that the analysis of data from any one aircraft experiment usually yields a consistent correlation between σ^o and wind speed, but different experiments yield different correlations (Stewart 1984). This suggests that factors other than those accounted for in the model functions are operative. SST as noted above is one such possible factor; surface films, non local effects such as swell, and atmospheric boundary layer stability are others.

With the limited data record available, it was felt that SST effects might be detectable, but other effects probably not. It is worth noting however that since we are dealing here only with speed biases, it would be possible to greatly extend the data base for collocation by using the whole undealised SASS data record, since different aliases have much the same speed.

Fig. 2.2a,b show the differences between SASS and SHIP in two latitude bands (a) equatorward of 30° and (b) poleward of 50°. Comparison shows that, at low wind speeds (<10 m/s), the bias is larger at higher latitudes. The magnitude of the effect is between 1 and 2 m/s.

The separation has been made by latitude: this is done to increase the number of collocations, since all ships report position, but not all report SST. Nonetheless, it is likely that the signature in Fig. 2.2 is mainly one of SST variation. Fig. 2.3 shows the climate average SST for September. Equatorward of 30°, the SST is between 25°C and 30°C, while poleward of 50° it is generally below 12°C.

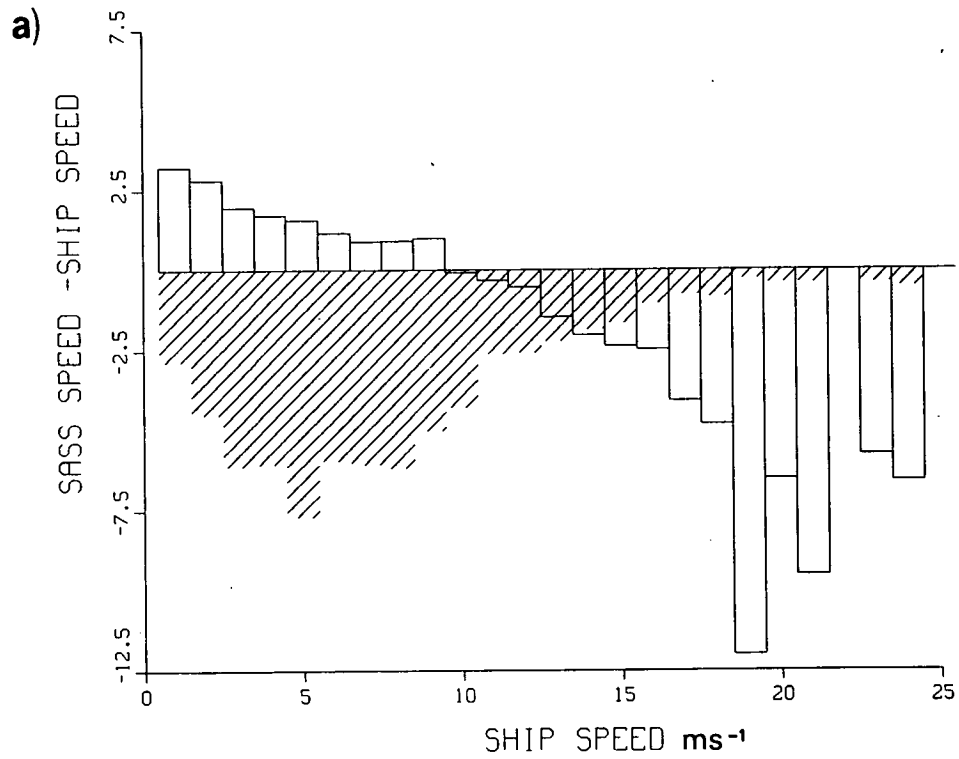

Fig. 2.2a As for Fig. 2.1a but with collocations restricted to the tropical belt between ±30°.

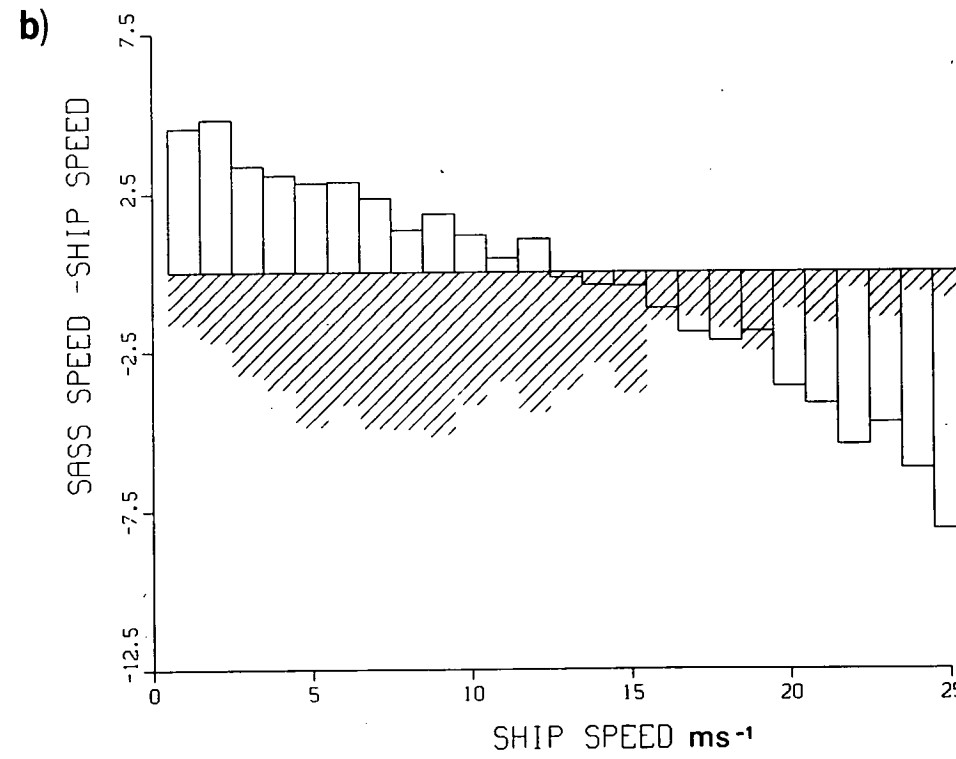

Fig. 2.2b As for Fig. 2.1a but with collocations restricted to the polar belt poleward of 50°.

This figure shows a larger speed bias at low ship speeds in the colder region.

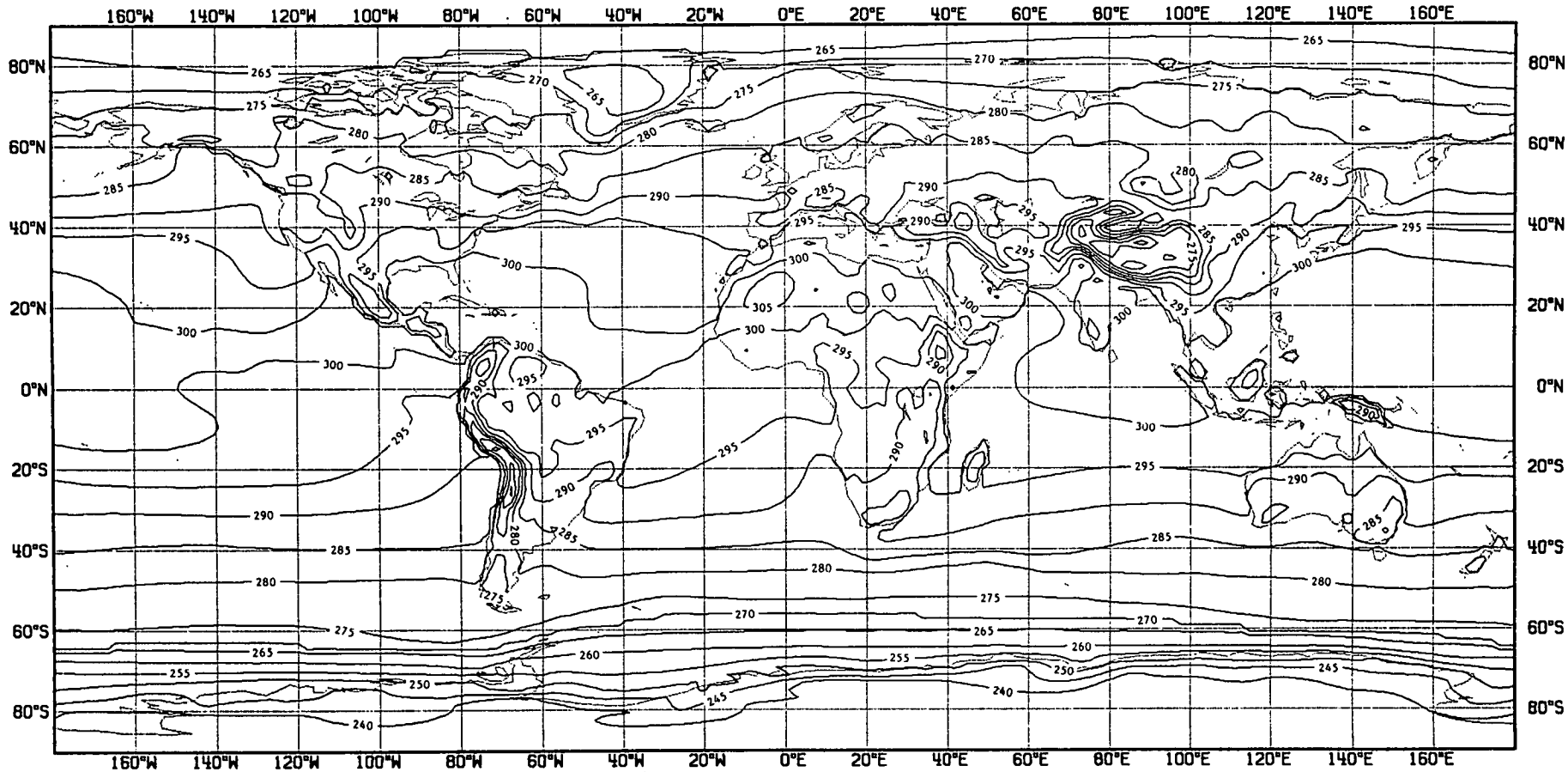

Fig. 2.3 Climatological sea surface temperature for September.

Woiceshyn et al. 1986 have also considered SST effects, collocating SASS data with data from the JASIN area (SST ~ 12.5°C) and with data from NDBO buoys (SST ~ 20°C). At low wind speeds they find an SST effect similar to that of Fig. 2.2. Fig. 2.2 however is based on a much larger data sample. The explanation offered by Woiceshyn et al is that at low wind speeds, data with low signal to noise ratio or negative σ^o is rejected by the quality control algorithm used by JPL. This is most noticeable for low σ^o, i.e. low wind speeds, and gets worse at lower temperatures. Rejecting low σ^o data gives rise to a positive bias, which is worse at colder temperatures. The data rejection has also been considered by Pierson and Donelan, 1986.

Figs. 2.2a and b show two other interesting effects

(1) For ship speeds between 4 m/s and 8 m/s SASS is high for both temperatures, but the difference is larger for the low temperature case. This is contrary to the results of Woiceshyn et al. 1986 who find SASS to be biased low in the mid speed range at low temperatures and high at higher temperatures.

(2) At higher wind speeds (> 14 m/s) SASS is biased low relative to ships. This is most pronounced in the warm water case. It should be noted however that this result is based on only a few collocations and needs further confirmation. Fig. 2.1f shows that the distribution of SASS v ship speed is not Gaussian, and so calculations of bias must be interpreted with caution.

The theory of radar return as a function of surface temperature is at present unclear, because of uncertainties in the wave spectrum at high frequencies. If the spectrum is as given by Lleonart and Blackman (1980) then the spectral energy density of wavelets should vary as the square root of viscosity, implying higher wind speeds at colder temperatures. This effect is also noticeable in the theory of Donelan and Pierson 1986, at speeds to 30 m/s. But because of lack of observations of the high frequency spectrum and its dependence on viscosity, no firm conclusion can be drawn. The results presented here appear to be in qualitative agreement with those of Donelan and Pierson (1986). The influence of SST on ERS-1 measurements may be less because the ERS-1 scatterometer uses a longer wavelength.

2.1.3 Influence of incidence angle

Schroeder et al. (1982) document the steps leading to the definition of the SASS-1 model function, an amalgam of earlier model functions, and note that greatest confidence is placed in the incidence angles from 20° to 50°. Outside this range and at lower wind speed, Schroeder et al. feel that the model is not so well defined and could be improved. In Figs. 2.4a-e, (SASS minus Ship) wind speed is plotted against ship wind speed as a function of incidence angle θ for (a) $18° < \theta < 25°$, (b) $25° < \theta < 35°$, (c) $35° < \theta < 45°$ (d) $45° < \theta < 55°$ (e) $55° < \theta < 70°$. These figures suggests that the speed bias at low wind speeds is indeed worse for the higher incidence angles ($> 55°$) than for the mid range incidence angles $25° < \theta < 55°$ but it is not clear that low incidence angles ($< 25°$) are worse. There is no evidence in Fig. 2.4 that the bias at high wind speeds depends on incidence angle. A period of several weeks may be necessary to reveal such a dependency based on ship reports.

Fig. 2.4 extends the incidence and geographical range of Jones et al. (1982) whose comparison is confined to the GOASEX observations. The results of Fig. 2.4 are broadly consistent with Jones et al. but differ in a number of ways; viz Jones et al. find the worst discrepancy averaged over all incidence angles in the speed range 5-10 m/s, whereas for Fig. 2.4 this range has generally small 'errors' at all incidence angles. The 'errors' in Fig. 2.4 at low and high speeds are larger than any 'errors' found by Jones et al.

2.2 Angular irregularities

Fig. 2.5a shows the angular difference between SASS dealiased wind direction and ship wind direction plotted as a function of ship wind direction relative to north. This figure gives some measure of the scatter in the directions which result from the combination of errors in the instruments (both SASS and ship), in the retrieval processing from $\sigma°$ to wind velocity, and in the ambiguity removal process (choosing the wrong alias). Figure 2.5a will not give a sharp indication of errors resulting from the instrument or the retrieval processing, since at that stage of processing, angles are measured relative to the spacecraft rather than with respect to north. A more enlightening way of diagnosing algorithmic problems is therefore to measure angles relative to the spacecraft.

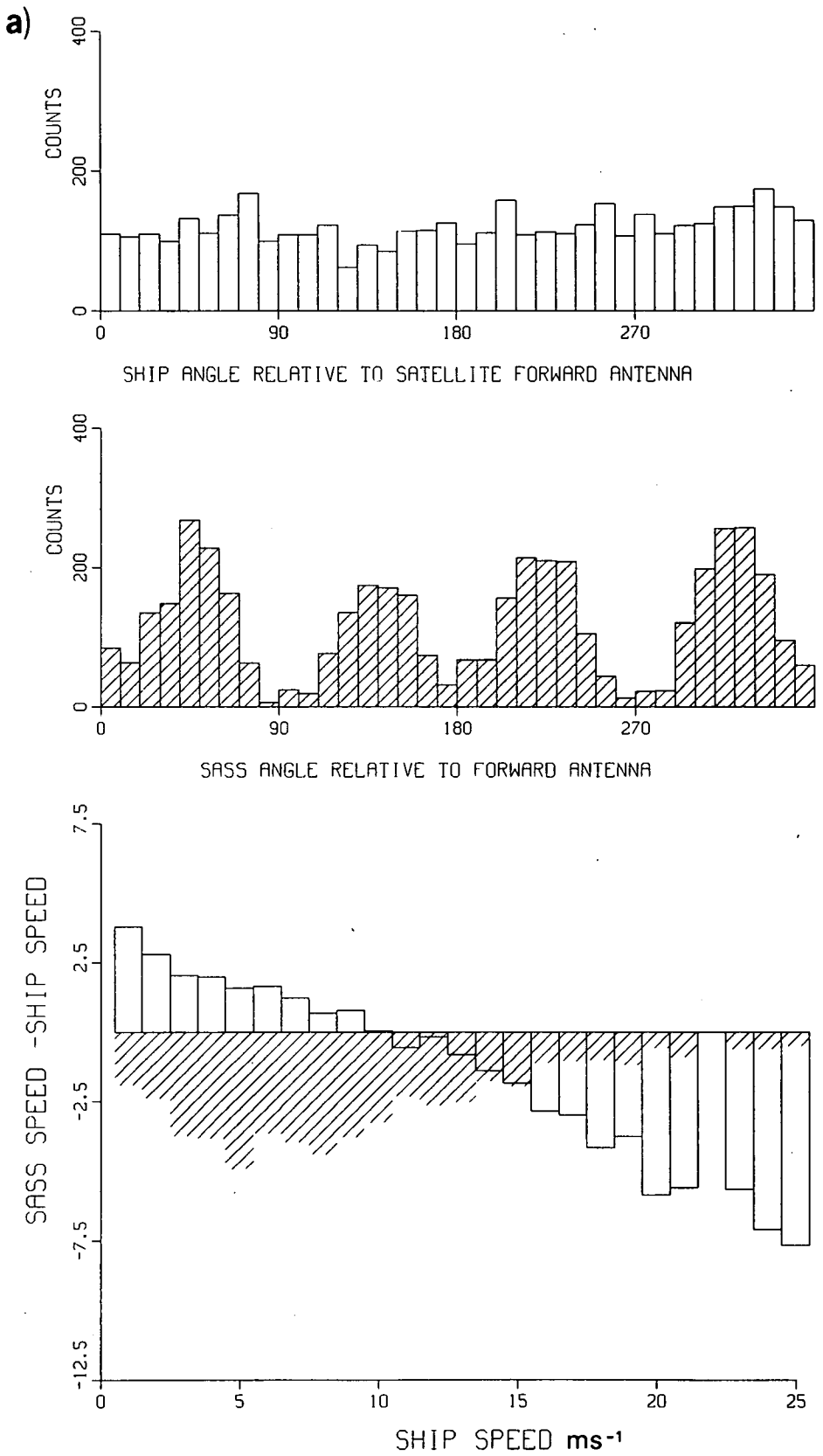

Fig. 2.4 a) Lower panel: Mean speed difference between SASS speed and collocated ship speed as a function of ship speed for incidence angles in the range 18-25°. Shading is as for Fig. 2.1a.
Middle panel: number of SASS collocations as a function of the wind direction measured relative to azimuth.
Upper panel: number of ship collocations as a function of ship wind direction measured relative to azimuth.

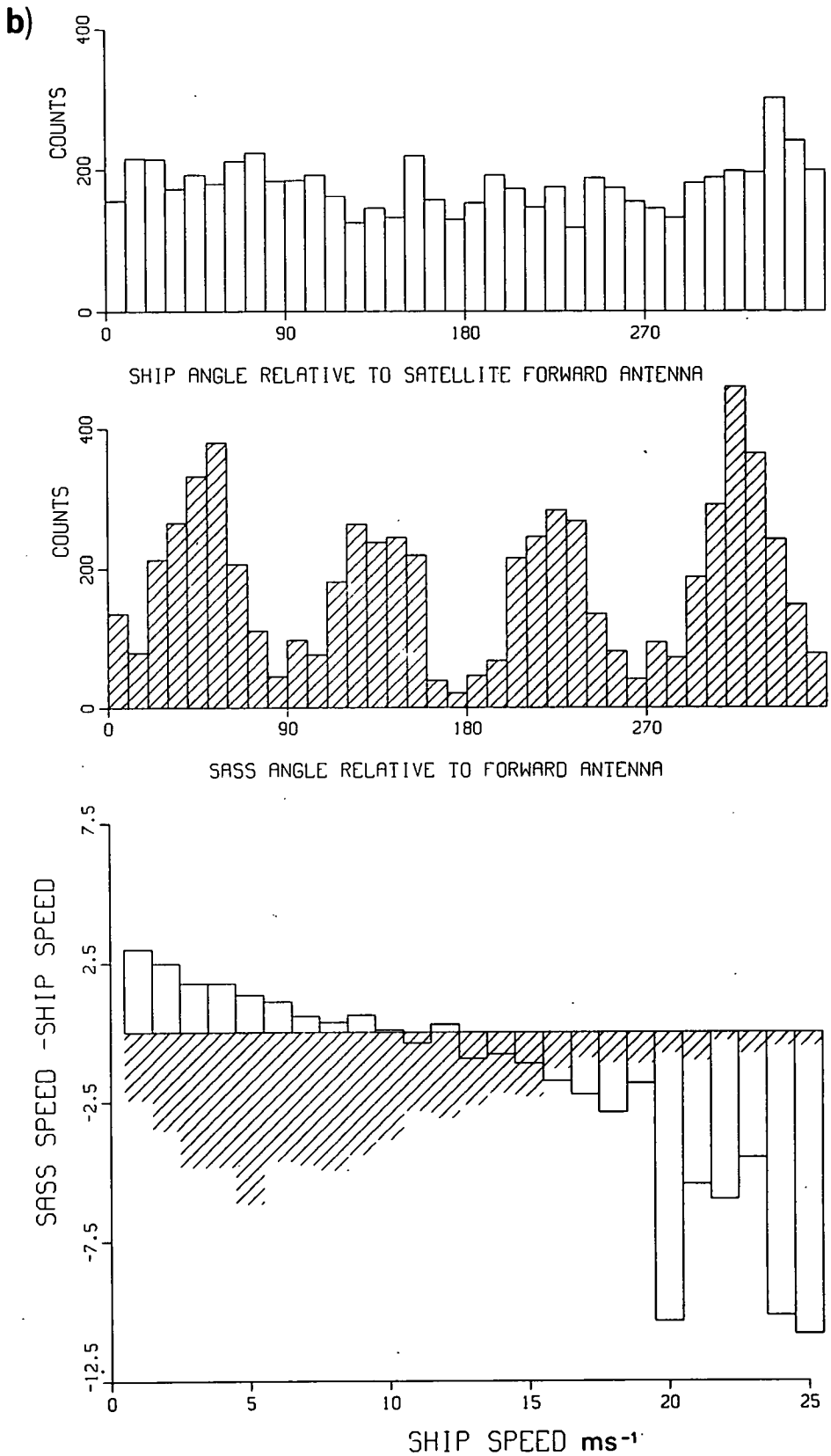

Figs. 2.4b-e are for increasing incidence angles: (b) 25-35°

c)

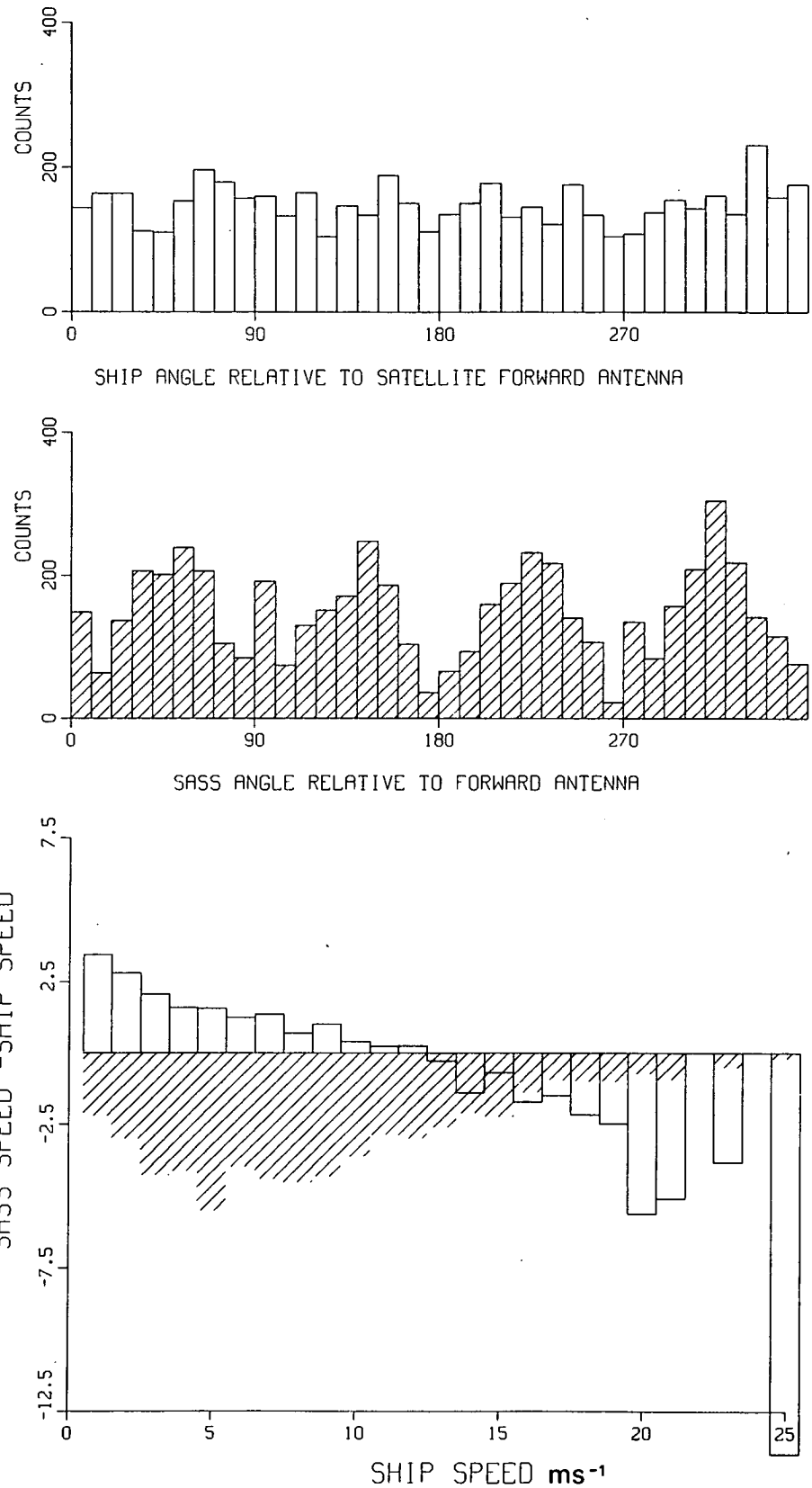

Figs. 2.4b-e are for increasing incidence angles: (c) 35-45°

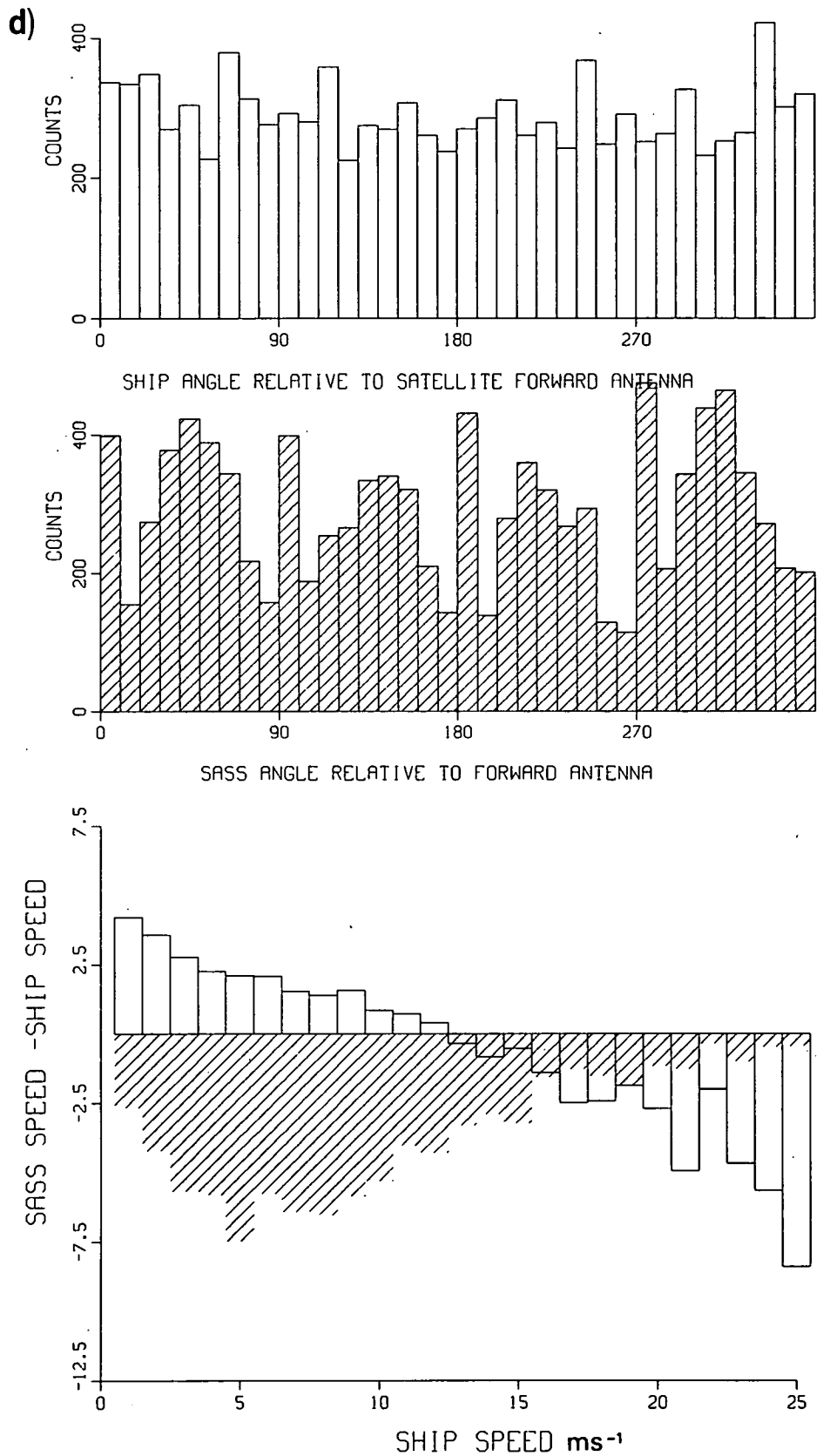

Figs. 2.4b-e are for increasing incidence angles: (d) 45-55°

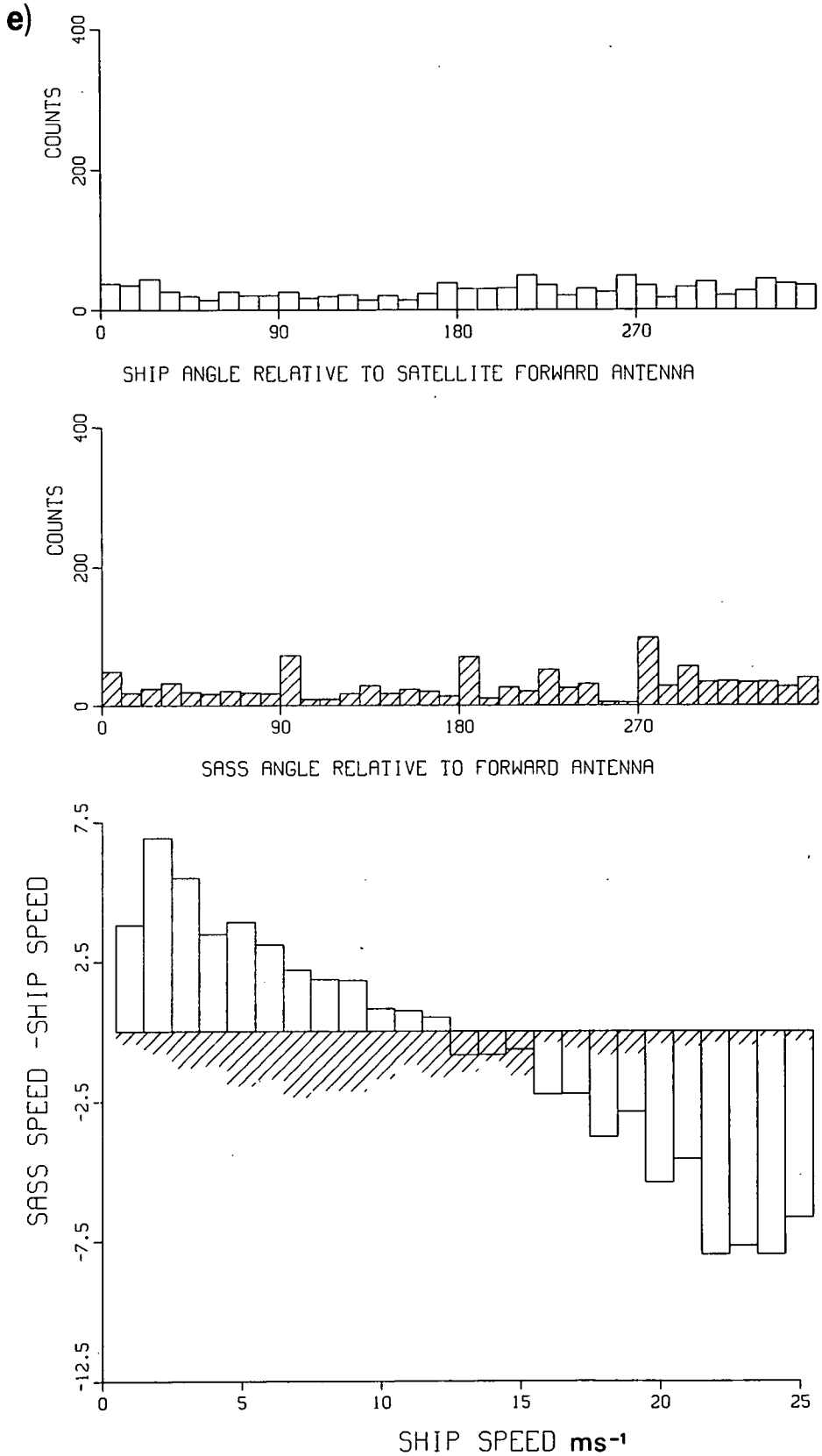

Figs. 2.4b-e are for increasing incidence angles: (e) 55-75°

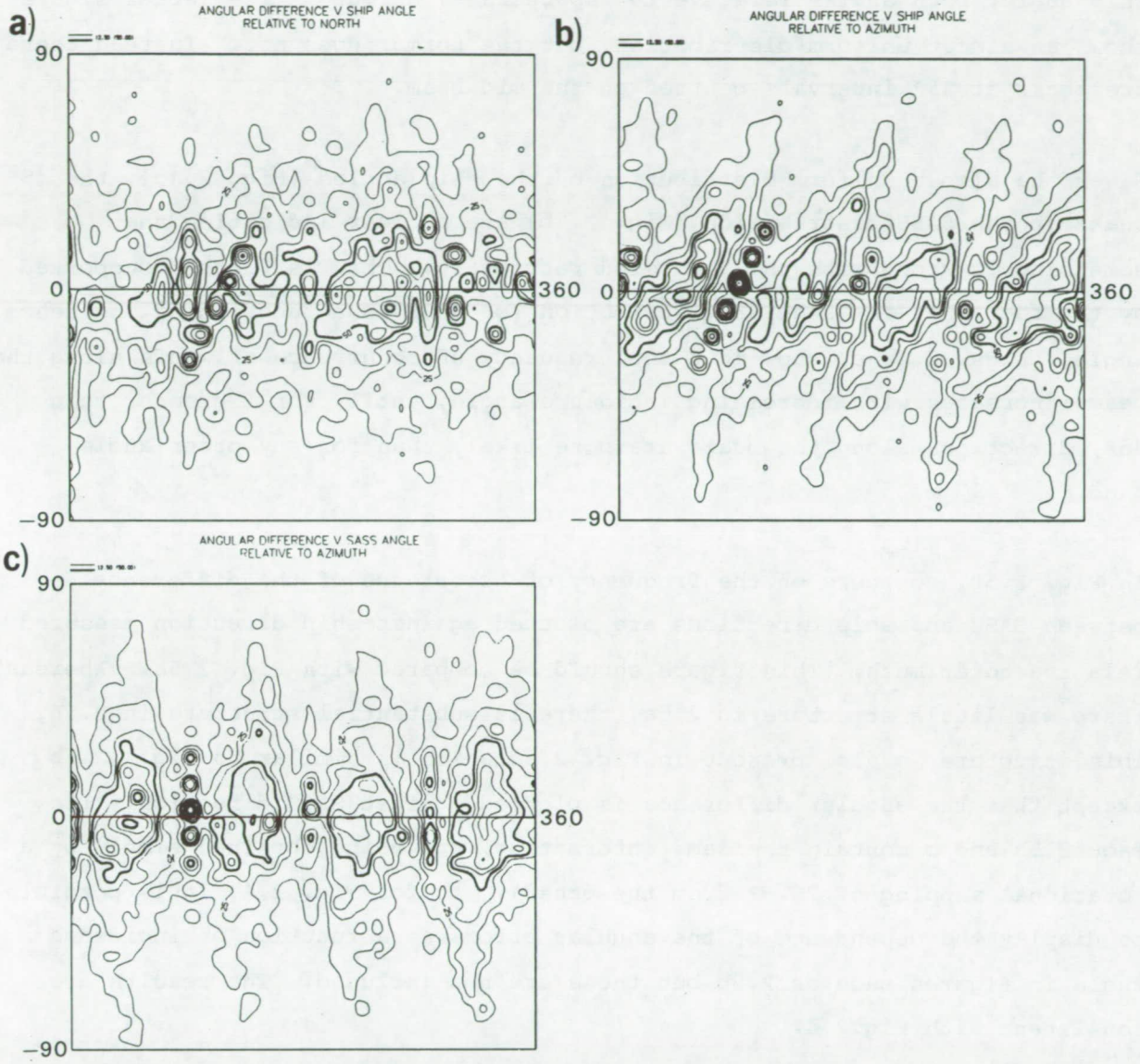

Fig. 2.5a Contour plot of the angular difference between SASS angle and ship angle plotted as a function of ship angle measured relative to north. The vertical axis ranges from -90° to +90°, while the horizontal ranges from 0 to 360°.

Fig. 2.5b As for 2.5a, but all angles measured relative to azimuth. (An angle of 0 means a direction along the forward beam).

Fig. 2.5c Angular difference plotted as a function of SASS angle measured relative to azimuth.

Fig. 2.1b is a histogram of the number of SASS observations for a given SASS angle, while Fig. 2.1c is a plot of the number of ship reports for a given ship angle, both angles relative to (spacecraft) azimuth. The latter figure shows an almost uniform distribution, but the former does not. Instead there are peaks at 45° intervals centred on the mid beam.

Given the almost uniform distribution of the ship angles (Fig. 2.1c), the 45° peaks in the SASS distribution (Fig. 2.1b) are a clear indication that something is wrong with the SASS wind retrievals. This is further supported by the fact that the angular distribution for SASS is a function of incidence angle. Figs. 2.4a-e, show that the frequency of occurrence of winds along the beams increases with increasing incidence angle, until, for θ greater than 45°, directions along the beams are more likely than for any other angle band.

In Fig. 2.5b, contours of the frequency of occurrence of the difference between SASS and ship directions are plotted against ship direction measured relative to azimuth. This figure should be compared with Fig. 2.5a. Whereas, there was little structure in 2.5a, there is substantial structure in 2.5b. This structure is also present in Fig. 2.5c which is similar to Fig. 2.5b except that the angular difference is plotted against SASS direction. (In fact 2.5b and c contain the same information, one being obtained simply by a rotational mapping of 26.5° from the other). As for Fig. 2.4, it is possible to display the dependence of the angular errors as a function of incidence angle in figures such as 2.5b but these are not included. The results are consistent with Fig.2.4.

Fig. 2.5c shows the spread of angular error as a function of angle, when all wind speeds are considered. Fig. 2.6a and b shows the same information when speed filters are applied. Only speeds below 6 m/s are included in Fig.2.6a. The banding, so evident on Fig. 2.5c is again in evidence, but the spread of error is larger. This is perhaps not totally surprising since at low speeds, the angles might be expected to be harder to determine. In Fig. 2.6b, only speeds $>$ 5 m/s are selected. Comparison of Figs. 2.5c, 2.6a and 2.6b shows that the angular irregularities exist regardless of speed. There is an indication that the angular error is larger at low speeds, but this needs further investigation

Other differences between SASS directions and ship or model directions may exist. For example, SASS velocities often have a large cross isobaric component (see also Section 4). It is possible to investigate such questions, but this has not been done.

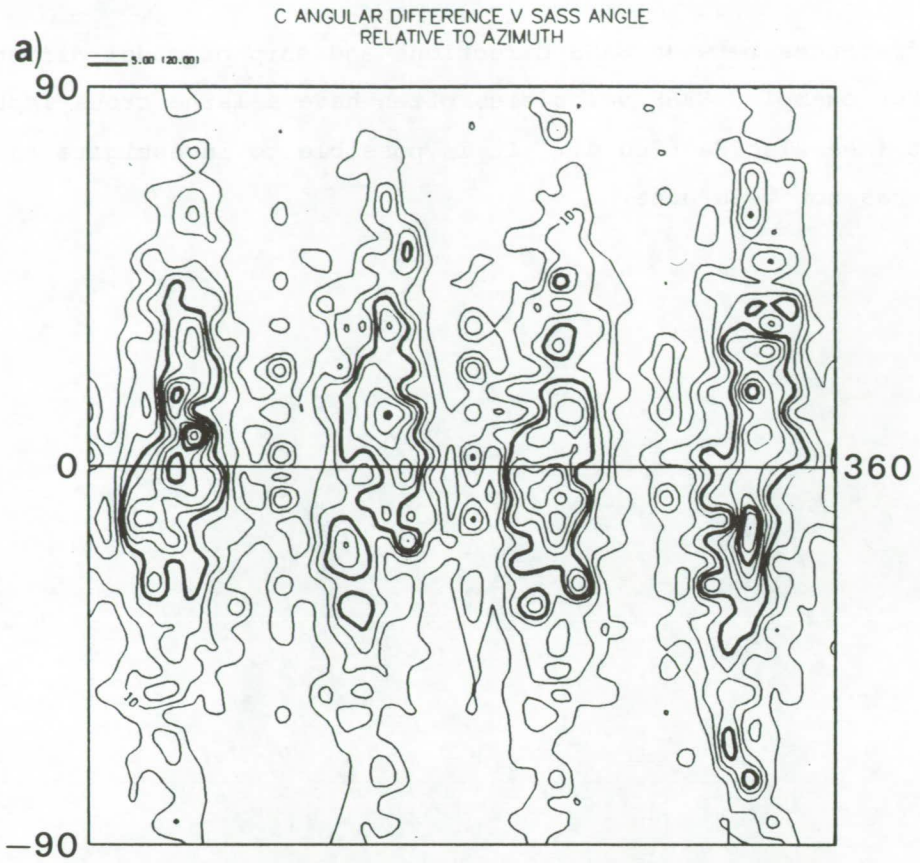

Fig. 2.6a As for Fig. 2.5c, but only for speeds less than 6 m/s.

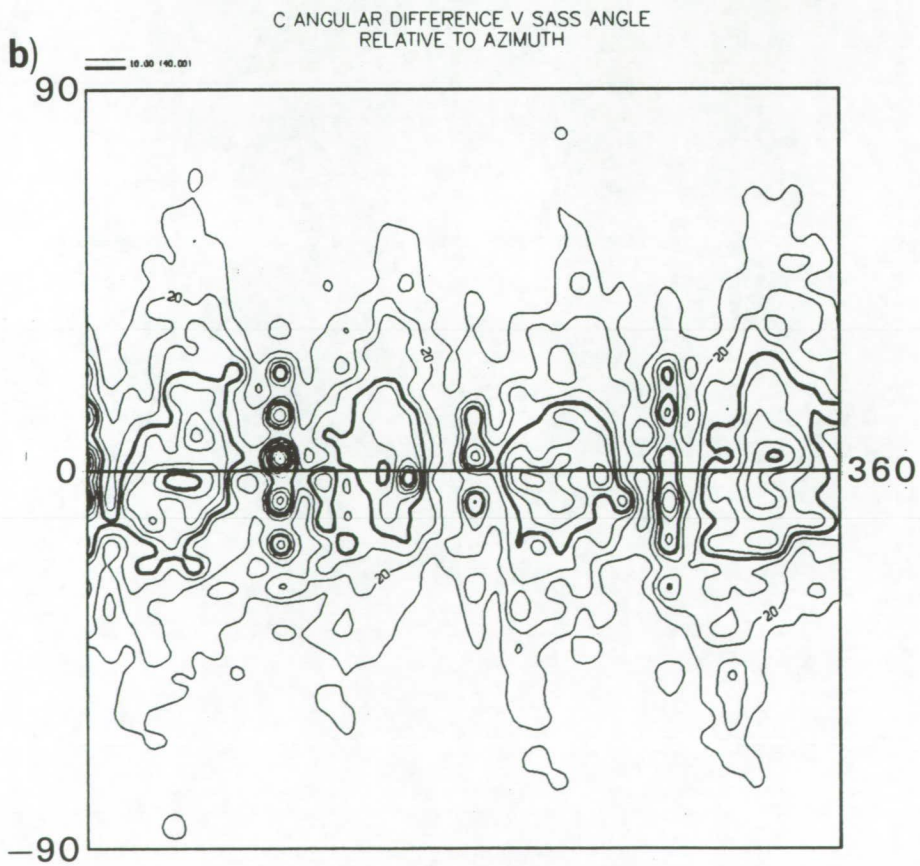

Fig. 2.6b As for Fig. 2.5c, but only for speeds greater than 5 m/s.

3. DATA ASSIMILATION

3.1 Introduction

The volume of data required to define the state of the atmosphere far exceeds the volume of data available at any given time. To improve the definition of the current atmospheric state, meteorologists have developed a number of techniques to combine current observations with earlier observations projected forward in time to the current time; these techniques are known generically as data assimilation. Data assimilation requires an accurate forecast model, an analysis algorithm and an initialisation algorithm. In the ECMWF and many other systems, data are grouped in six hour bins and treated as if they were valid at the mid point of the time interval. The forecast model provides a background field for the analysis in the form of a 6-hour forecast valid at the same time and made from the last analysis. The analysis algorithm makes a minimum variance statistical combination of the background field and the data. The initialisation algorithm is a (slight) technical modification of the analysis to prevent noise being generated in the forecast for the next six-hour period. In this section, we report data assimilation experiments on SASS data with the April 1986 ECMWF operational analysis/forecast system. The highest resolution possible is used (T106) for the model which produces the 6 hour forecast or first guess (FG). All longer forecasts were also done at T106 resolution.

Two main assimilation experiments were carried out, NOSASS and AESASS. The former, as the name implies, is an assimilation in which SASS data is not used, and represents the control run. Although SASS data is not used it is still passed to the analysis routines and so departures of the SASS data from the model first guess and initialised analyses can be calculated. Those data which would have been rejected, had the data been actively assimilated, can also be identified. The AESASS is the experiment in which SASS data is actively assimilated. Both experiments ran from 6Z on the 6th September to 18Z on the 17 September inclusive.

A third short (1 day) experiment (ALINOS) was run using SASS data from the extended SASS data tape but now including azimuth and incidence angle information (see Appendix A). The starting condition was the 12Z first-guess on 10th September produced by the NOSASS experiment. This experiment is discussed in Sections 3.4.1 and 3.4.2.

In Section 3.2 a brief description of the analysis cycle is given. The procedures used are quite involved, and so will not be reported on in detail. The reader is referred instead to reports by Lorenc (1981), Hollingsworth and Lönnberg (1986), Lönnberg and Hollingsworth (1986) and Shaw et al. (1987) for a more thorough description. In Section 3.3, specific features of the analysis relevant to the way SASS data is used are listed. The forecast model can be considered as another instrument, with its own error characteristics. A comparison of the forecast model with SASS measurements is discussed in Section 3.4. As noted earlier (see also Appendix A) the assimilation of SASS data used measurements from the short dealiased tape which does not contain information on azimuth and incidence, so the main comparison is with respect to speed, but a short assimilation experiment (ALINOS) in which SASS data from the longer aliased tape is passed to the analysis but not used allows a brief angular comparison.

In Section 4 the differences in the analyses produced with and without SASS data are discussed and the impact of assimilation of SASS data on medium range forecasts assessed.

3.2 DATA ASSIMILATION

An analysis, if it is to be as accurate as possible, must supplement information from the currently available observations by two means:

1. Information from earlier observations.
2. Knowledge of the likely structure and scales of atmospheric motion, and of the balance which is usually observed between the various fields (mass, wind, humidity) of the atmosphere.

In a data assimilation scheme both of these are provided with the help of a numerical model of the atmosphere, which can update information from past observations to the current analysis time, and assimilate all the data into a consistent multivariate three dimensional analysis which represents the atmospheric motion in a realistic way. If the main use of the analysis is to provide initial conditions for a numerical forecast, the advantage of using a numerical model outweighs the main disadvantage, which is that biases and inaccuracies in the model's formulation and limitations to its resolution mean that the final analysis does not always accurately represent all the detail available in the observations.

Ideally, observations should be inserted into the assimilating model at the valid model time. However, this is difficult to organise, particularly if sophisticated analysis methods are used to help ensure that the information is inserted into realistic scales of motion, with approximate balance between the various fields. At ECMWF a compromise 6 hourly intermittent data-assimilation is used. Observations from a 6 hour period spanning the nominal analysis time are used to correct a 6 hour forecast made from the previous analysis. Deviations of the observations from the forecast are analysed to give increment fields which are then added to the forecast fields.

Since the analysis methods cannot represent the atmosphere's balance as accurately as the model can, the model equations are used subsequently in a non-linear normal mode initialisation. The balance achieved by this is sufficiently realistic that even fields sensitive to the balance, such as the vertical velocity, are meteorologically realistic. For this reason, the initialised fields may be considered to be the analysis, despite the fact that the uninitialised fields usually fit the individual observations somewhat better.

The initialised analysis is then used as initial conditions for a 6 hour forecast, using ECMWF's prediction model. Since we use the forecast field in the next analysis, we also estimate its statistical uncertainty, so it can be given appropriate weight. The highest available resolution for the model is used (viz T106, which uses a horizontal resolution of 1.2 degrees for calculations in physical space).

As the main purpose of the analysis is to produce initial conditions for the forecast model, the same vertical coordinates are used in the analysis as in the forecast model. However, the majority of the observations are reported on standard pressure levels and therefore the data are presented to the analysis schemes at 15 standard pressure levels: 1000, 850, 700, 500, 400, 300, 250, 200, 150, 100, 70, 50, 30, 20 and 10 hPa. Thickness and precipitable water observations are given for layers defined by the standard pressure levels. The analysed variables are geopotential height, and northward and eastward components of wind on a regular latitude/longitude grid with a resolution of 1.875° and at model levels.

The analysis method used to combine observations and model first guess is an extension of optimal interpolation (Eliassen 1954 and Gandin 1963) to a multivariate three-dimensional interpolation of deviations of observations from a forecast field (Lorenc, 1981). This technique allows consistent use to be made of observations with different error characteristics, and takes into account their spatial distribution. Because of the various assumptions made in using linear regression and error covariance modelling, the interpolation is not truly optimal and the name 'statistical interpolation' is preferred. The abbreviation OI will be frequently used.

Linear relationships can be specified in a statistical interpolation scheme between meteorological variables that are analysed simultaneously. The relationships used in the ECMWF scheme cause the analysed corrections to the forecast to be locally non-divergent and approximately geostrophic, but with the geostrophic relationship relaxed near the equator. The hydrostatic relationship enters in the conversion of temperature observations to thicknesses.

The scheme has been designed for a vector processing computer especially suitable for the efficient solution of large linear systems of equations. In contrast, the logical operations usually required for selecting only the 'best' data in order to keep the systems small do not exploit the full speed of a vector processing machine. Thus instead of the small systems, typically of order 10 to 50, used in other schemes, the ECMWF scheme uses large systems of order 200 or more. This also enables the full potential of the multivariate three-dimensional statistical analysis method to be exploited, since within such a large number of data it is possible to include height, wind and thickness data for several layers of the atmosphere. For example only by three-dimensional use of the data can optimum use be made of a surface pressure observation, a set of satellite temperature soundings, and a cloud motion and surface wind. The thickness and thickness gradient (thermal wind) information in the soundings increases the "zone of influence" of the pressure and wind data.

During the pre-analysis stage, the observations are sorted into boxes approximately 660 km square. Several tests are applied to the data to identify and exclude 'erroneous' observations from the data set that is used

for the analysis. The tests are first against the first-guess (FG), then against neighbouring observations in the same box and finally the full multivariate check by the OI equations.

Primitive equation models, unlike quasi-geostrophic models, generally admit high frequency gravity wave solutions, as well as the slower moving Rossby wave solutions. If the results of the analysis scheme are used directly as initial conditions for a forecast, subtle imbalances between the mass and wind fields will cause the forecast to be contaminated by spurious high-frequency gravity-wave oscillations of much larger amplitude than are observed in the real atmosphere. Although these oscillations tend to die away slowly due to various dissipation mechanisms in the model, they make the forecast noisy and they may be quite detrimental to the analysis cycle, in which the six-hour forecast is used as a first-guess field for the next analysis. The synoptic changes over the six-hour period may be swamped by spurious changes due to the oscillations, with the consequence that at the next analysis time, good data may be rejected as being too different from the first-guess field. For this reason, an initialization step is performed between the analysis and the forecast, with the object of eliminating the spurious oscillations.

The principle of the method is to express the analysed fields in terms of the normal modes of free oscillation of the model atmosphere, then to modify the coefficients of the fast moving gravity modes in such a way that their rate of change vanishes.

3.3 Aspects of the use of SASS data in the assimilation cycle

In what follows we note some special aspects which affect the use of scatterometer data in the assimilation.

(1) All appropriate types of observations are used in the analysis. They include: reports from surface land and sea platforms (SYNOPS and SHIPS); radio sonde and pilot reports (TEMPS and PILOTS); satellite wind reports (SATOBS); aircraft reports (AIREPS); satellite thickness reports (SATEMS); and drifting buoy reports (DRIBUS).

(2) The 10 m wind is calculated from the wind at the lowest model level according to

$$U_{10} = U_{30} \frac{\ln\left(\frac{10+z_o}{z_o}\right)}{\ln\left(\frac{30+z_o}{z_o}\right)} \qquad \text{where } z_o = \text{roughness length,}$$

which in turn is calculated from the Charnock formula over ocean and is specified over land. The lowest model level is about 30 m above the surface.

(3) There are 15 standard pressure levels, the lowest being 1000 mb. All surface (ship, buoy, SASS) wind speeds are taken to be at 10 m. The increment or difference between the observation and first guess (OB-FG) is calculated, and then assigned to the 1000 mb level. No correction is made for stability.

(4) The statistical analysis algorithm ought to be provided with accurate statistics on the observational errors. The scatterometer winds almost certainly have spatially correlated errors, but nothing is currently known about that aspect of the errors. The scatterometer winds are therefore specified to be uncorrelated. The presence of spatial correlation in the observation errors would have a marked impact on the spatial filter properties of the analysis algorithm (Hollingsworth, 1987).

(5) Preliminary tests suggested that the rms error assigned to SASS observations should be 3.6 m/s for both zonal and meridional components. This is the same as for surface wind speed measurements from ships but lower than the error of 5.4 m/s assigned to DRIBU's. The larger the assigned observational error the less weight is given to an observation.

(6) Information on the statistics of short-range forecasts enters through the prediction error covariance function. This at present is taken to be the sum of terms which are the product of a vertical correlation and a horizontal correlation. The vertical extent to which surface observations can influence the atmosphere is related to the vertical

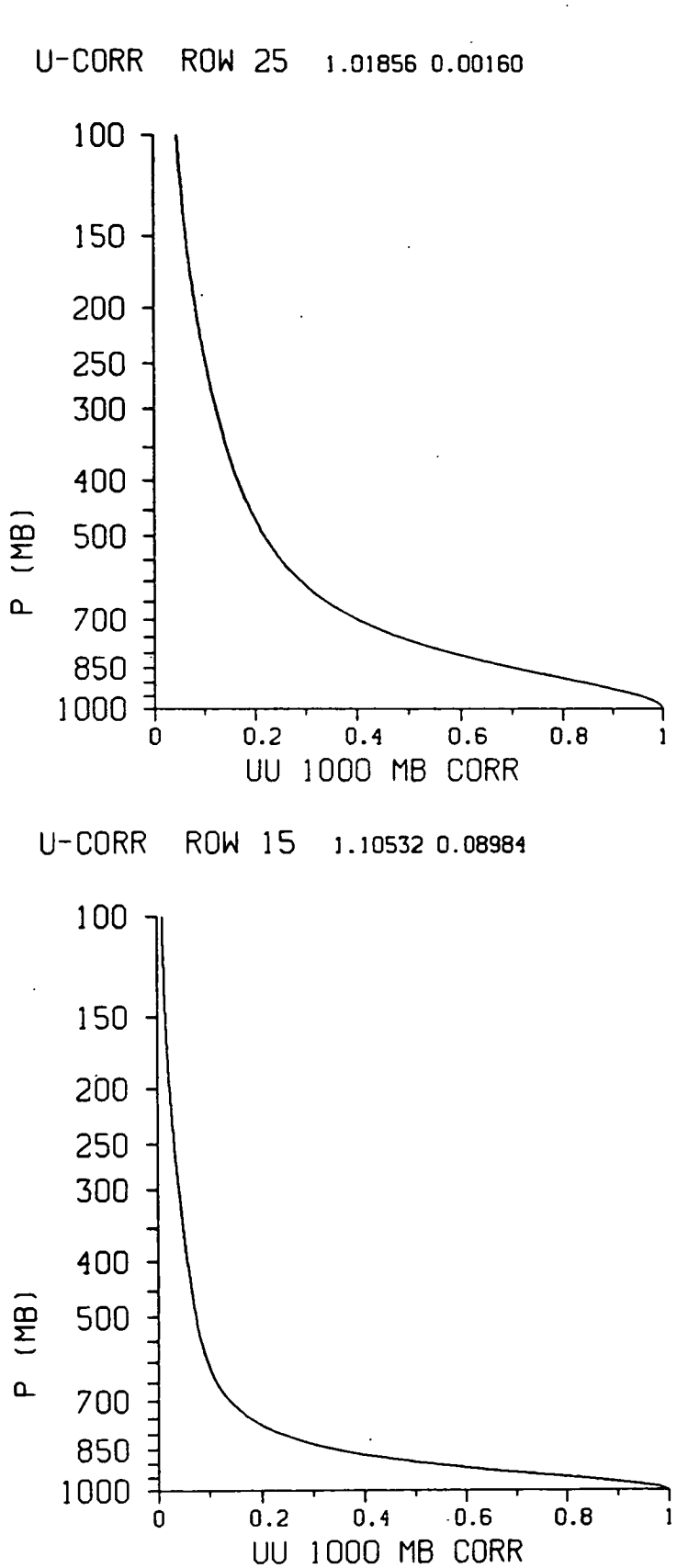

Fig. 3.1 Vertical correlation function used to extend in the vertical the departure of the surface observation from the first guess.
a) mid latitudes, b) tropics.
From Per Unden, personal communication.

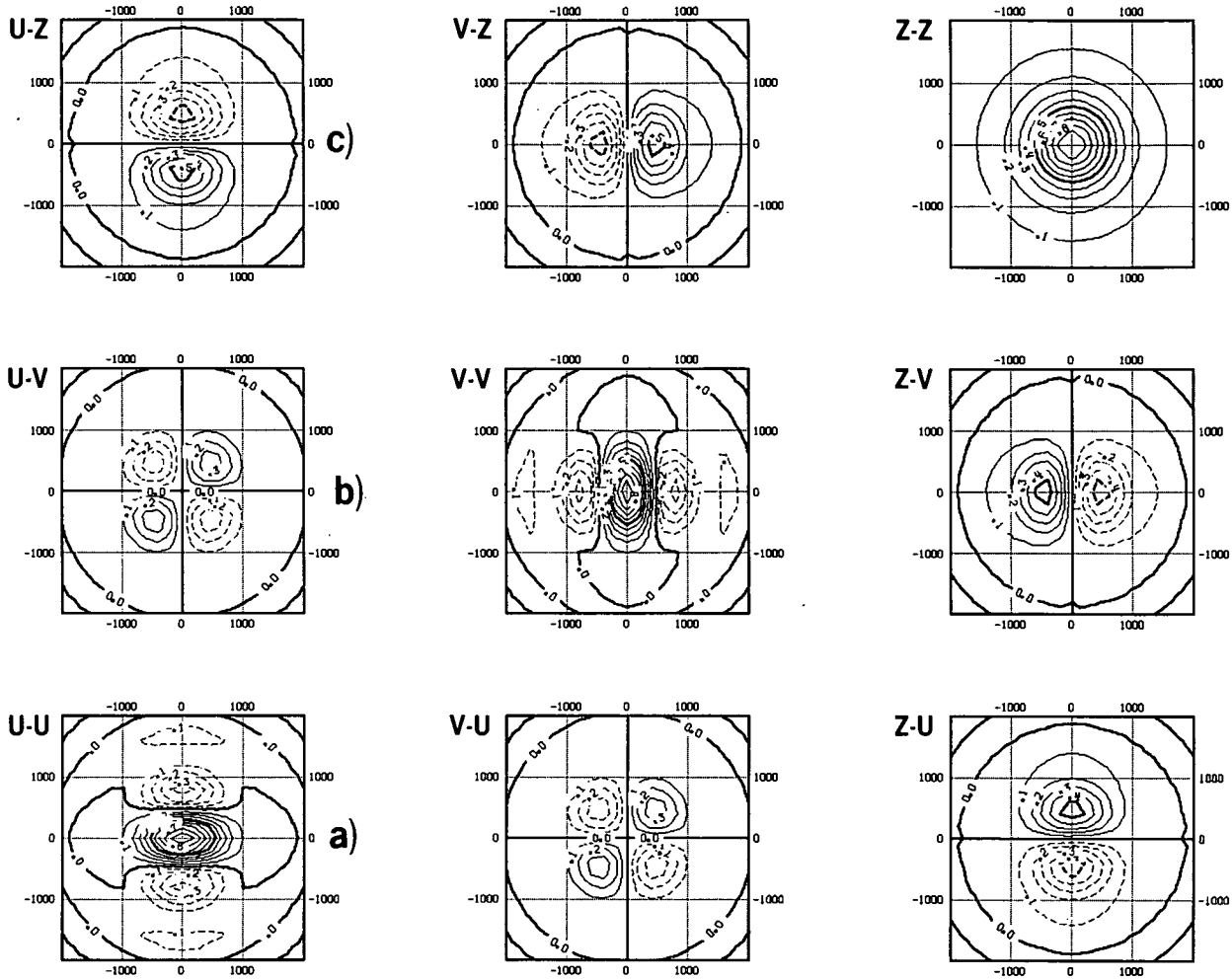

Fig. 3.2 The horizontal correlation function used to extend the departure of the surface observation from the model first guess in the horizontal. From ECMWF Research Manual 1: Data Assimilation, P. Lönnberg and D. Shaw.

The departures (OB-FG) are calculated for both components (zonal and meridional). A zonal velocity can influence (a) the zonal velocity (b) meridional velocity and (c) height (by geostrophy).

These correlation functions depend on latitude by a similarity transformation. (The spatial scale for the tropics is double that shown and 1.2 larger for the SH).

correlation. This is a function of latitude and is shown in Fig. 3.1 for the extratropics (a) and tropics (b). The influence has dropped to less than one third of its surface value by a height of 800 mb in the tropics but extends to 600 mb in the extratropics.

The extent to which observations influence the analysis in the horizontal is illustrated in Fig. 3.2. One imposes physical relationships between analysis variables such as geostrophy, non divergence and hydrostatic balance. The extent to which an observation of the u component of velocity can influence the u component, the v component and the height as a function of distance from the observation point is shown in panels a, b, c respectively. These functions are expanded in the tropics by a factor of 2 (component length scale = 1000 km) and by 1.2 in the Southern Hemisphere, but the shape is universal.

(7) The O.I. procedure acts as a spatial filter. The analysis will draw to the data on the large scale and to the model first guess on the small scale. (Hollingsworth 1987). This is discussed more fully in section 4.2.3.

(8) Not all data is presented to the analysis. The O.I. procedure involves inverting matrix equations. Ideally one would like to analyse the whole atmosphere at once. But this is not practical, so instead the domain is broken up into boxes (1144). Even within these boxes it is not always possible to use all data if there is an abundance of data. So consistent observations are combined to form super observations. In the use of N very close observations they will be combined to give one "superob" with an error of $\sigma/\sqrt{N}$. The analysis will combine this one superob with the model FG and filter out any smaller scale structure in the observations. Because scatterometer data is quite dense, it will be frequently superobbed. Data of different types can be superobbed provided the data agree. Approximately 40-50% of the SASS data is superobbed.

(9) The analysis, as well as filtering noise from the data, can be used to check the quality of the data. Several levels of checks are incorporated, in addition to obvious checks for reporting errors. The checks are

(1) departures from the first guess. If this is too large the datum is flagged.

(2) departure of the observation from an OI analysis made excluding that observation. If this is too large the datum is flagged.

For all data which pass the first level of checks (reporting errors) etc., departures of the observation from the first guess and from the analysis are recorded. In the case of SASS data a departure from the analysis is only calculated after initialisation. The details of the ECMWF quality control procedures are discussed in Shaw et al. (1987); some examples of these quality control checks will be given in Section 4.

3.4 A statistical comparison of SASS data with the First-guess and analysis Wind Fields

3.4.1 Comparison of model speed and SASS speed

In Section 2.3, it was shown that SASS speeds differed from ship speeds especially at low and high wind speeds. In this Section the model will be treated as an instrument and comparison made between SASS and the model first guess (FG) or initialised analyses (IN). In Fig. 3.3 speed histograms of (a) model FG speed v SASS speed and (b) analysed speed (IN) v SASS speed are shown for the AESASS experiment. The comparison is over all latitudes. In (a) one can see that the biases observed in Section 2 are very much in evidence here also. In (b) one can see that the model analysis has responded to the SASS data and the speed agreement is much improved. However, by the next observing time (6 hrs later) the fit has returned to being like (a) i.e. in a statistical sense much of the SASS induced modifications especially at high wind speeds have been lost - the model and SASS do disagree at higher speeds. It may be argued that the first-guess also has many ship reports and therefore that the fit of Fig. 3.3 may be reflecting partially the influence of ships. The influence of ship reports may be tested by comparing SASS with the first-guess in the Northern and Southern Hemispheres separately, since there are few ship reports from the Southern Hemisphere. Fig. 3.4 shows the NH case

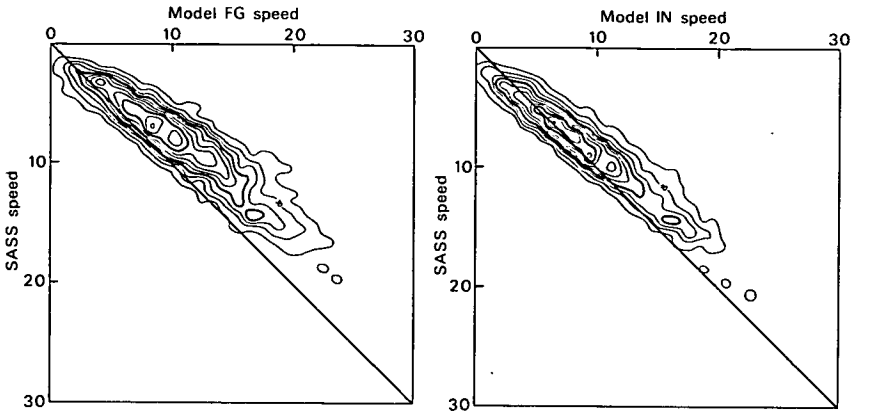

Fig. 3.3 Left-Contour histograms of model (FG) speed (across) v SASS speed (down). The axes range from 0 m/s to 30 m/s.

Right-Histograms of (IN) Analysis speed (across) v SASS speed (down). The axes range from 0 m/s to 30 m/s.

Only data for the six hour wind centred on 12Z on 11th September from the AESASS experiment are used.
Comparison of left and right hand diagrams show the extent to which the FG has been altered by the SASS data. (Best seen by turning the diagram through 90°).

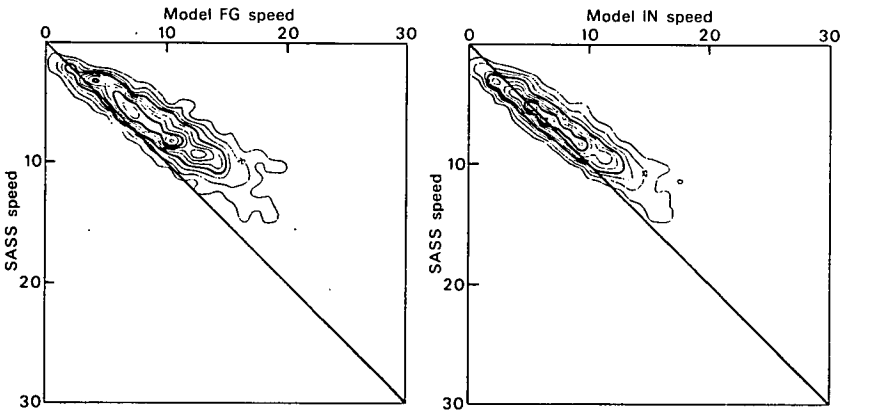

Fig. 3.4 As for 3.3 but only Northern Hemisphere.

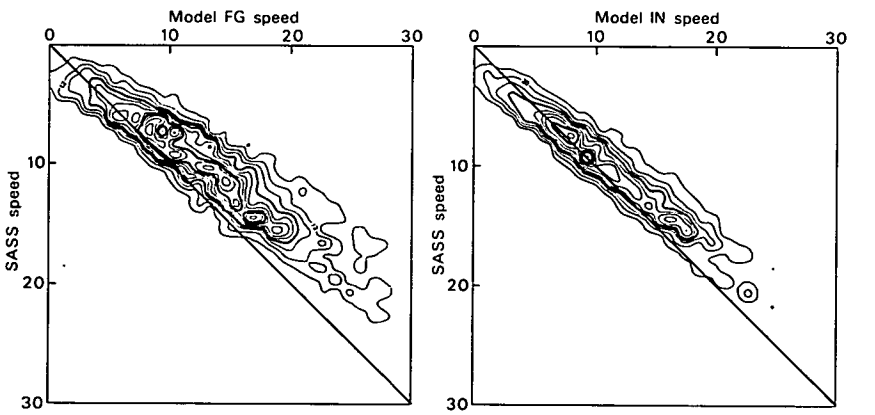

Fig. 3.5 As for 3.3 but only Southern Hemisphere.

The speed range is much larger in this latter case but Fig. 3.3, 3.4 and 3.5 all show the positive bias at low speeds and negative bias at high speeds commented on in Fig. 2.1, when SASS was compared with ship data.

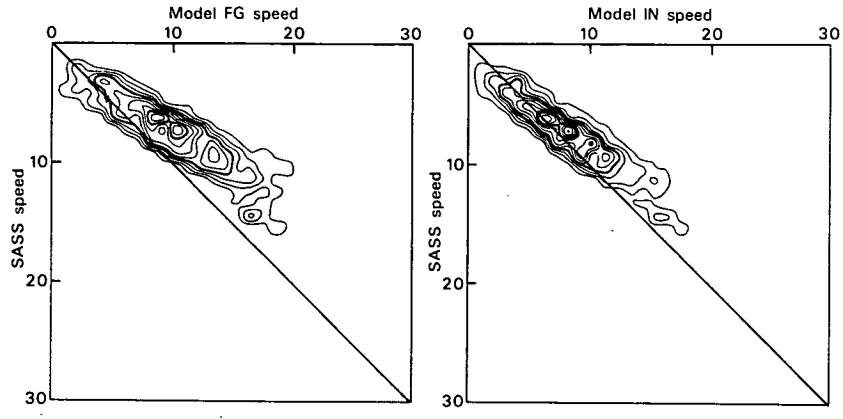

Fig. 3.6 Similar to Fig. 3.4 but corresponding to the region equatorward of 20°.

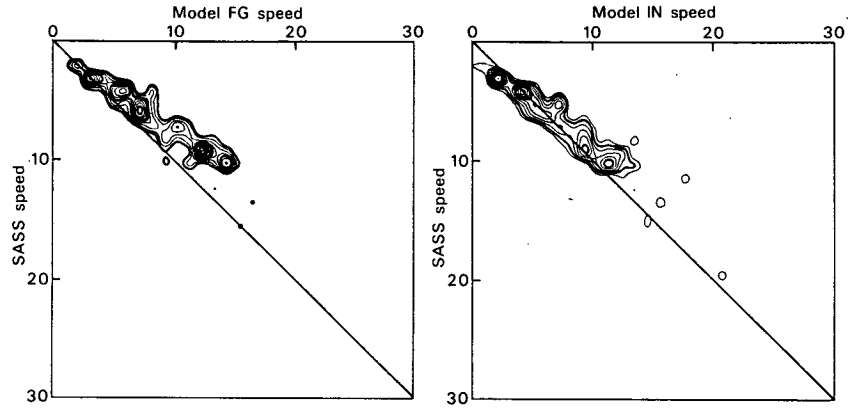

Fig. 3.7 As for Fig. 3.6 but poleward of 45°N.

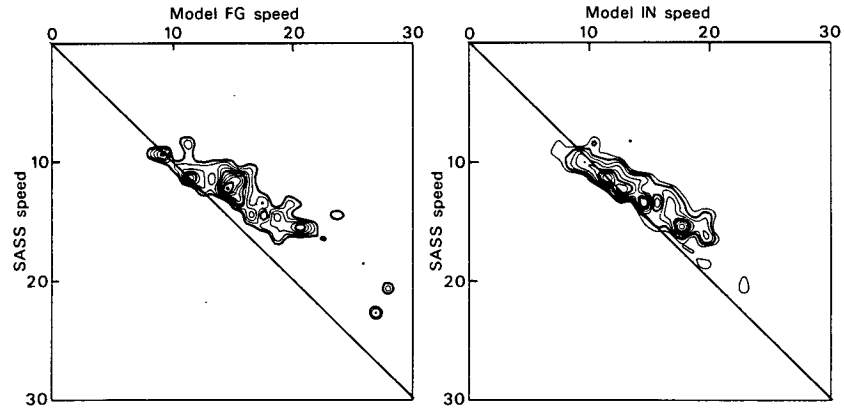

Fig. 3.8 As for Fig. 3.6 but poleward of 45°S.

The positive bias at low speeds is evident (in low latitudes) in 3.6, but not so clearly in high latitudes in 3.7 or 3.8. All Figs show negative bias at high speeds, but the magnitude of the bias differs. For a model FG speed of 12m/s, the most probable SASS speed in Fig. 3.7 is 9.5 m/s while in Fig. 3.8 it is 11.5 m/s. This difference could result from geographical model bias. If the SASS speed bias is the same in both hemispheres, then the difference could result from the forecast model winds being biased high in the NH relative to those in the SH. The difference could also result from factors not contained in the SASS model function.

and Fig. 3.5 the SH case. In both, at high wind speeds SASS speeds are low compared with the atmospheric model. This same tendency is evident in the equatorial band (Fig. 3.6). The speed bias at low wind speeds is also evident on Figs. 3.3 - 3.6 inc.

The SASS coverage, being global gives the opportunity of comparisons in different parts of the globe. For example, Figs. 3.7 and 3.8 show the speed histograms, polewards of 45°N and 45°S respectively. A difference in mean speed between the two regions resulting from seasonal as well as geographical differences is to be expected, and so the histograms look rather different, with the SH having much stronger winds. The point of interest is that for both Fig. 3.7 and 3.8, the collocation shows a high speed bias of the model relative to SASS i.e. the line of maximum probability is not at 45°. In the NH, at a model speed of 12 m/s, the SASS measured speed is ~ 9 m/s, i.e. biased quite strongly low. By contrast in the SH, the equivalent SASS-measured speed is ~ 11.5 m/s, biased a little low but 2.5 m/s higher than its NH counterpart. This could indicate some problem with the forecast model. Alternatively, it could indicate that the SASS measurements are subject to some other effects not included in the SASS-1 model function. Examples include the possibility of a greater abundance of surface film in the NH than in the SH, or a greater influence of non local waves (swell) in the SH. The latter effect is addressed by comparing wave models with altimeter data to give a further estimate of the accuracy of the model winds in Part II of this report. Spatial plots of the average difference between SASS and model FG and IN are also informative (Hollingsworth et al. 1986).

Figs. 3.3 to 3.8 also show the collocation comparison of the SASS with model analysis (panel b). Comparison with panel a shows the influence the SASS has on the first guess (FG) during analysis. The analysed winds now fit the SASS data better but not perfectly: there remains a high speed bias.

This can be clearly seen on Fig. 3.9a when first-guess (FG) speeds and analysed (initialised) speeds are plotted against SASS speed for the AESASS experiment on 11 September at 6Z. This figure clearly shows that compared with the model FG speed, SASS is low at high wind speeds. In fact, the difference is quite comparable to that found on Fig. 2.1a. For example the difference between SASS and FG at a model FG speed of 25 m/s is ~ 8 m/s, while

the difference between SASS and ship at a ship speed of 25 m/s is ~ 9 m/s. The assimilation of SASS data slows down the model speeds so that the difference between SASS and initialised wind speeds is ~ 6 m/s at a model speed of 25 m/s. Two further points should be noted:

(1) the point at which SASS speeds agree with the forecast model is ~ 5 m/s, considerably lower than the cross over point of Fig. 2.1a which is above 10 m/s.

(ii) For high model speeds (> 22 m/s), it would appear that the SASS data is saturating - SASS speeds in excess of 18 m/s being rare at least on this occasion. Further, the analysis can not adjust to this low bias and the fit of SASS to IN is also particularly flat.

In Fig. 3.9b, SASS speeds are compared to first guess and initialised speeds from the NOSASS experiment for 6Z on the 11 September. The agreement is very similar to that between SASS and FG in the AESASS experiment. Analysis does not improve the fit to the data, in the case of Fig. 3.9b.

Another way of displaying the influence of the SASS on the assimilation is shown in Fig. 3.10a for 3 latitude bands, polewards of 30°N (left), the tropical band (central) and the southern ocean polewards of 30°S (right). In this figure, the frequency of a given wind speed departure of the zonal wind is plotted against the magnitude of the departure from the first-guess and from the initialised AESASS analysis. After analysis, the histogram is much sharper in all cases showing that the analysis has drawn to the data. For comparison, a similar figure is shown in Fig. 3.10c for the NOSASS experiment, showing that the fit to SASS data in this experiment is no better after analysis than before, implying that the improvement in fit of Fig. 3.10a results from the influence of the SASS data itself. For comparison, with Fig. 3.10a, Fig. 3.10d, shows the fit before and after assimilating ship data: there is little improvement in the rms fit after analysis in the case of ships in contrast to the fit to SASS which does improve. Fig. 3.10e shows a histogram for 6Z on the 11 September. The purpose of this diagram is to show that quite skewed histograms do occur. The SASS data and the model first guess are in disagreement at this time, by 25 m/s in some places.

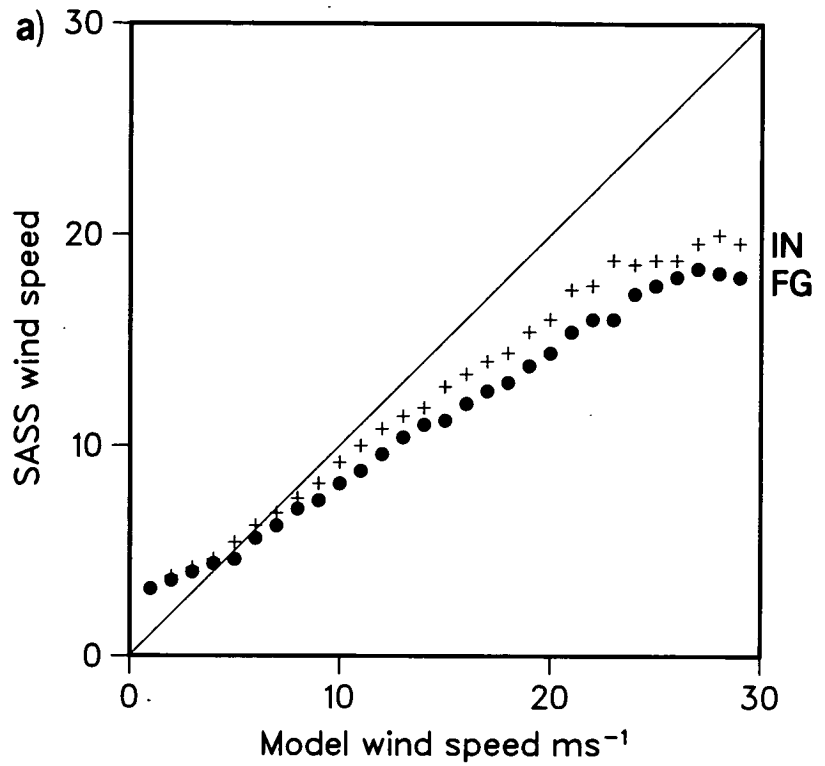

Fig. 3.9a Comparison of SASS speed with model first guess and initialised analysis (IN) for 6Z on 11th September from the AESASS experiment. This figure shows a large bias between SASS and FG comparable to that of Fig. 2.1 at high speeds. There is also a low speed bias.

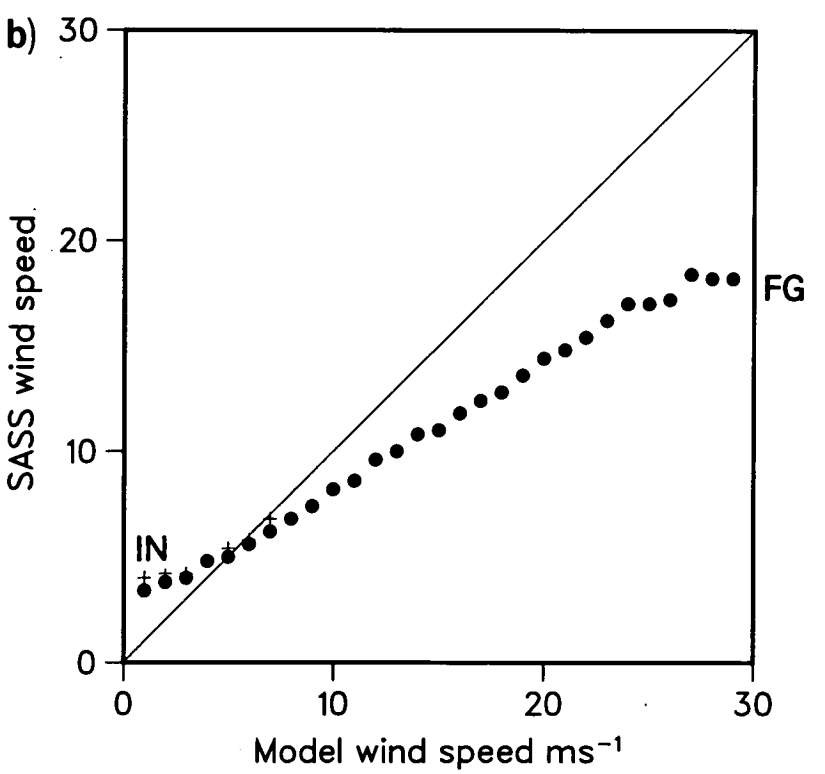

Fig. 3.9b Comparison of SASS speed with first guess and initialised analysis for the same time as 3.9a, but from the NOSASS experiment.

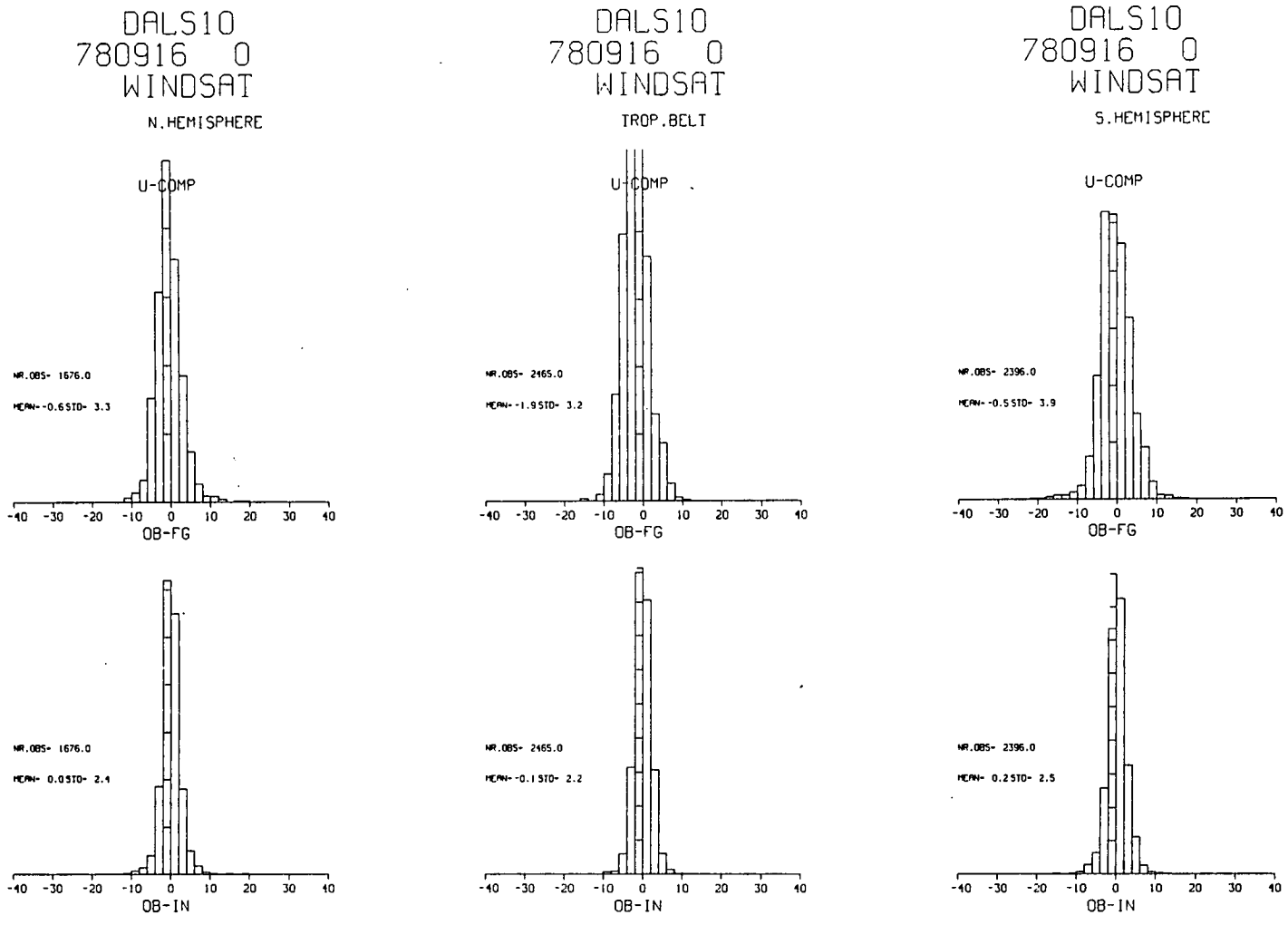

Fig. 3.10a Histogram of departures of SASS zonal wind component from model wind at 10 m for the AESASS assimilation FG (upper) and initialised analysis (lower). In all three regions, NH poleward of 20°, tropics, and SH poleward of 20°, the histograms are sharper after assimilation showing the extent to which the data is used. The tropical wind is frequently biased with respect to the FG (model stronger than SASS) but this is removed by the analysis.

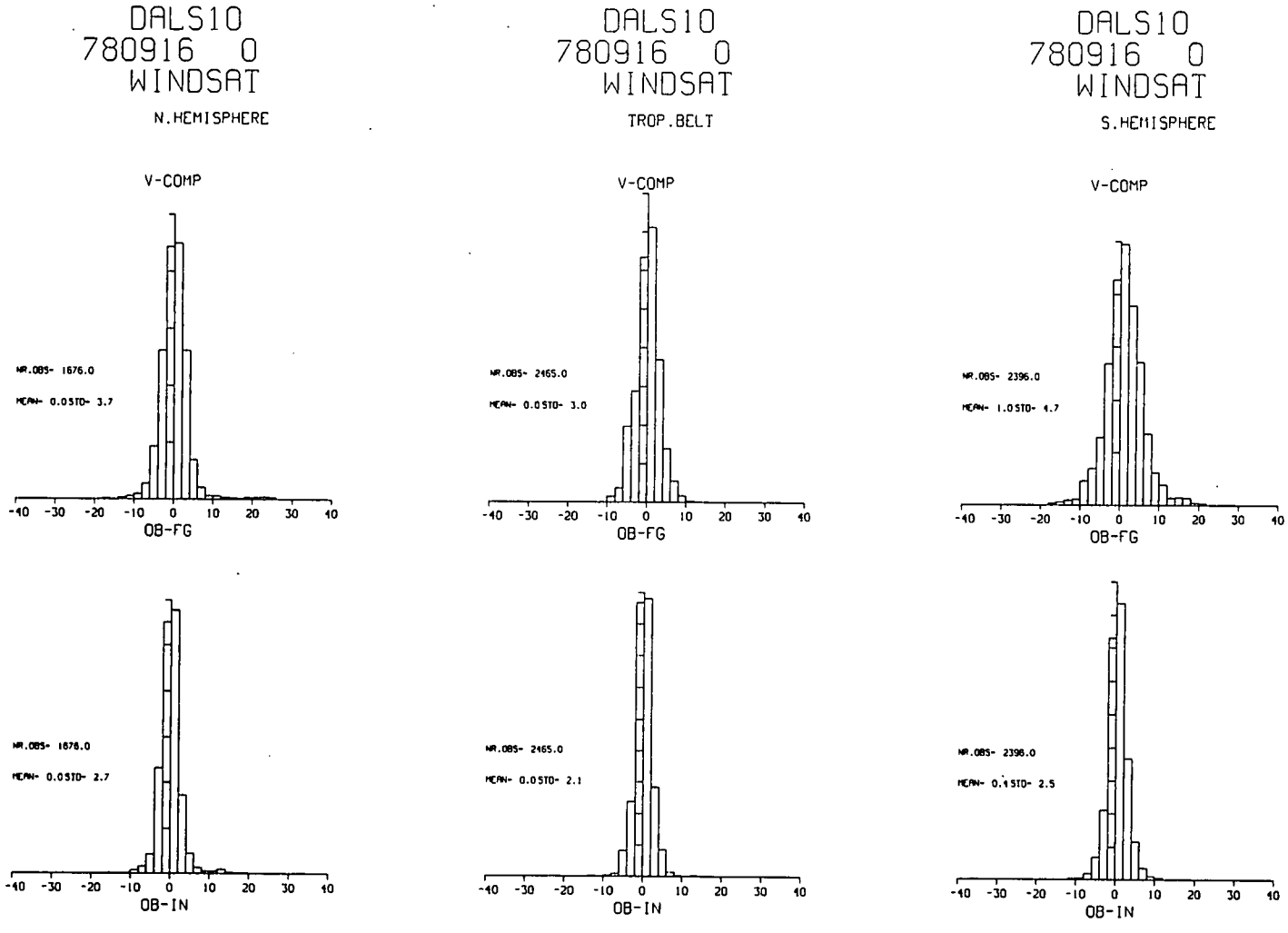

Fig. 3.10b As for 3.10a but for the meridional wind component.

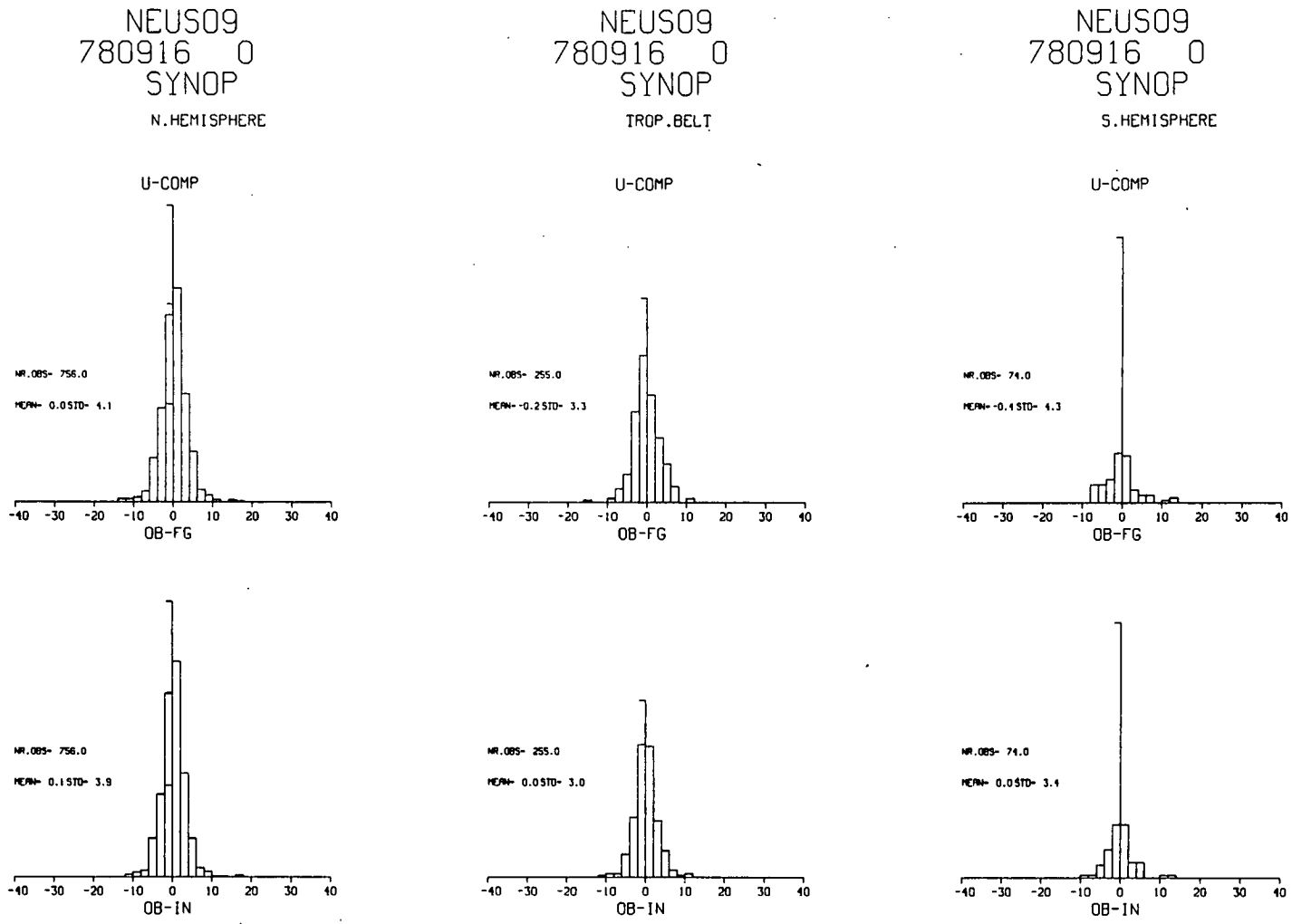

Fig. 3.10c As for 3.10a but for the NOSASS analysis.

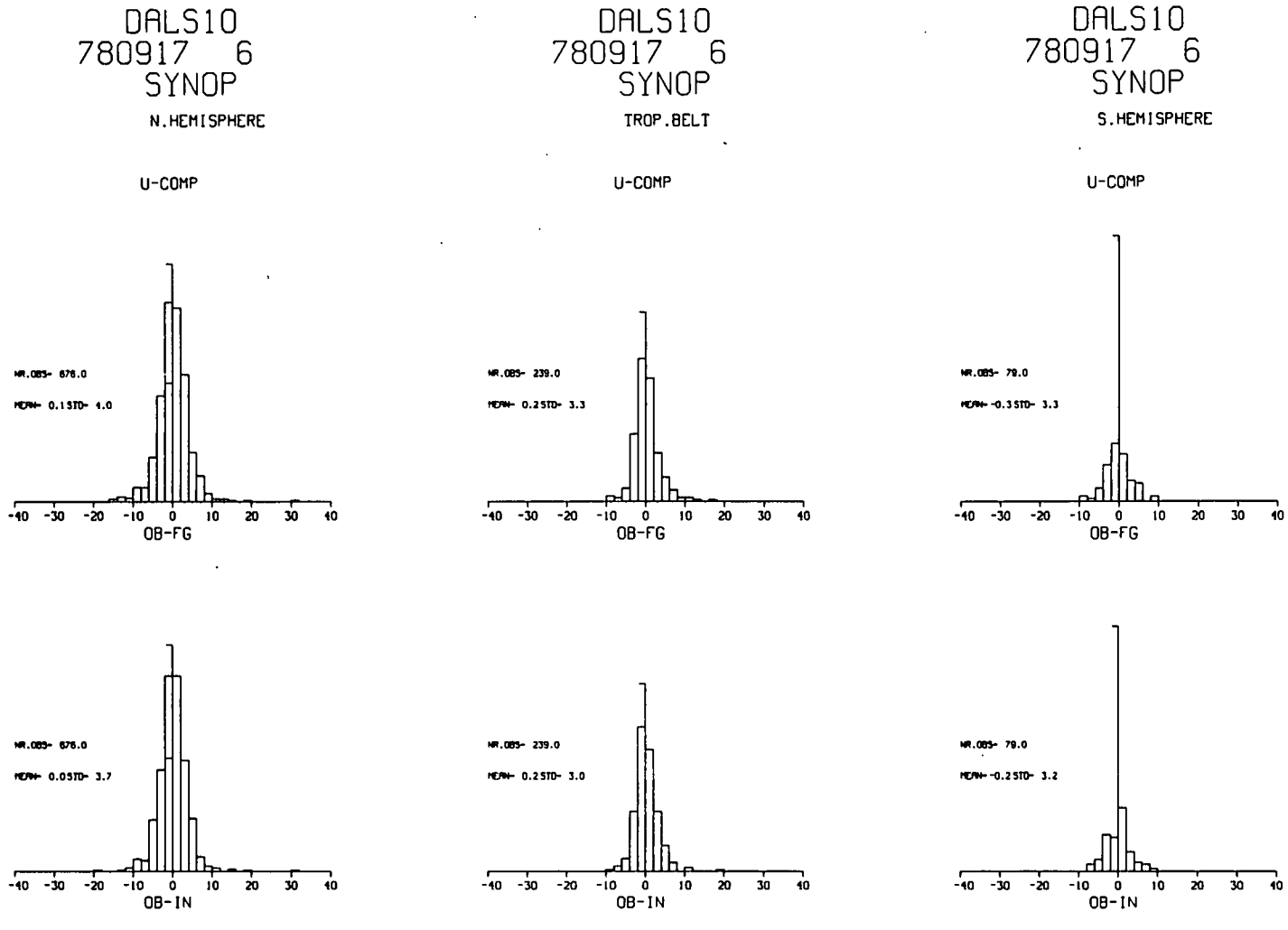

Fig. 3.10d As for 3.10a but for ships.

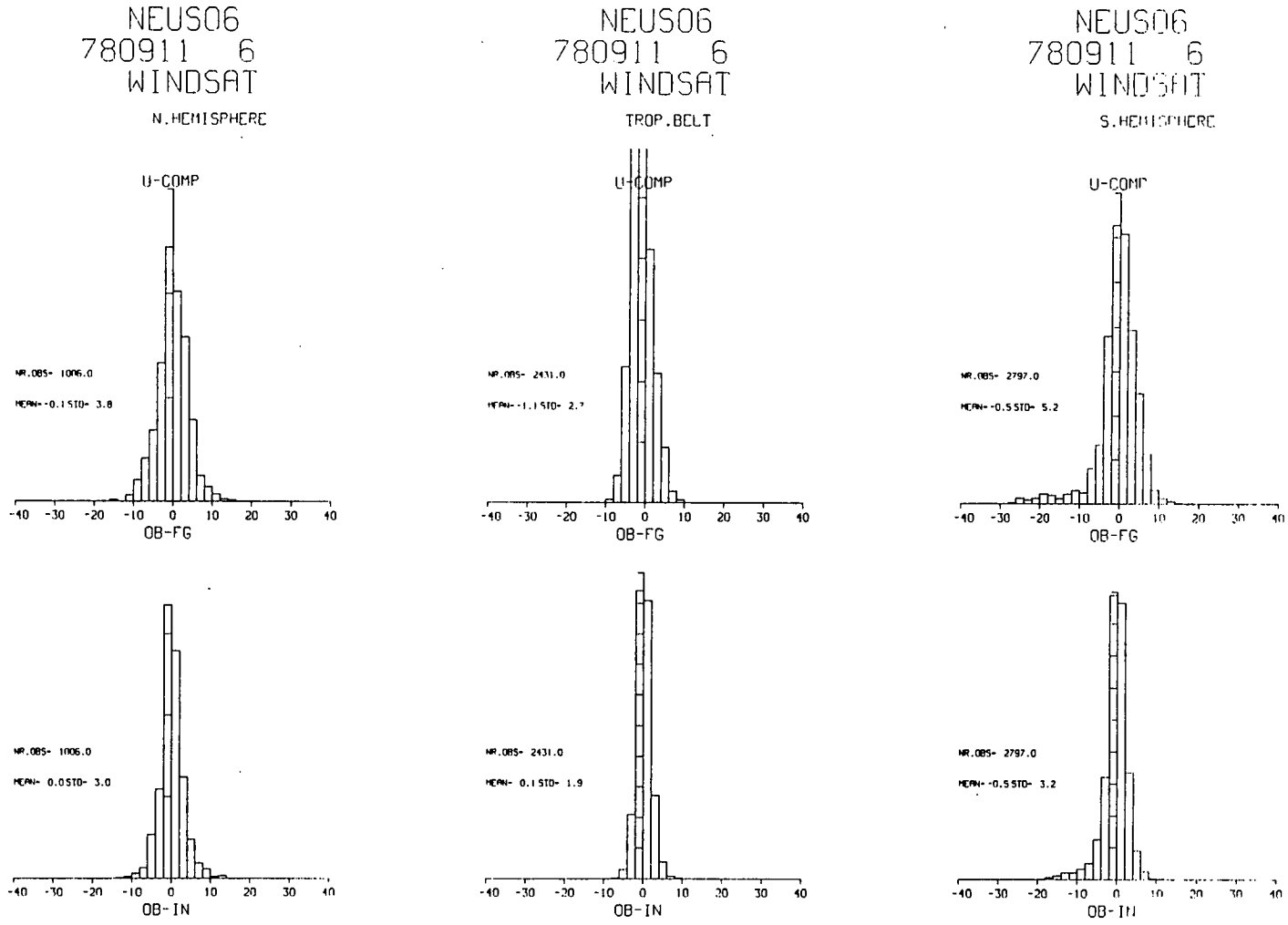

Fig. 3.10e As for 3.10a but at a different time to show that the histogram is sometimes skewed. This indicates a major difference between SASS and first guess at this time, largely but not completely corrected by the analysis.

A comparison of the mean of the departures (i.e. bias) shows that there is only a small bias when averaged over all speeds in both northern and southern hemisphere. (In the Northern Hemisphere it is usually negative i.e. the first guess has higher mean speed, but less than 1 m/s. In the Southern Hemisphere it can be of either sign but is again usually less than 1 m/s).

In the tropics, by contrast, the bias is larger (usually between 1 m/s and 2 m/s) and is always negative. (FG stronger than SASS). This is despite the fact that SASS is biased high at low wind speeds. The fact that it is biased low with respect to the model at intermediate wind speeds dominates the low wind speed bias since most data correspond to the trades with speeds of order 8-10 m/s. The fit to the meridional component of velocity is shown in Fig. 3.10b. The speed bias in the tropics in the meridional velocity component is less than in the zonal component. The reasons for this merit study but the question has not be pursued.

3.4.1.2 Dependence of speed bias on incidence angle

As noted earlier, the main assimilation experiments used data from the short SASS tape for which azimuth and incidence angles are not available. A short assimilation experiment (ALINOS) was run with data extracted from the extended SASS tape and including azimuth and incidence angle information. The results from the ALINOS assimilation are discussed here.

In 2.1.3 it was noted that when SASS speed was collocated with ship speed, there was a suggestion (Figs. 2.4a-e) that the outer incidence angles were less accurate than the inner and middle incidences, at both low and high wind speeds, but the results were tentative because of the paucity of collocations at high ship speeds. When collocating with the model, a collocation is possible for every SASS report, so the number of collocations increases, which is a great advantage. Table 3.1 gives mean differences between SASS and model FG for speeds greater than cut offs of 16, 20 and 24 m/s, and in brackets the number of collocations. The same incidence bands as for Figs. 2.4a-e are used. No separation has been made for hemisphere or latitude so the numbers probably are most influenced by the Southern Hemisphere westerlies. Based on this table, there is some evidence to suggest that the outer incidence band has a greater speed bias than the mid and inner incidence bands and that the

mid incidence angle is more accurate. One should bear in mind that although the number of 'collocations' is quite large only a 'snap-shot' view is being sampled, and not enough synoptic events are being sampled, so this comparison should really extend over a few days. The magnitude of the difference between model and SASS could reflect an error in either SASS or model or both, but the nature of the dependence on incidence angle (if any) should be independent of meteorological model error. For this reason the dependence on incidence angle is most probably due to the instrument or the wind retrieval algorithm.

Minimum speed / Incidence angle	16 m/s	20 m/s	24 m/s
18 - 25	6.3 (335)	7.5 (157)	8.5 (60)
25 - 35	6.1 (410)	7.4 (185)	9.1 (77)
35 - 45	5.8 (423)	7.1 (189)	8.8 (66)
45 - 55	6.2 (964)	7.8 (431)	9.4 (182)
55 - 65	6.4 (213)	8.2 (106)	10.3 (47)

Table 3.1

Mean speed difference between SASS speeds and model FG speed as a function of incidence angle. In calculating the differences, all deviations above the minimum model speeds noted, are used. The number in brackets give the number of collocations. Data for 12Z on 10th September from ALINOS.

3.4.2 Angular comparison

Fig. 3.11 is a contour plot of SASS angle v model FG angle for incidence angles between 25° and 35° when angles are measured relative to azimuth. This figure exhibits clustering with gaps at 180°, 270° as well as at 90°. This clustering was also noted in connection with collocated ship reports (Section 2.2). Fig. 3.11 is based on data for only the time 12Z on 10th September. If angles were measured relative to north, clustering would still occur because not all wind directions would be uniformly sampled. But on different realisations the clustering moves around whereas it does not when angles are measured relative to azimuth. Together with the results of Section 2.2, Fig. 3.11 strongly suggests that the error lies in the SASS retrievals.

3.4.3 Long term adjustment of analysis to the data

In the AESASS experiment, SASS data is supplied every 6 hours to the analysis. One might expect that after some time the FG and analyses of the AESASS experiment will fit the SASS data better than those from the NOSASS experiment. In Fig. 3.12a the rms error of fit of the FG and analysis is plotted for the Northern Hemisphere, tropics and Southern Hemisphere for the last 9 analyses (2¼ days) of the AESASS experiment. The shaded region indicates the fit to the analysis, the unshaded bars the fit to the FG for the zonal component of velocity. (Fig. 3.10a corresponds to time 2 of Fig. 3.12). Figure 3.12a should be compared with Fig. 3.12b which corresponds to the NOSASS experiment. For the Northern Hemisphere, the fit of the SASS data to the NOSASS FG is slightly worse than the fit to the FG from the AESASS experiment of Fig. 3.12a. The differences however are small, corresponding to almost no statistical improvement. In the tropics, the AESASS FG always fits the SASS data better than the NOSASS FG with an improvement of ~ 1m/s (Taking the square root of the difference of the square of the average rms values).

In the SH, the effect is larger: the mean rms fit to the FG drops from 4.44 m/s in the NOSASS experiment to 4.18 m/s in the AESASS experiment. This implies that there has been an improvement of $(1.5\ m/s)^2$ in the FG error variance in the case where SASS is used over that when it is not used.

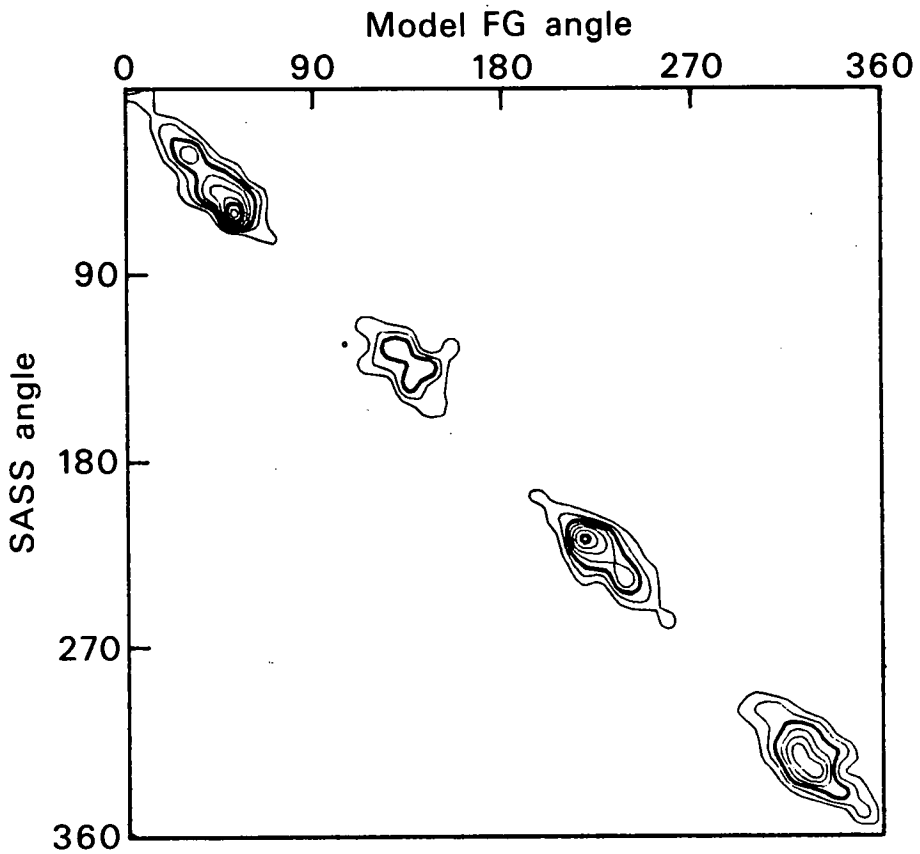

Fig. 3.11 Contour plot of frequency of occurrence of SASS direction v model FG direction. Both directions are relative to azimuth. Only data from a single synoptic time September 10, 12 UTC ± 3 hours from the ALINOS experiment is compared. The incidence angle is between 25 and 35°.

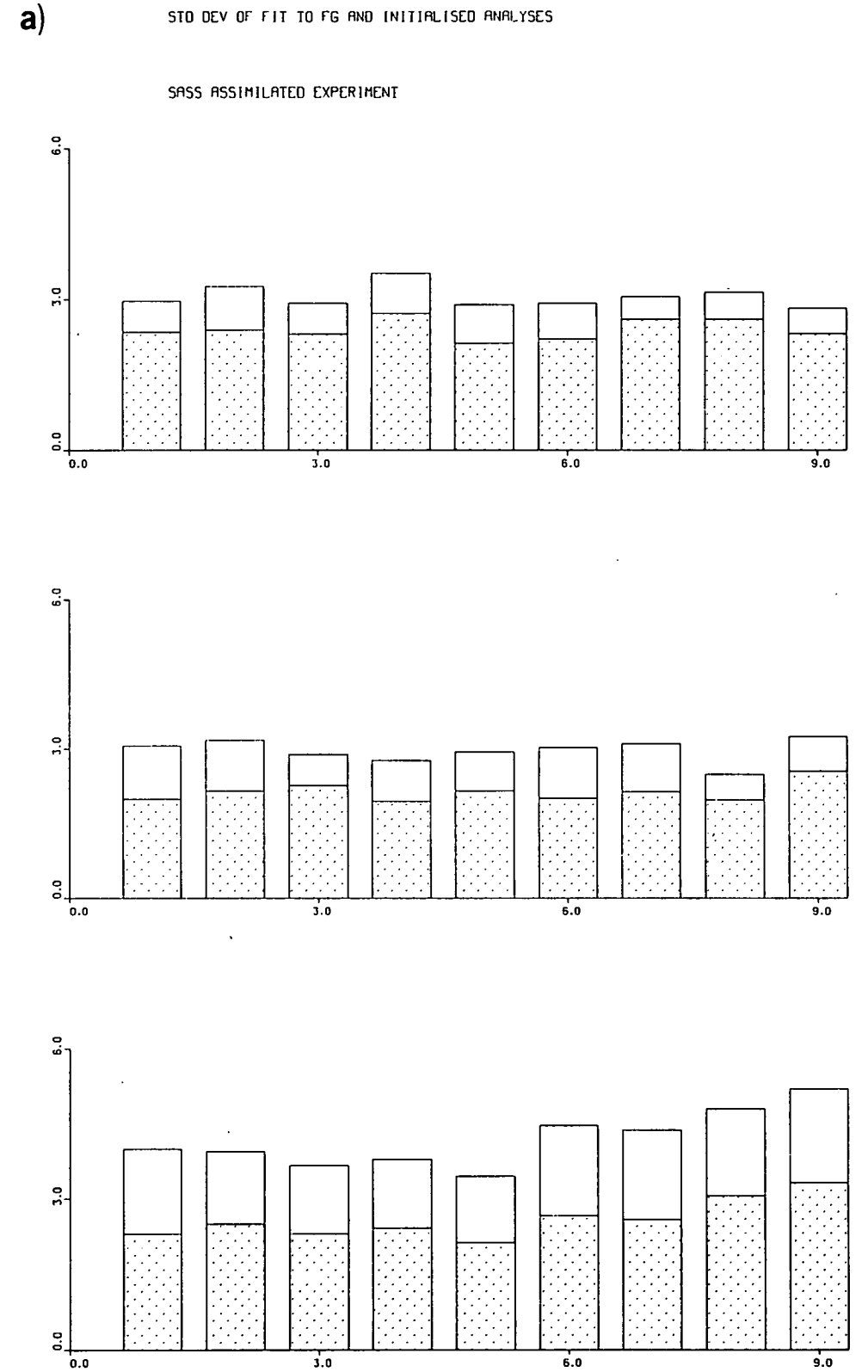

Fig. 3.12a Rms fit of SASS data to AESASS FG (no shading) and AESASS initialised analyses IN (shaded) for the last 2¼ days of the AESASS assimilation. The upper panel is for NH poleward of 20°N, middle panel for the tropics equatorward of 20°, and lower panel for the SH poleward of 20°S.

This figure shows the improvements of fit to the SASS after analysis. It is largest in the SH.

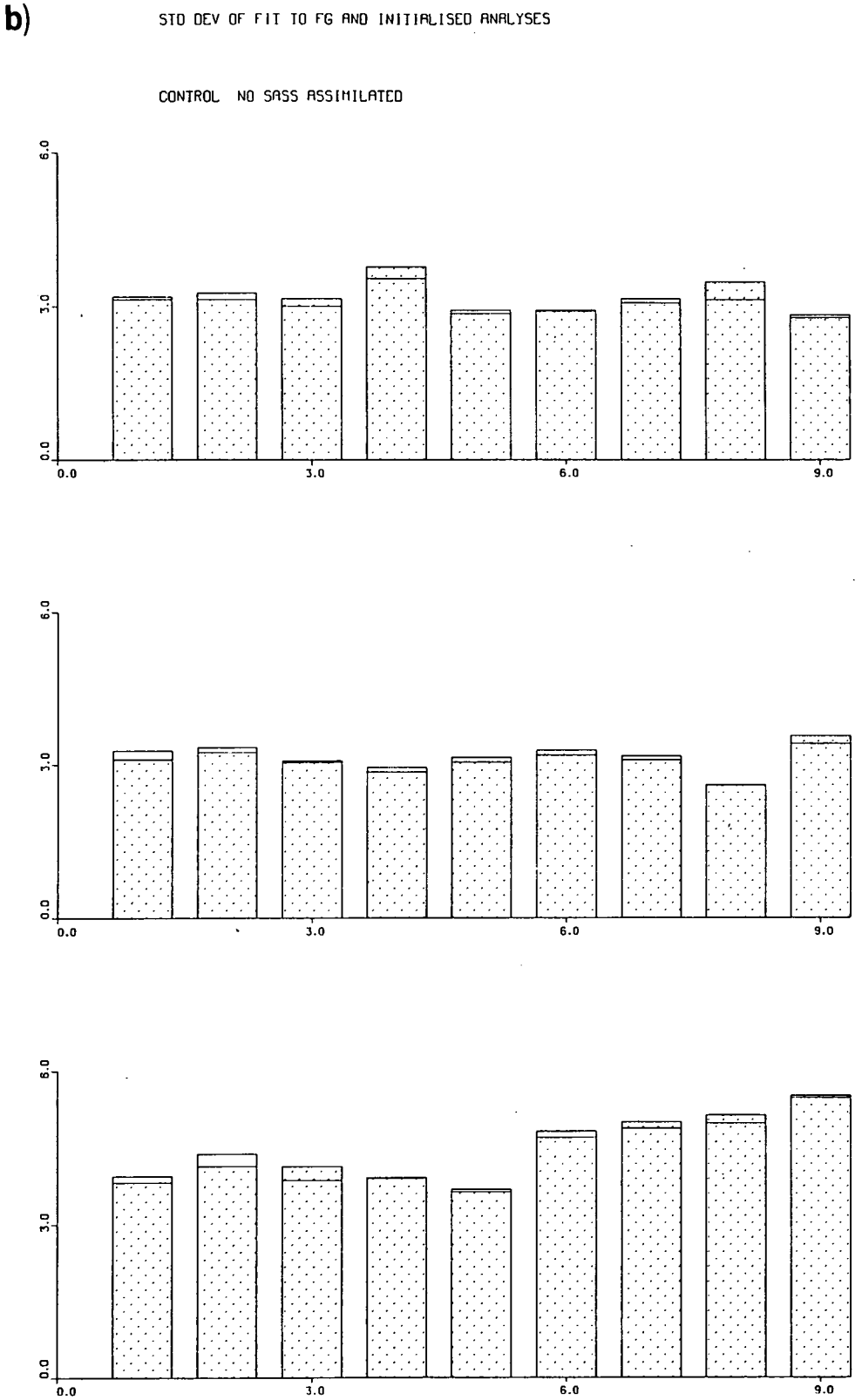

Fig. 3.12b As for a but for the NOSASS assimilation. Comparison with (a) for the NH shows that the SASS fits the FG from the AESASS case only marginally better than the NOSASS i.e. there is little memory in a statistical sense of the fact that SASS data has been assimilated for some 10 days previously. However, in the tropics and SH the SASS data fits the AESASS FG's better than it does the FG from the NOSASS. In the NOSASS case, the fit of the SASS to the initialised field may be better or worse than the fit to the FG.

4. Analysis and Forecast Studies with SASS Data

4.1 Introduction

Satellite-borne instruments have the potential of filling the gaps in the observation network. This is especially true in the Southern Hemisphere, but it is also true that in the Northern Hemisphere the conventional observation network, particularly over the oceans has significant gaps on any observing period (see Fig. A1). In this section we will consider the impact of SASS data first on analyses and then on forecasts from those analyses. If there is no impact on the analyses, there will be no impact on the forecast, but the reverse is not necessarily true. Further, changes in the analyses as a result of assimilating SASS data need not lead to improved forecasts.

In view of earlier studies (Baker et al., 1984; Yu and McPherson, 1984) it is likely, especially in the mid latitude northern hemisphere, that the observation network is able to identify the large scale structure. The impact of SASS on forecasts is therefore likely to be intermittent, having little impact much of the time, but perhaps having noticeable impact on those occasions when other observations fail to resolve a feature but SASS does. The results however are also likely to depend on the procedures used for assimilating the data.

The first SASS analysis and forecast impact studies were conducted manually by a team of meteorological analysts from the Atmospheric Environment Service (AES - Canada), NOAA-PMEL, UCLA, and JPL, led by Dr. Steven Peteherych (1981a, 1981b). Marine surface pressure analyses that included the influence of SASS wind data with conventionally available data were made in an operational environment at the AES regional forecast centres in Vancouver and Halifax. Comparisons were made of these surface analyses (using SASS data) with operational surface pressure analyses using conventional data only. The studies showed that the inclusion of SASS data in the analyses resulted in more accurate placement of significant meteorological features, e.g. storms, fronts, and other strong wind regions, and that in 75 percent of the case studies, it was judged that significant marine forecast improvements were made -- in particular, that for the storm that resulted in damage to the ocean liner Queen Elizabeth II (QEII).

Only a few groups (e.g. Atlas et al., 1984, Baker et al., 1984, Duffy et al., 1984, Yu and McPherson, 1984) have performed global numerical weather prediction (NWP) model experiments to study whether the assimilation of the single-level high-resolution measurements from the satellite-borne SEASAT scatterometer, which provides global measurements of the surface wind field, could positively impact numerical prediction capability. Duffy and Atlas (1986) noted that these studies essentially showed that 72-hour forecasts made from initial conditions that included Seasat surface winds were not significantly better than 72-hour forecasts where Seasat scatterometer (SASS) wind data had been excluded.

For their NOAA-NMC global NWP model experiment, Yu and McPherson (1984) assimilated SASS data for only 48 hours and conducted only one 72-hour NMC forecast for the July 1978 period. They cycled 3 successive passes through the SASS wind data in their scheme for objectively dealiasing the SASS data, i.e., they dealiased the SASS data in three successive passes beginning with the 2-direction measurements, then the 3-direction ones, and finally they removed the ambiguities from measurements with 4-direction solutions. In addition, they employed an empirical vertical correlation function (Bergman, 1979) to link the influence of the surface wind field to the lower layers of their model. They found large differences in the Southern Hemisphere for the single 72-hour forecast between wind and height analysis with and without assimilating SASS wind data, but the paucity of observations made quantitative verification impossible.

Baker et al. (1984), Atlas et al. (1984), and Duffy et al. (1984) performed forecast impact studies utilizing about one week of SASS data. Baker et al. and Atlas et al. utilized the NASA-GSFC-GLA fourth-order NWP model with a 4° by 5° latitude/longitude resolution grid, while Duffy et al. performed their experiments with a 2.4° by 3° latitude/longitude grid operational forecast model called NOGAPS (Navy's Operational Global Atmospheric Prediction System -- essentially the UCLA GCM, see Arakawa and Lamb, 1977) used by the U.S. Navy. Both the NASA-GSFC-GLA and NOGAPS SASS impact studies used the SASS wind data objectively dealiased during the assimilation cycles for the NASA GSFC-GLA experiment that picked SASS directions closest to the 4° by 5° grid wind directions of the first-guess wind field with a 3-pass-scheme similar to that of Yu and McPherson. Essentially, the only "new" independent information introduced during the assimilation cycle from SASS were the SASS speeds for

all the three global experiments cited above since the 2-direction-solution SASS measurements only comprise about six percent of the total. Duffy et al. concluded that "The objective verifications show that SASS data had a small effect on forecasts made from the Navy's NOGAPS model." They further concluded that this was true in both the northern and southern hemispheres in agreement with the results of Yu and McPherson (1984) and Baker et al. (1984).

In the NOGAPS experiment the surface winds were never used directly in the analysis -- the NOGAPS system itself sees only the surface pressure field. The difficulty experienced by Duffy et al. was complicated by the fact that Navy's sea level pressure analysis was not readily available to them, so they substituted the NASA-GSFC-GLA sea level pressure analysis program (a three-pass Cressman successive correction scheme described by Baker et al., 1984) in their NOGAPS/SASS experiment.

In the NASA-GSFC-GLA experiment to examine the usefulness of SASS data, Baker et al. noted that, even in the Southern Hemisphere, the positive impact of SASS data was only evident if the VTPR temperature soundings from the polar orbiter were excluded from the observational database. This suggested some redundancy between the two data sets with regard to their individual positive impacts on Southern Hemisphere forecasts.

Unlike the above experiments that studied the usefulness of SASS data in global NWP models, several investigators (Anthes et al., 1983, Aune and Warner, 1983, and more recently Duffy and Atlas, 1986) used SASS wind data in limited-area numerical studies of the Queen Elizabeth II (QEII) storm for the period September 8-10, 1978. Several operational NWP models failed to predict the intensification and explosive development of this storm in which the QEII suffered damage and in which the fishing trawler Captain Cosmos was lost. The numerical experiments of Anthes et al. and Aune and Warner used the coarse-grid (4° by 5° lat/long) objectively-dealiased SASS data produced by NASA-GSFC-GLA. The latter found the impact of the SEASAT data to be small. In contrast, the numerical experiment by Duffy and Atlas (1986) showed that the inclusion of SASS data in the lowest level of the model (1000 mb) did have some effect on the cyclogenesis and the predicted central pressure of the QEII storm. The latter study differed from the Anthes and Aune and Warner studies in two important respects. First, the SASS data set utilized by Duffy and

Atlas was dealiased by analysts as described by Baker et al. (1984), and Wurtele et al. (1982) (and corresponds to the dataset used in this report). More importantly, however they allowed the corrections to the surface wind by the SASS measurements during the assimilation to influence the upper level wind through the use of an empirical vertical correlation function (see Bergman, 1979) following Yu and McPherson (1984). When the analyst-dealiased SASS data were included at the lowest level without the ad hoc incorporation of the vertical correlation function, the prediction was virtually unaffected.

4.2 Synoptic Impact of SASS on analysis

4.2.1 Differences between AESASS and NOSASS analyses

In Fig. 4.1 the difference between analysis from the NOSASS and AESASS assimilation experiments are shown for 12UTC on September 9, 10 and 16. Differences for both 1000 mb wind and the height of the 1000 mb surface are shown. North of 20°N, differences are usually small, but can be as large as 10 m/s (for example 12UTC on the 10th or 12UTC on the 16th). The spatial scale of the changes is usually quite small, despite the fact that the analysis will act to damp small scale features. [Since this was our first experimentation with scatterometer data, no special steps were taken to adapt the analysis filter to the properties of the scatterometer data. Work is underway to improve the response of the analysis on small scales. It will also be essential to determine the spatial error correlation properties of the ERS-1 data as early as possible in the lifetime of the satellite]. Some of this small scale structure could come from the model, being generated earlier in the assimilation and cascaded down scale. In the tropics also, the changes can approach 10 m/s. By contrast in the Southern Hemisphere, wind changes can be 20 m/s, and are a mixture of large and small scales. The height changes can be in excess of 135 m or (17 mb).

In Fig. 4.2, for September 9, the differences are plotted with a smaller contour interval (2 m/s as opposed to 5 m/s in Fig. 4.1) to illustrate more clearly the changes that are taking place in the tropics. Because of the speed bias (Section 2.1.2) it is not clear that these changes are necessarily beneficial. The magnitude of the change is about 2m/s. For a mean wind of 5 m/s, this can lead to a large change in stress, since stress depends

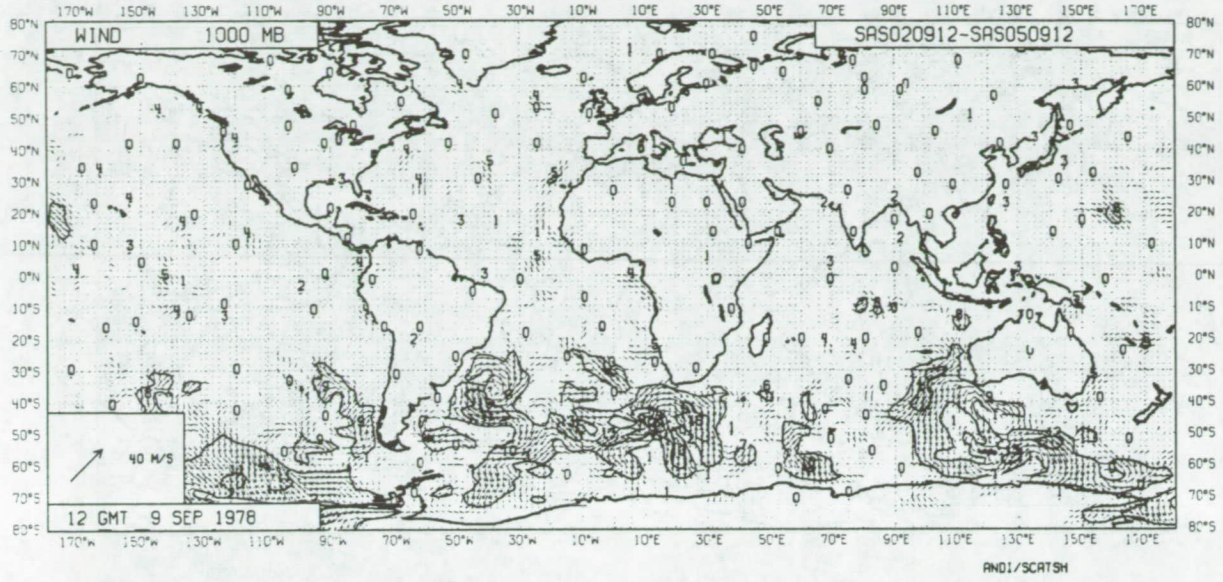

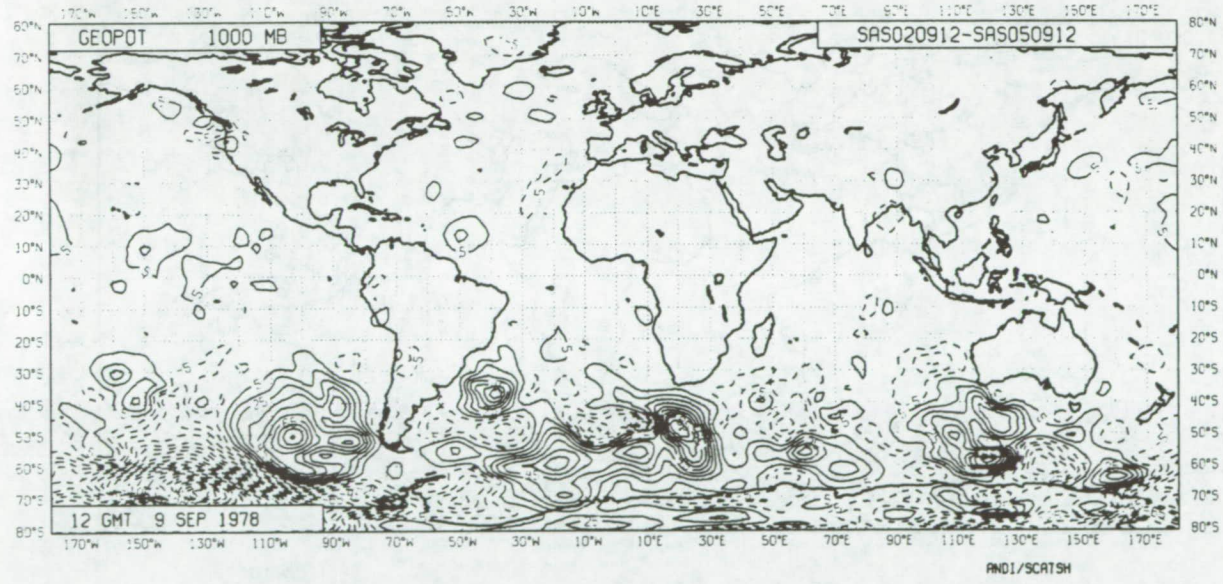

Fig. 4.1 A series of plots of differences between analyses from the NOSASS and AESASS assimilations for winds at 1000 mb (upper) and the height in metres of the 1000 mb surface (lower). In the NH and tropics differences in height are small (~10m or 1 mb) while wind changes can be up to ~10m/s. The differences are usually small scale. In the SH, by contrast both the magnitude and scale of the changes are larger. (To convert metres to mb, divide by 8).
a) September 9 1978, 12 GMT. Contour interval for speed is 5 m/s; contour interval for height is 10 m starting from ± 5 m.

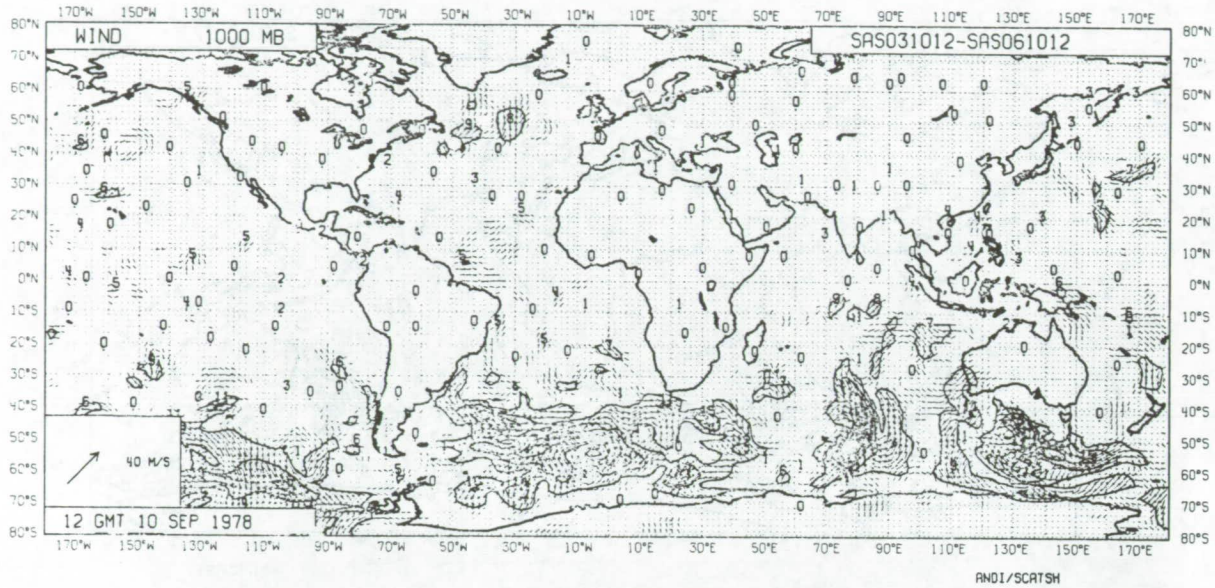

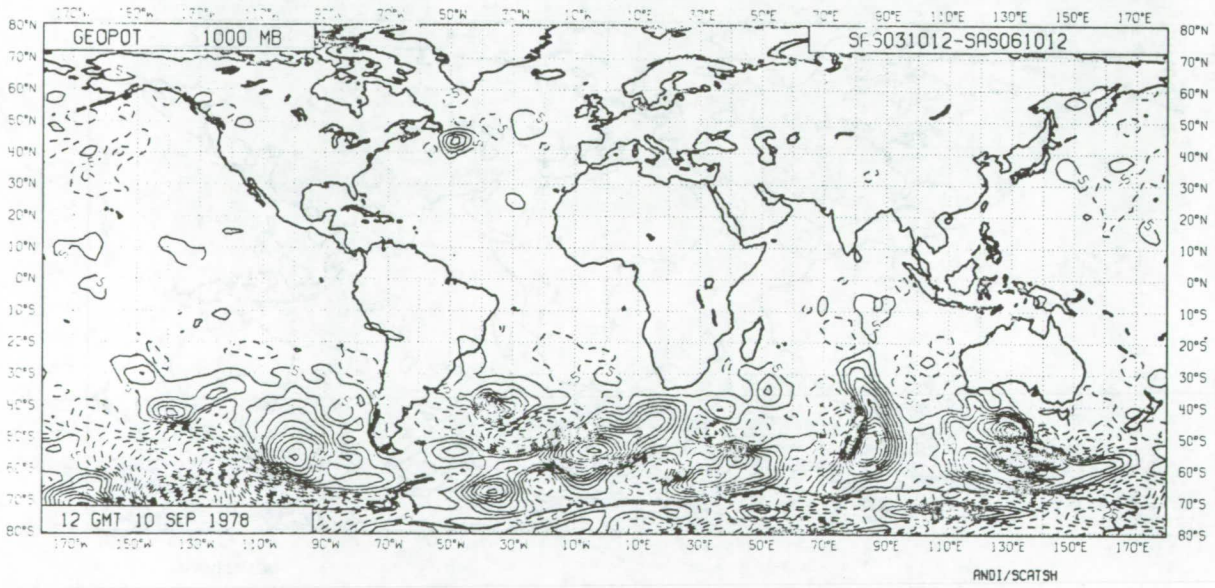

Fig. 4.1 b) September 10 1978, 12 GMT

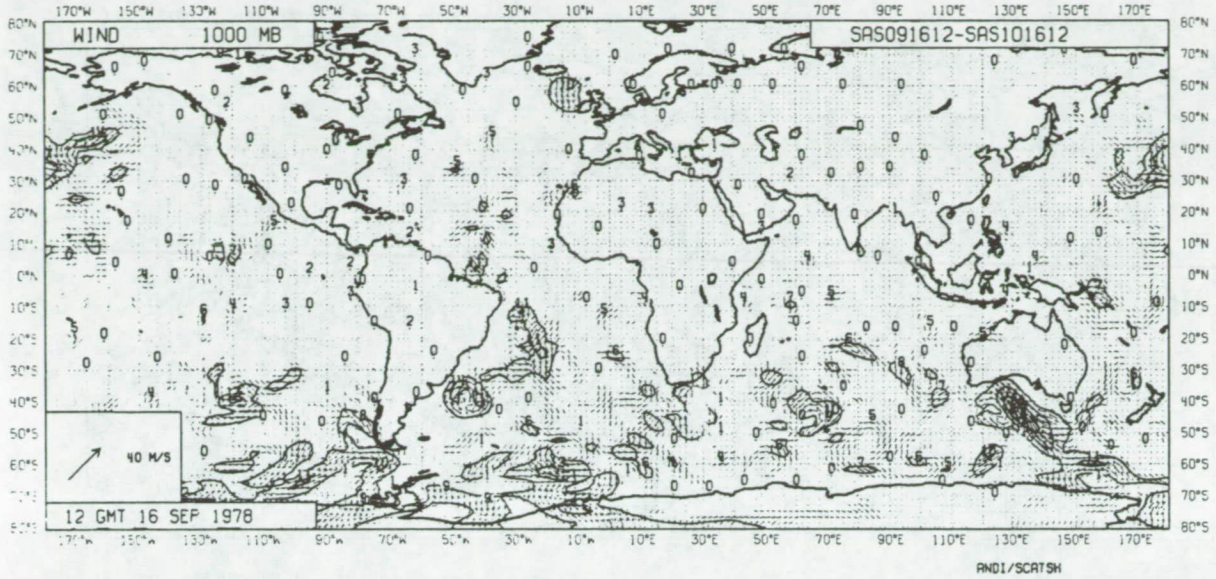

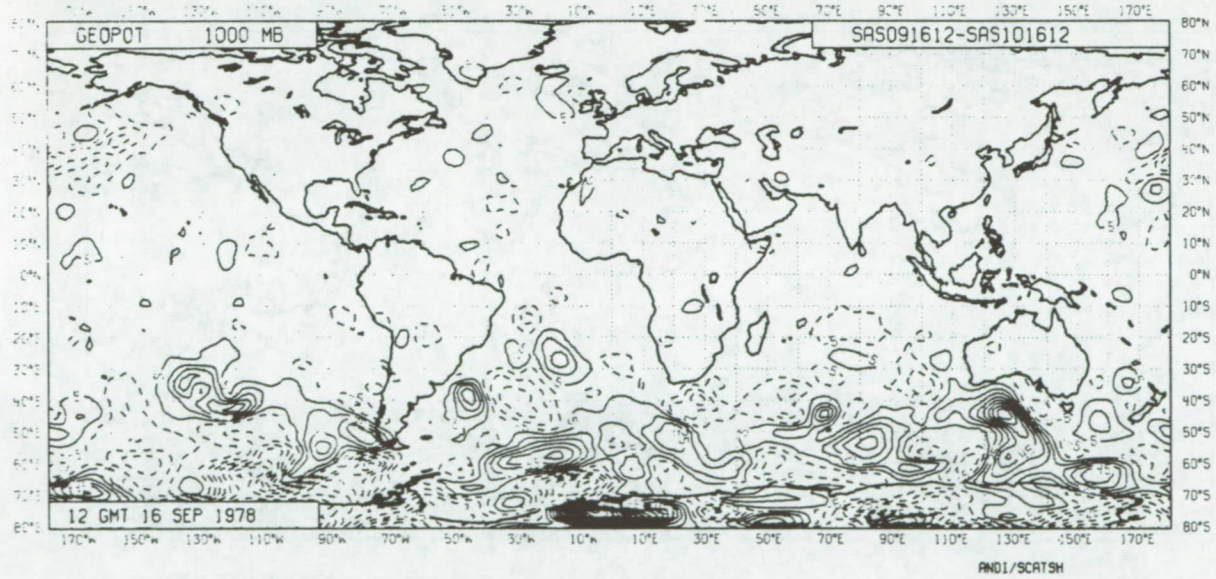

Fig. 4.1 c) September 16 1978, 12 GMT

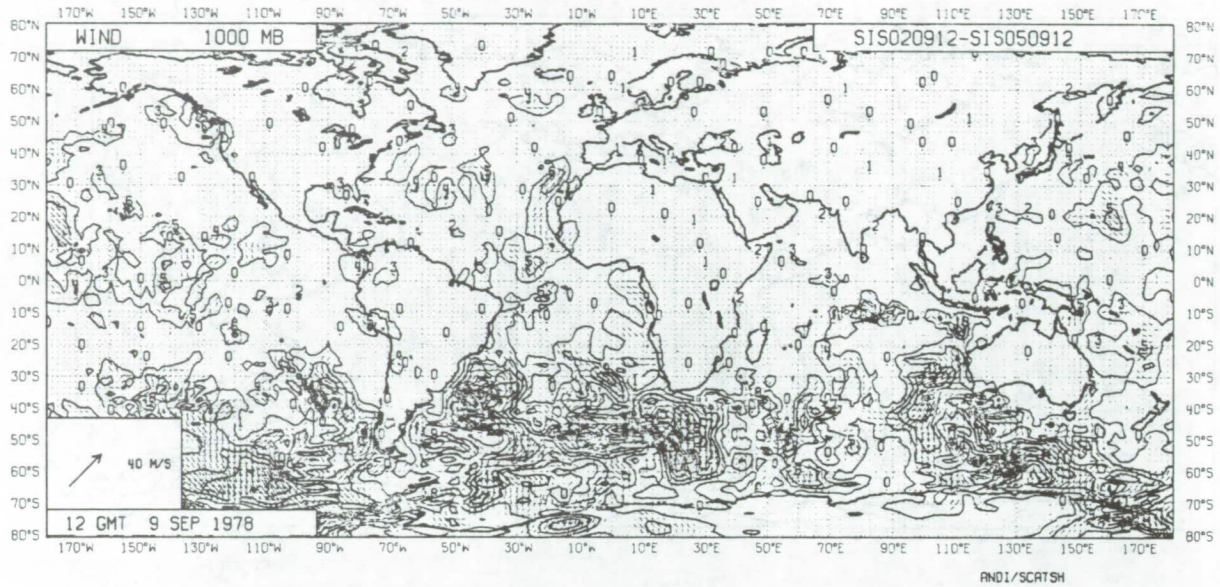

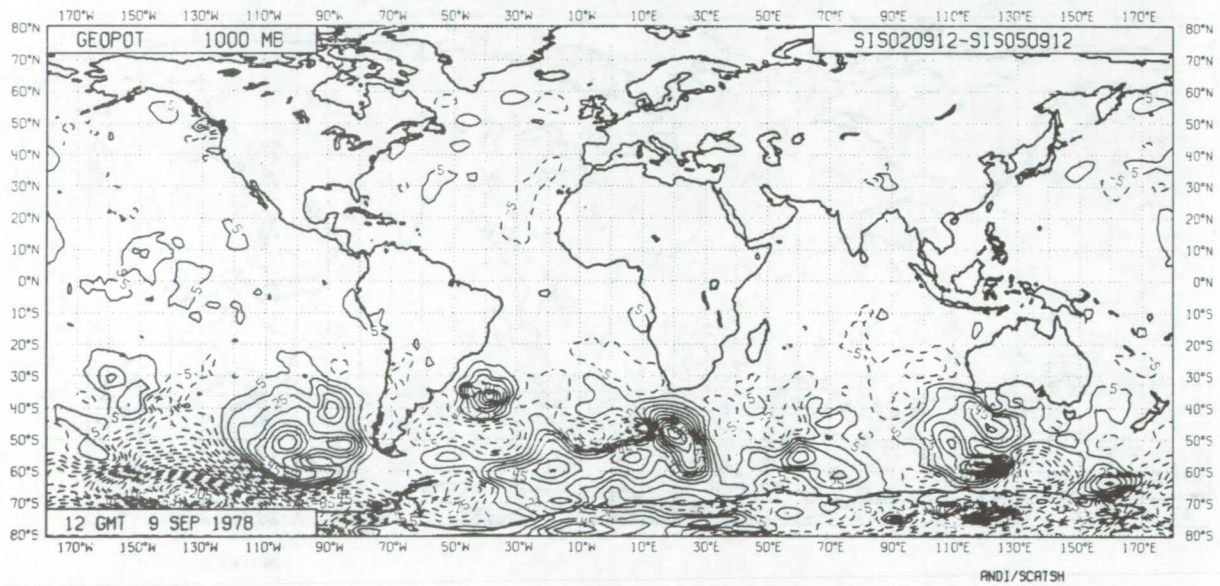

Fig. 4.2 Difference between the NOSASS and AESASS analyses for September 9 1978, 12 GMT after initialisation showing that the changes introduced by the analyses survive initialisation (c.f. Fig. 4.1a). The contour interval is 2 m/s for wind speed to show that changes are being made in the Tropics of about 2-3 m/s.

quadratically on wind speed. It is important that ERS-1 should not have a bias in low latitudes: wind stress is of crucial importance for driving ocean models for TOGA.

4.2.2 Retention of SASS data by the analysis

Fig. 4.1 illustrates differences in analyses before initialisation. It is possible that initialisation could filter out some of the changes, if the influence of SASS is projected mainly on to gravity waves and not on to planetary wave modes.

In Fig. 4.2, the differences between the NOSASS and AESASS initialised analyses for 12Z on 9th September are shown indicating that the changes in the uninitialised analyses (Fig. 4.1) do survive initialisation.

That the changes induced by SASS in fact survive for several days was further tested by an experiment AESNOS in which SASS data was supplied at the start of the experiment 06 UTC on September 6 but not subsequently. The experiment ended at 12 UTC on September 8. Analyses from the AESNOS assimilation were then compared with corresponding analyses from the NOSASS assimilation. Differences in the AESASS and NOSASS analyses in the Southern Hemisphere present at 12 UTC on September 8 can be traced back to differences in the analyses at 06 UTC on September 6. At high latitudes of the Southern Hemisphere, the amplitude of disturbances in the 1000 mb height was typically only 1/3 the size of the original disturbance. If there were no other data in this region, then the analysis at 12 UTC on September 8 and a forecast to 12 UTC on September 8 from the analysis at 06 UTC on September 6 would be very similar. Differences between forecasts made from 2 different analyses do not necessarily immediately amplify. Some differences may be damped especially over the first day or two, before amplifying. If there is data, then this would also tend to prevent amplification of the differences, and if there were 'enough' data, to damp the differences. On the other hand, if the information in the SASS data was being projected mainly on to gravity waves, these would rapidly propagate and dissipate and the information in the SASS data be quickly lost. It would appear that this is not happening in the high latitudes of the Southern Hemisphere though examples can be found at lower latitudes where information is lost over the 2-day period.

4.2.3 Synoptic Examples of differences between FG, analyses and SASS

Superposition of SASS data on plots of the first guess (FG) or analysis can be useful for identifying possible inconsistencies between FG and SASS. Only a few examples can be provided, for illustration. In general, the qualitative agreement in the Northern Hemisphere is good. Fig. 4.3a illustrates a small scale cyclonic structure south east of Japan at 152°E, 23°N, which is well represented in both FG, and SASS. To the South and North however, there are several regions where the SASS winds change abruptly by 90° in a way that appears unmeteorological. The most likely source of error is the ambiguity removal procedure.

Fig. 4.3b shows the corresponding differences between the SASS winds and those of the initialised analysis (scaled up by a factor of 10). This figure shows immediately that even though the general agreement in position of the cyclonic vortex is very good, there are substantial differences between the model velocities and the SASS data (up to 7.5 m/s).

Fig. 4.4a shows the North West Atlantic analysis for 12Z on September 11. The main feature is the QEII storm, which appears well represented in both SASS data and the analysis. Fig. 4.4b however shows that differences in SASS and model velocities can be as large as 16 m/s, with differences of 3-6 m/s being common. On Fig. 4.3b and Fig. 4.4b each vector difference between SASS and model analysis or FG is given a code of the form ABCD. Most are 0031. "A" refers to comparison of the observation with the FG and "B" with the Optimum Interpolation. A zero means that the ECMWF quality checks considered the observation correct, a 1 that the observation is probably correct, 2 probably wrong, 3 definitely wrong. The C digit identifies the point in the sequence of quality checks where the B flag was set (3 indicates checking in the O-I) and a 1 in position D means the observation was used. Because SASS data has speed dependent errors only a rather tolerant quality control is applied. Thus as Fig. 4.4b shows only a few observations are questioned and none rejected. This constraint can be tightened if the data quality improves, or can be used to find only the largest differences between SASS and model. To illustrate, Fig. 4.4c shows only those SASS observations which differ from the model FG by more than 5 m/s and Fig. 4.4d shows those which differ from the initialised analysis by more than 5 m/s. The differences between these figures shows the extent to which the analysis has drawn to the data.

a)

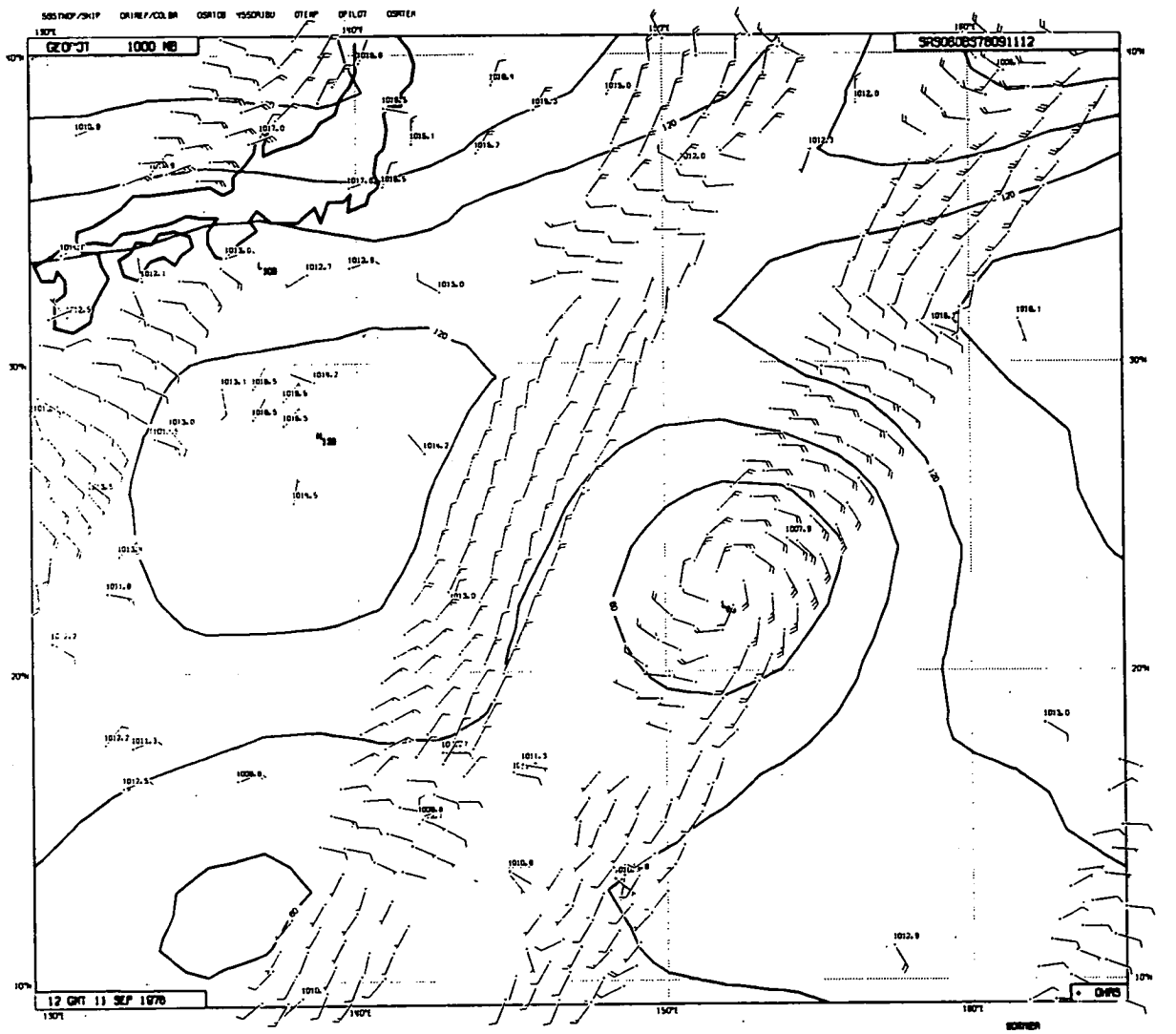

Fig. 4.3a Analysis from the assimilation experiment at 12Z on 11th September. Superimposed, are SASS and ship observations. The agreement in the location of the cyclonic feature is very good but Fig. 4.3b shows that significant differences in speed remain. Abrupt wind changes are visible e.g. at 140°E.

b)

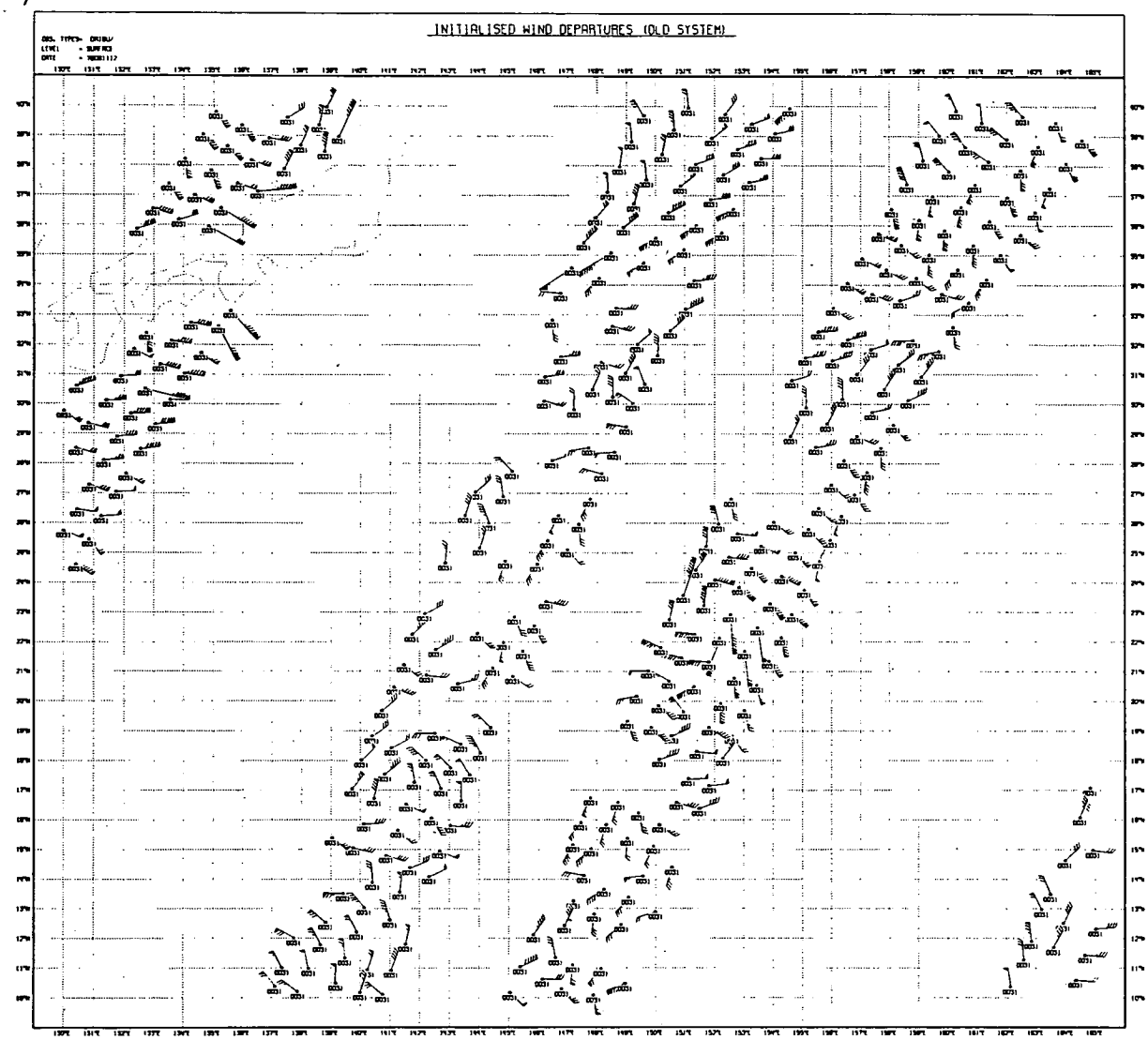

Fig. 4.3b Differences between analysis and SASS measurements. The usual meteorological convention is used except that one barb is .5 m/s and one fletch is 2.5 m/s. The coded information is explained in the text.

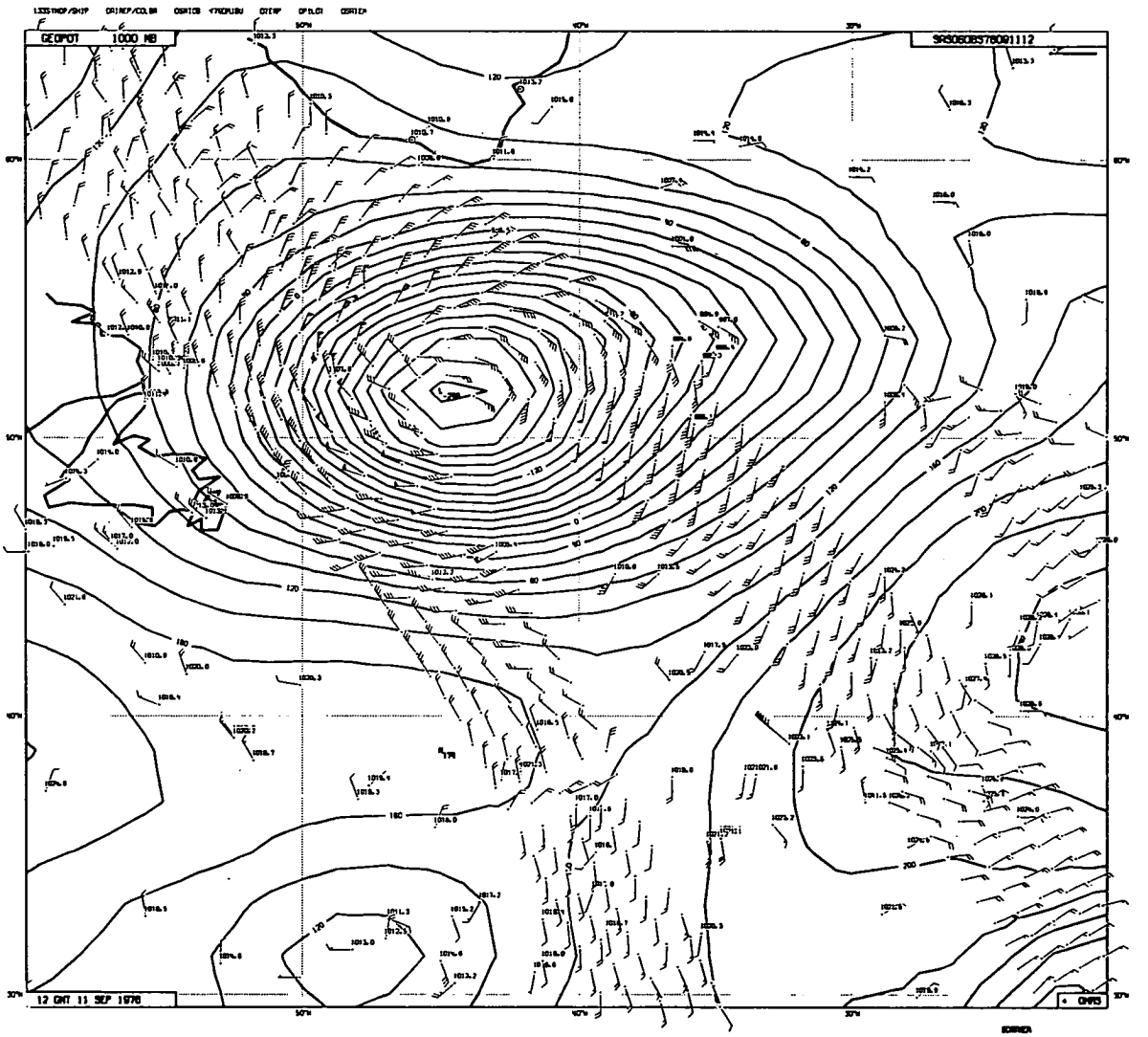

Fig. 4.4a As for 4.3a but for the QEII storm. Ship reports show surface pressure in hPa.

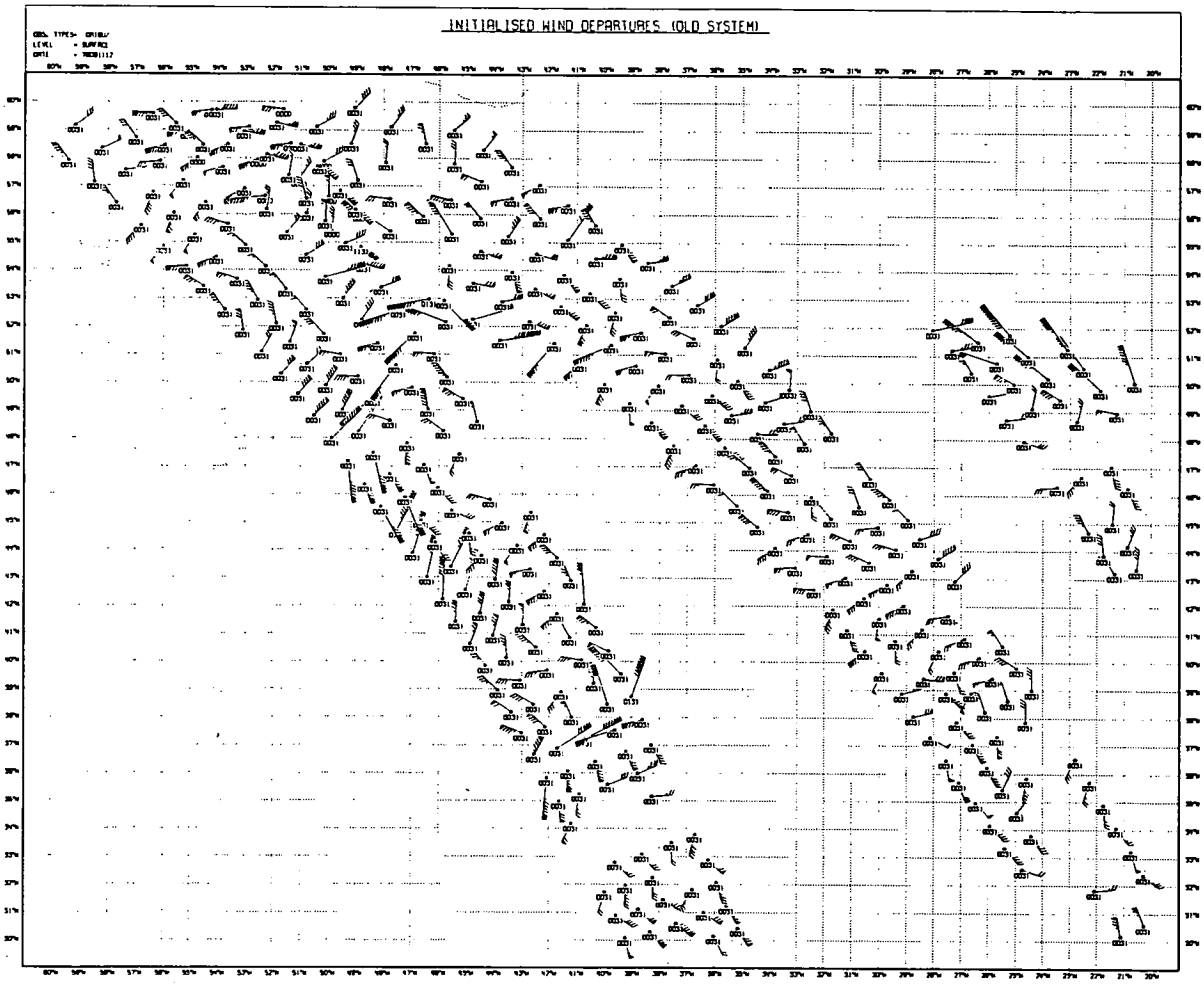

Fig. 4.4b As for 4.3b but for the QEII storm.

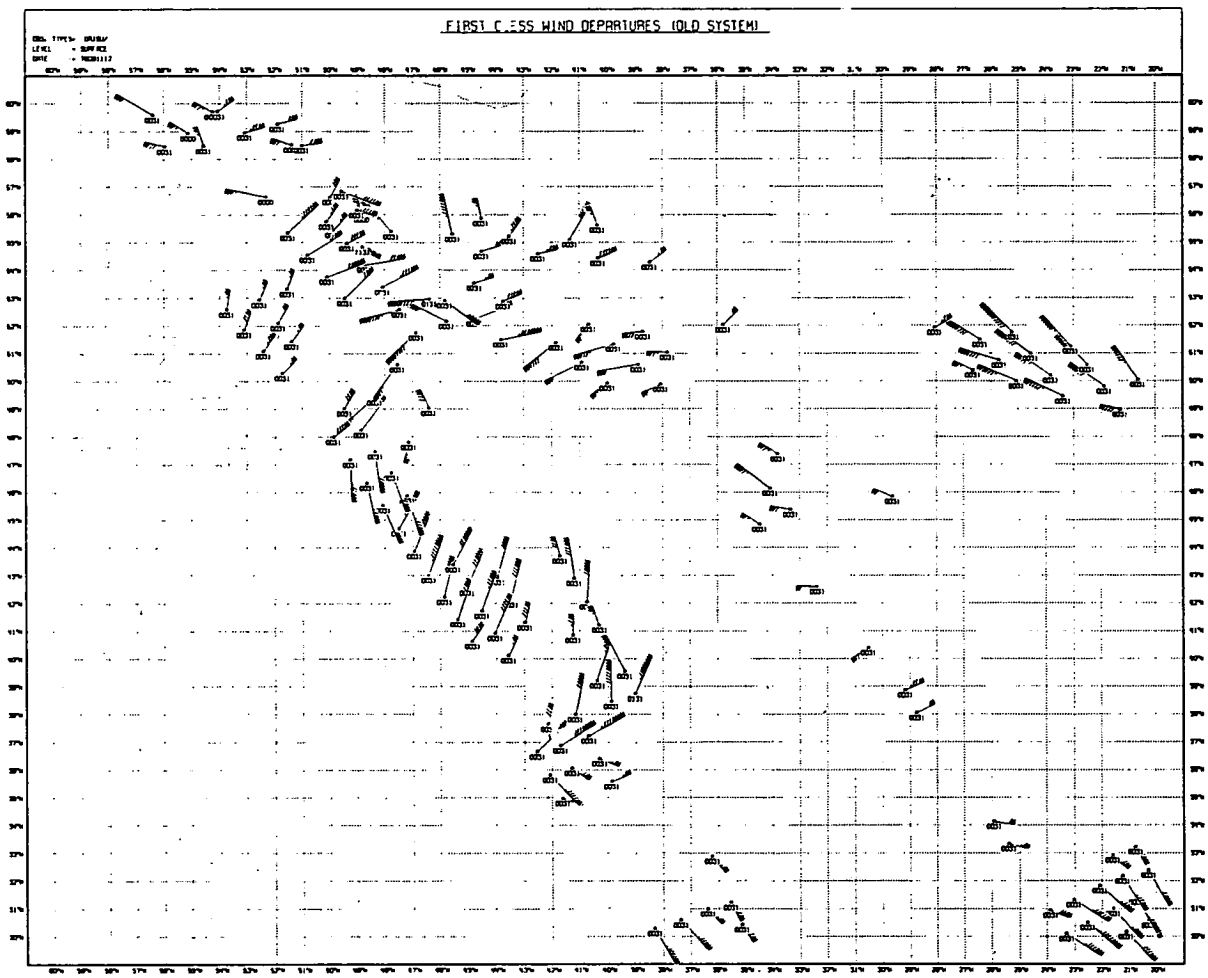

Fig. 4.4c Differences between model FG and SASS measurements. Only those measurements differing by more than 5 m/s are plotted.

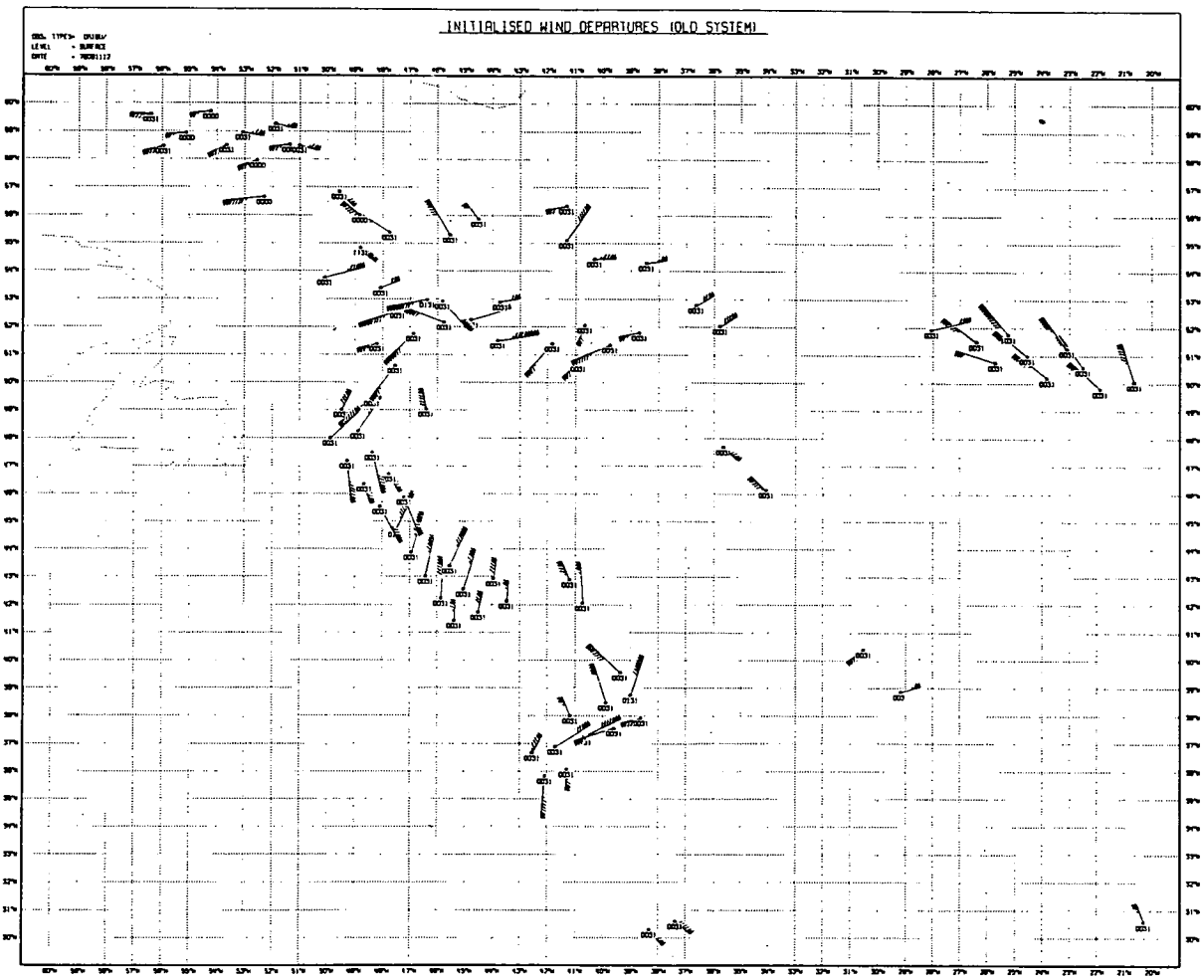

Fig. 4.4d As for 4.3c, but the differences between IN and SASS measurements.

One can see, from Fig. 4.4a, some areas where the wind vectors change abruptly (near 48°W, 44°N for example) and blow markedly across the isobars. Near 40°W, 38°N the SASS winds are unrealistic. Note also the strange ship report at 32°W, 39°N which illustrates the quality problems that can occur with any type of wind data.

Fig. 4.5 shows a very sharp front in the SASS data near 160 W. This front is present in the model also but much less sharply defined. Present numerical models are not able to use such small scale information in the data to maximum effect, but progress in this direction is likely by the time data is available from ERS-1.

In the case of the front on Fig. 4.5 the abrupt change in the SASS wind direction by 90° is probably correct. There are many examples however (see Figs. 4.3, 4.4, 4.5) where abrupt changes in SASS directions are probably incorrect. (Recall also the angular irregularities noted in SASS data in Section 2.2).

4.3 Impact of SASS data on forecasts

A number of forecast experiments have been run, listed in table 4.1. The starting dates were partly chosen to include specific synoptic events we wanted to forecast, such as the QEII and Ark Royal storms. Others were to test whether the model was rejecting the SASS data.

4.3.1 The QEII Storm

As indicated in 4.1, one study which has found a beneficial impact of SASS data on a forecast, is that of Duffy and Atlas (1986) for the QEII storm. This storm is of interest because of the failure of the NMC and Fleet Numerical Weather Centre (FNWC) operational forecast models to predict its intensification. It began as a shallow baroclinic disturbance approximately 100 km west of Cape Cod at 12Z on September 9th. During its movement out over the ocean, the low developed explosively, deepening by an estimated 60 mb in 24 hrs to a minimum pressure of 945 mb at 12 UTC on September 10th. (Gyakum 1984).

24 hour forecasts from 12 UTC on September 9th by the NMC-LFMII model (horizontal resolution 190 km) gave a central pressure of 1000 mb, while the FNWC model (horizontal resolution 381 km) forecast a pressure of 999 mb. The forecasts of the location of the centre of the storm and of the wind strength were likewise poor.

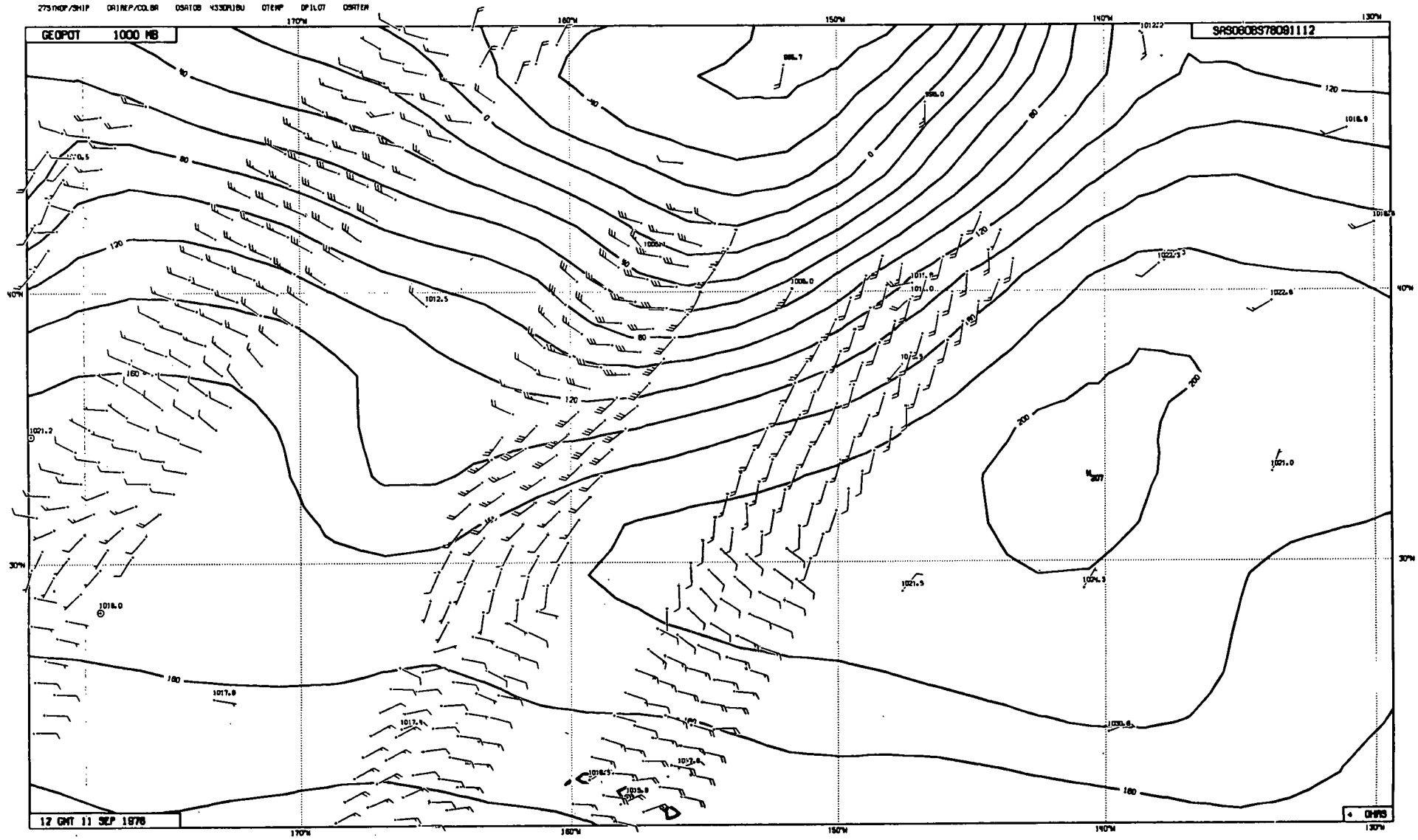

Fig. 4.5 As for 4.3a, but illustrating a sharp frontal feature in the SASS which is only diffusely represented in the analysis.

Table 4.1

Forecast Experiments

Code Name	Start date/ hour	Duration (days)	Starting analysis	Comment
DYJ	0912	10	NOSASS	QEII
DYK	0912	10	AESASS	Storm
EDN	1212	10	NOSASS	
EDM	1212	10	AESASS	
EDL	1500	10	NOSASS	Ark Royal
EF9	1500	10	AESASS	Storm
EIJ	1612	2	NOSASS	
EIM	1612	2	AESASS	

Duffy and Atlas used a limited-area fine-mesh model (horizontal resolution approx. 100 km) for their study. In their experiment without SASS data, the results are only slightly better than the NMC-LFMII model (the central pressure at 00Z on the 11th was 1000 mb, with peak surface (at an undefined height) winds of 21 m/s). When SASS data was used however the forecast improved - the low intensified by 12 mb to 988 mb, with peak winds of 37 m/s (at an unspecified height). Although SASS data led to an improvement in the forecast, the forecast even with SASS cannot be considered good: there was a positional error of ~ 1000 km and a central pressure error of more than 10 mb (taking a 100 km square average central pressure of ~ 975 mb for 00 UTC on the 11th). The peak intensity of the storm occurred earlier (12Z on 10th) but Duffy does not show his results for this time. His comments however suggest that he did not have a more intense forecast at 12 UTC on 10th so at that time his pressure errors were probably more than 30 mb for the SASS forecast, (taking a 100 km square central pressure of 955 mb at 12 UTC on the 10th - Anthes et al. 1983).

In Fig. 4.6, the 24 hour surface pressure forecast for 12Z on the 10th is plotted (a), together with the verifying analysis (b), both for the AESASS experiments. At this resolution the forecast for the position of the QEII storm appears quite accurate. Fig. 4.7 is a plot of the location of the QEII storm for the period 12 UTC on the 9th to 12 UTC on the 14th as gauged by (a) the German manual surface analysis, (b) the forecast from the AESASS analysis of 12Z on the 9th. The position of the storm in the AESASS analyses is not

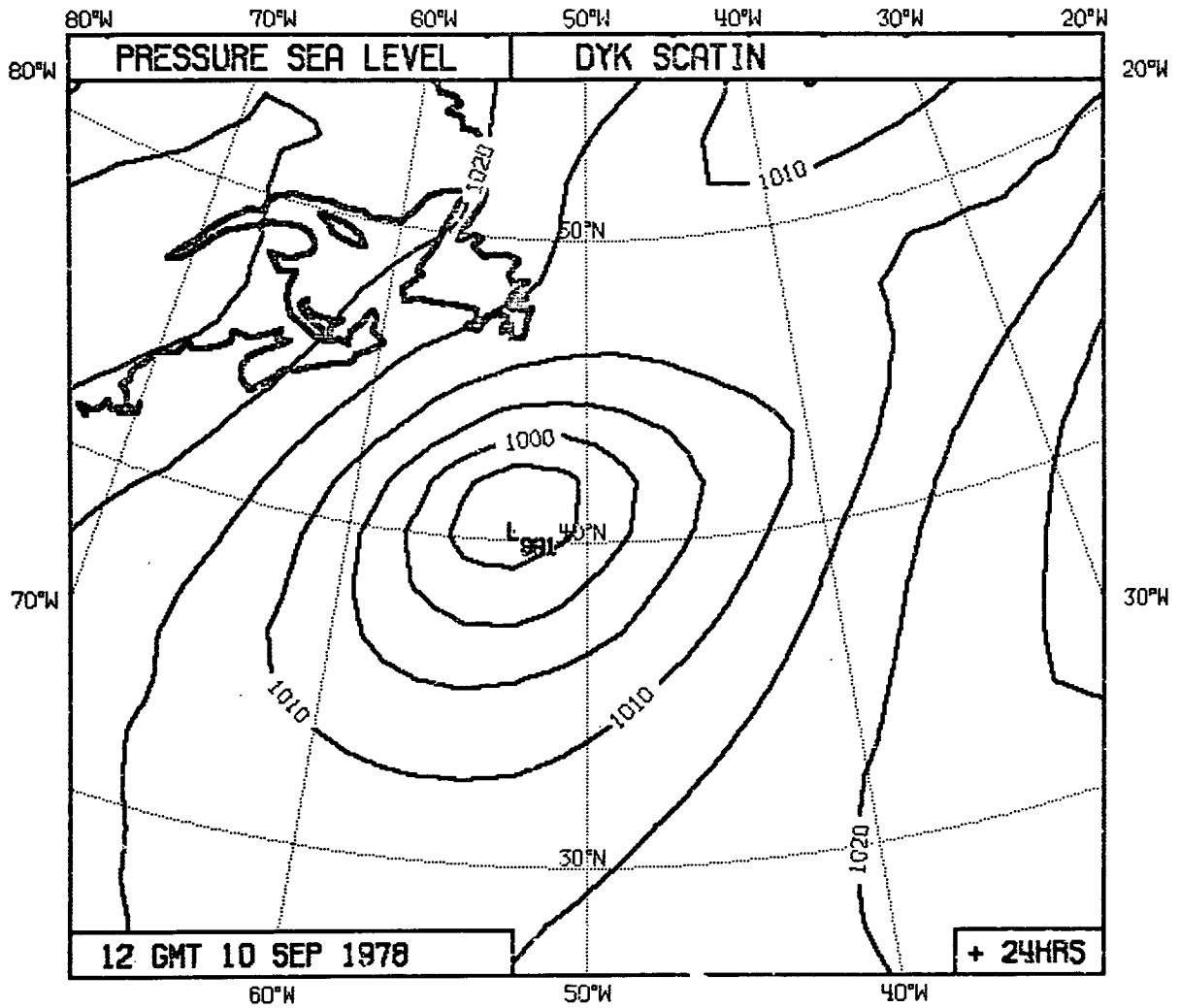

Fig. 4.6a 24-hour surface pressure forecast for 12Z on 10th September from the AESASS forecast DYK.

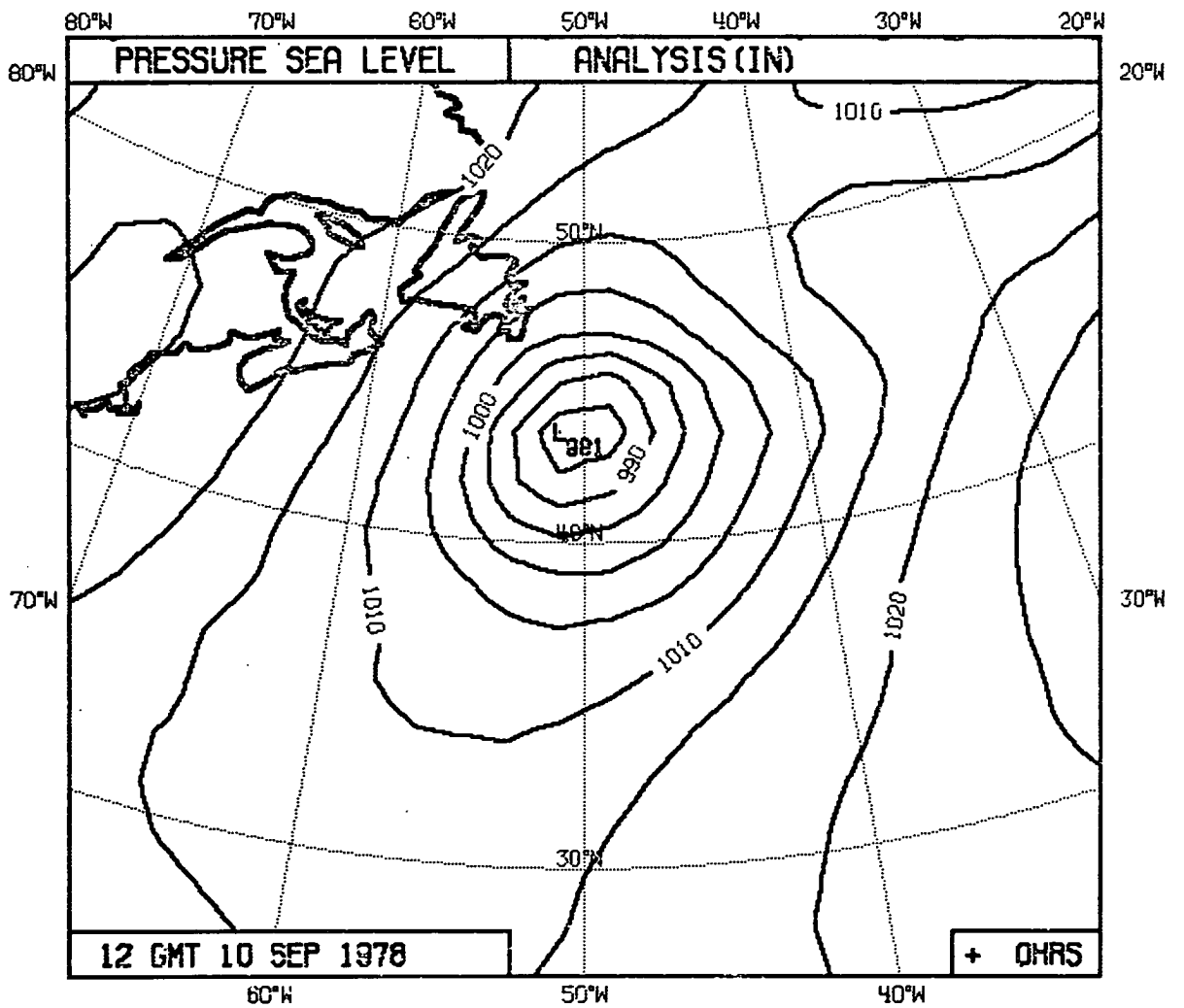

Fig. 4.6b Verifying analysis for 12 Z on September 10.

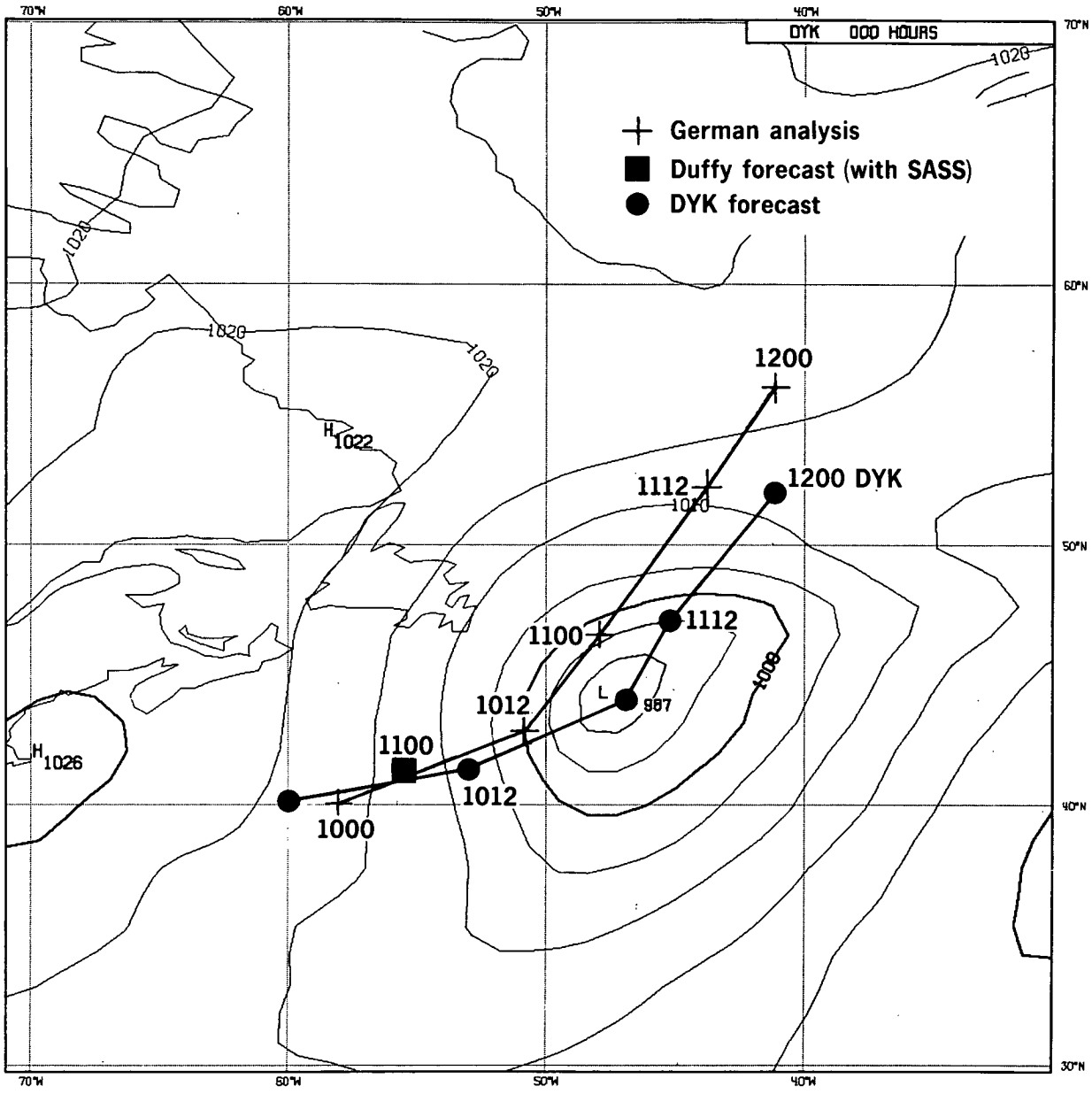

Fig. 4.7 Track of QEII storm from AESASS forecast and German analyses. The location of the QEII storm as forecast by Duffy et al. at 00 UHT on 11 September is plotted. Contours of height of 1000 mb surface for this time are shown for the AESASS forecast.

shown but follows closely the German analyses. One can see from Fig. 4.7, that the model forecast has modest errors in position. For example, at 00 UTC on the 11th, the error is approximately 300 km. This is substantially less than the position error of Duffy and Atlas at this time (1000 km).

In Fig. 4.8 the central pressure from a number of sources is plotted for the period between 12 UTC on the 9th and 00 UTC on the 14th September. Not only is there a wide variation in the central pressure forecast by different models, there is a wide variation in the analysed values. In particular, both NMC and the German analysis probably seriously underestimate the central pressure at 12 UTC on the 10th, 00 UTC on the 11th and 12 UTC on the 11th. [The AESASS analyses are probably closer to the truth at 12 UTC on the 11th]. Pressures and positions of the QEII storm from the NOSASS analyses, and the forecast from the NOSASS analysis have not been plotted. The NOSASS analyses hardly differ from the AESASS analyses values (as Fig. 4.1 confirms) suggesting that the SASS data agreed well with the other in-situ data. Fig. 4.9 shows the difference in the NOSASS and AESASS forecasts (DYJ and DYK) after (a) 24 hours (b) 84 hours. There is very little difference between the 2 forecasts, anywhere in the NH even after more than 3 days. (This is not really surprising since the analyses for 12Z on the 9th were very similar).

From Fig. 4.8, one can see that the forecast by the ECMWF model is not substantially better in amplitude than Duffy and Atlas at 00 UTC on the 11th, but the position of the low is much better forecast (Fig. 4.7). We conclude therefore that the ECMWF forecast is significantly better than Duffy and Atlas. Unlike Duffy and Atlas, we do not find SASS data to have had any important beneficial impact on the forecast. Duffy and Atlas find substantial changes in the low level analysed wind fields as a result of asimilating SASS. This is not the case for our analyses (Fig. 4.1). It would therefore appear that one interpretation of the results is: if the assimilation of conventionally available data is not very good, assimilating SASS data can help; but the better the assimilation of conventionally available data the less impact SASS has. One should note however that the ECMWF forecast, while better than Duffy and Atlas's, still did not capture well the rapid deepening between 00 UTC and 12 UTC on the 10th. A resolution of 100 km is probably not adequate to resolve such intense features: a resolution nearer 50 km may be necessary, Orlanski and Katzfey (1987). It would be interesting to repeat this experiment with a higher resolution assimilation, and 50 km resolution SASS data.

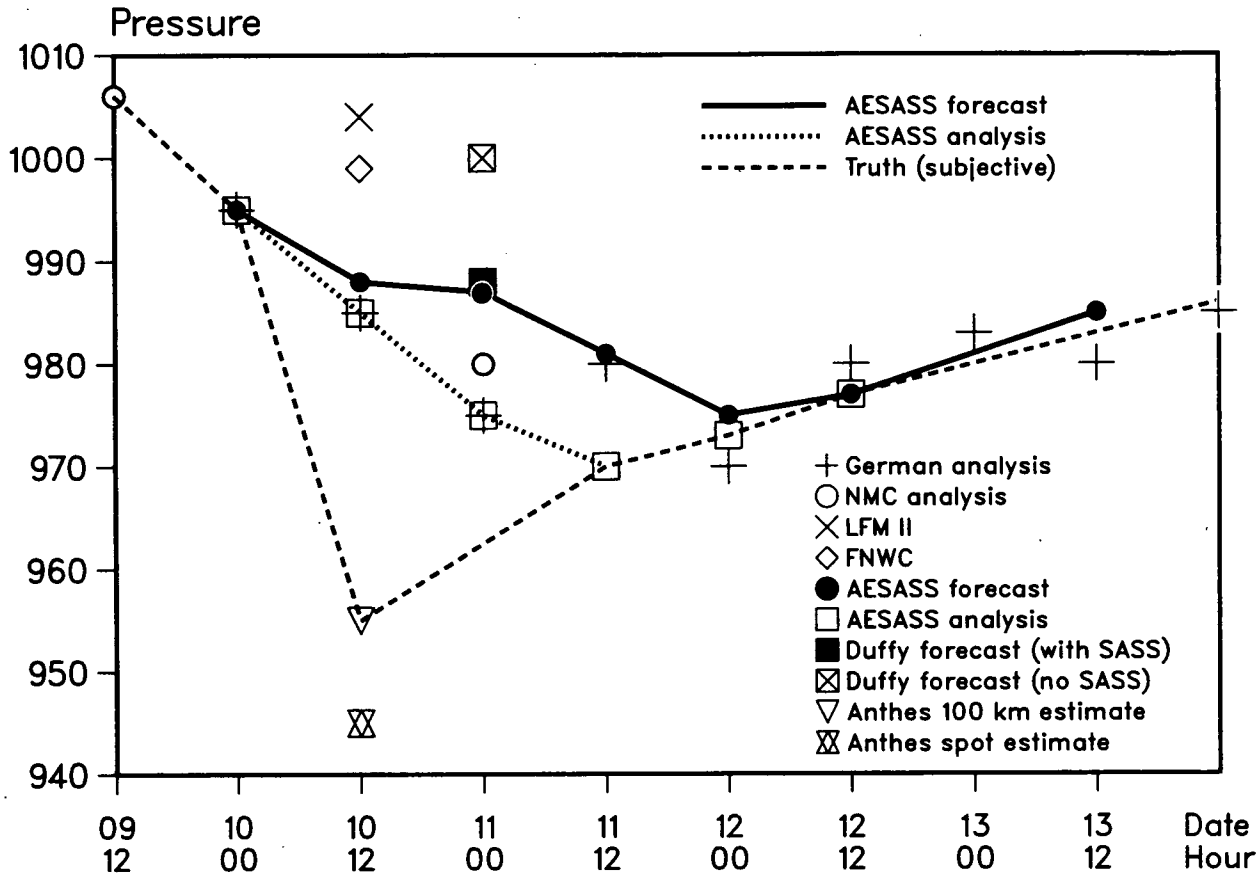

Fig. 4.8 Time evolution of surface pressure as gauged by a number of analyses or forecasts. No forecast reproduces the rapid deeping between 00 UHT and 12 UHT on the 10th September.

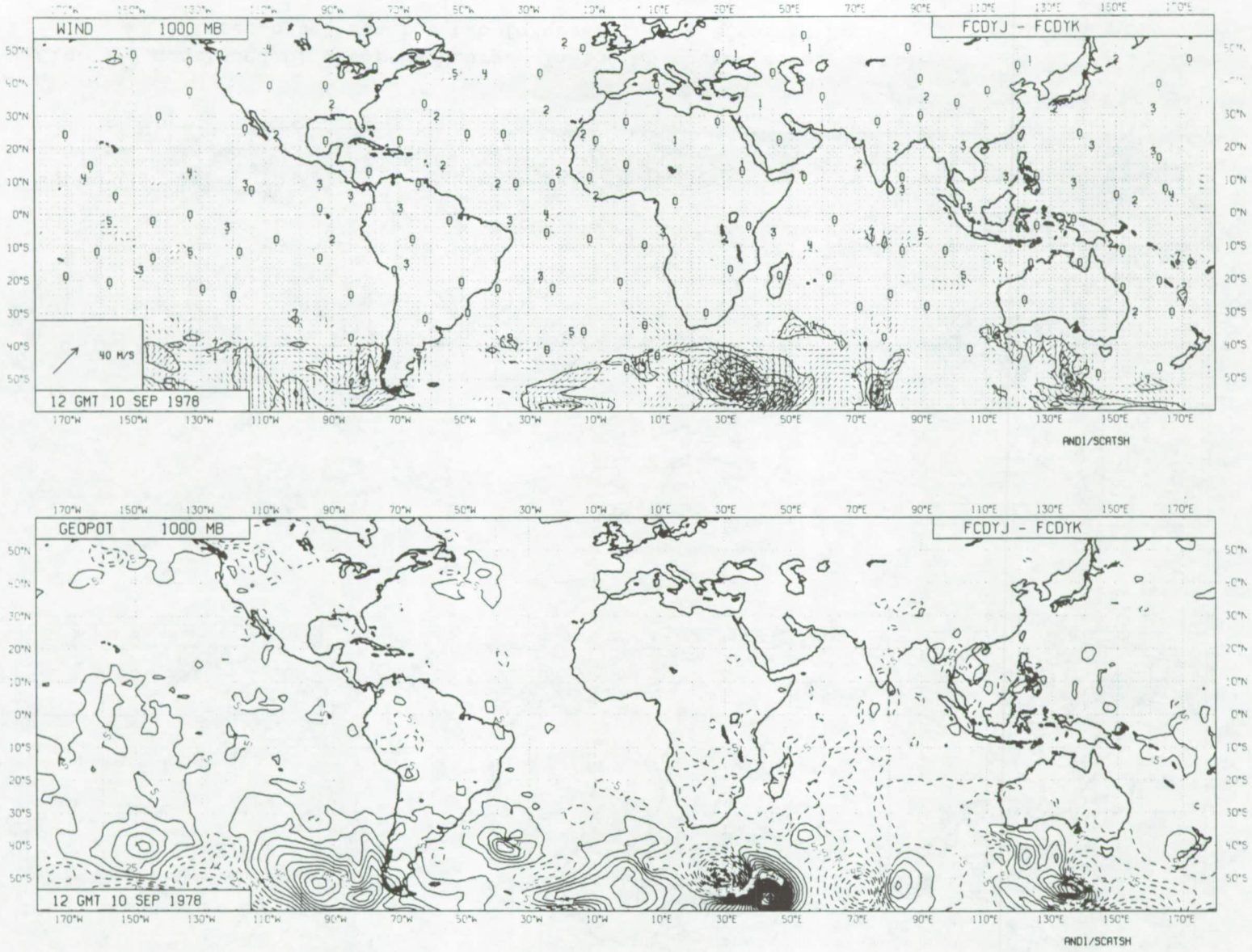

Fig. 4.9 Difference between forecast from the AESASS and NOSASS analysis of September 9, 12 UTC (called DYJ and DYK in table 4.1) (a) after 24 hours

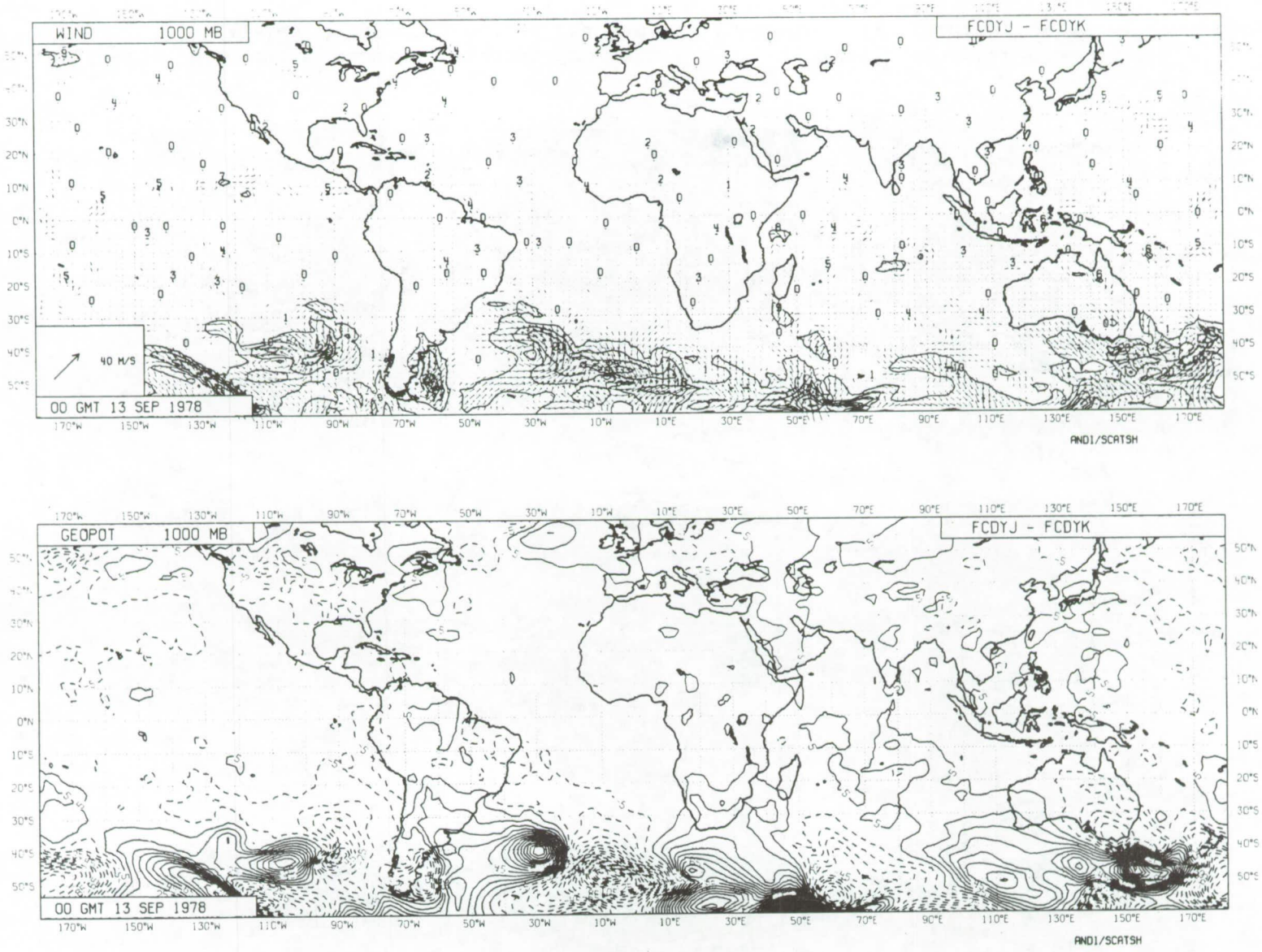

Fig. 4.9 continued b) after 84 hours. In the NH there is very little difference between the two forecasts, even after 84 hours

4.3.2 Impact of SASS on the Ark Royal Storm

The Ark Royal Storm occurred on September 16th and 17th, north of Scotland, during which time the NATO fleet including the Ark Royal was buffeted by this violent storm. (Peteherych et al. 1986). This storm which evolved from the tropical storm Flossie, was poorly forecast by operational centres. Peteherych et al found the SASS and SMMR moisture data useful for subjective analysis of the Ark Royal Storm. Here we will try to see if SASS data has any impact on the numerical forecast of the Ark Royal Storm. Two 10 day-forecasts (one from the AESASS analysis and one from the NOSASS analysis) were run from 00Z on 15th September, and two short (2 day) forecasts from 12Z on 16th September. (Table 4.1 gives a list of forecast experiments which have been carried out).

In Fig. 4.10 the intensity of the system is plotted for the German analysis, AESASS analysis and the (EF9) forecast from the AESASS analysis as a function of time. At the height of the storm 00Z on September 17, the location and intensity of the storm was well forecast in the 48 hr AESASS (EF9) run, although at 24 hrs and 36 hr there are both positional and intensity errors in this forecast. Fig. 4.11 shows the difference in the AESASS and NOSASS forecasts at 00Z on the 17th. Pressure differences are around 1mb, though wind speed differences of 6 m/s exist in the vicinity of the storm. Fig. 4.12 shows the 48hr AESASS forecast (EF9) surface pressure and 500 mb height fields and shows the intense storm in the Norwegian Sea.

In this experiment, as for the QEII, SASS has had little impact on the forecast of this storm, at least out to 3 days, in terms of position or intensity as measured by central pressure. There are however small scale differences in the wind field up to 6 m/s in the vicinity of the storm. While this may not be very significant meteorologically, it may make a substantial difference to the local wave field in a wave model driven by the forecast surface winds.

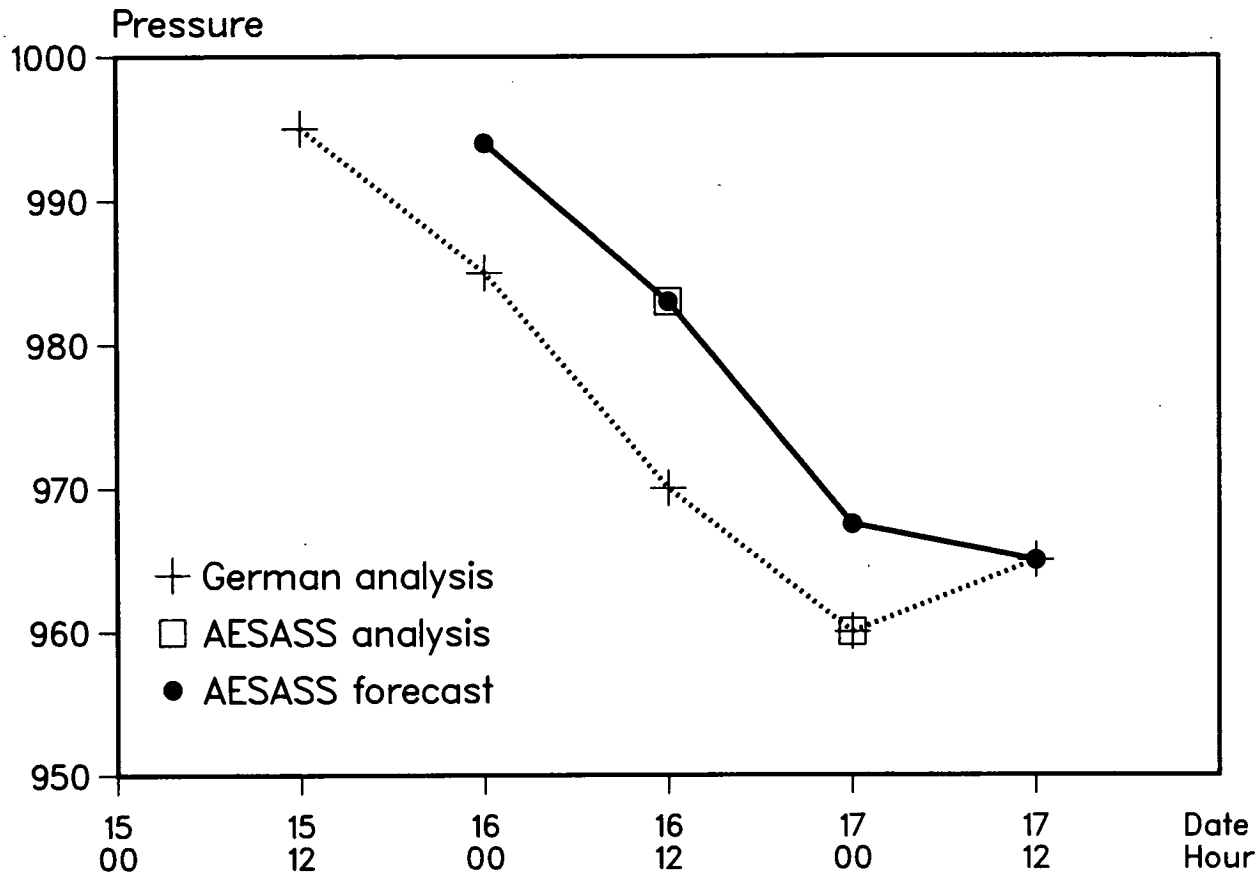

Fig. 4.10 Plot of the surface pressure evolution of the Ark Royal storm in the German analysis, the AESASS analysis, and the AESASS forecat from September 15, 00 UTC.

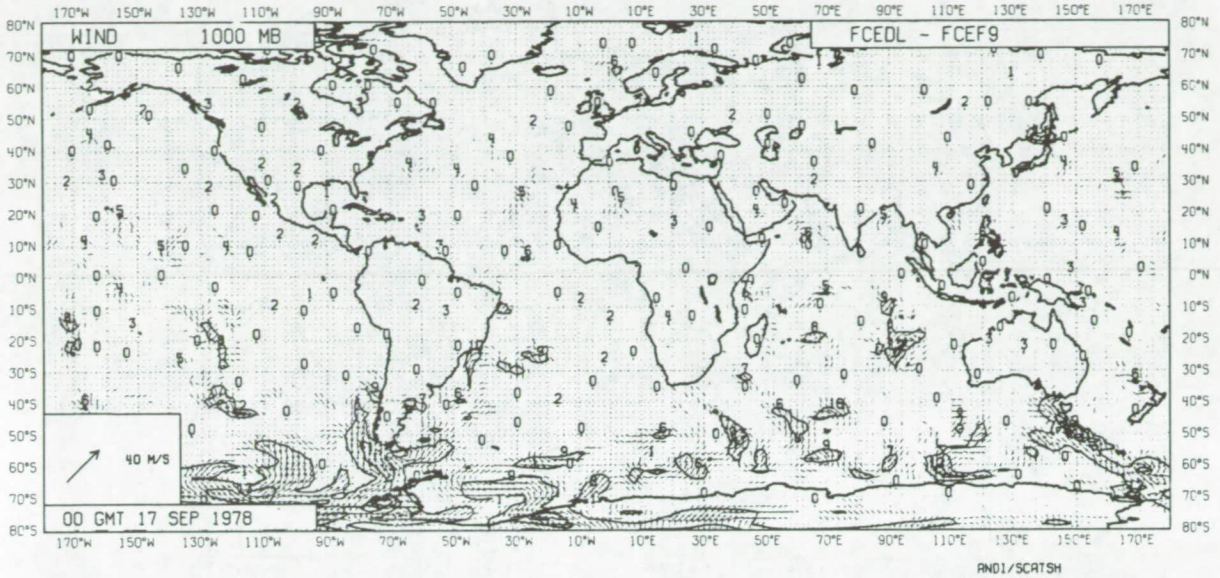

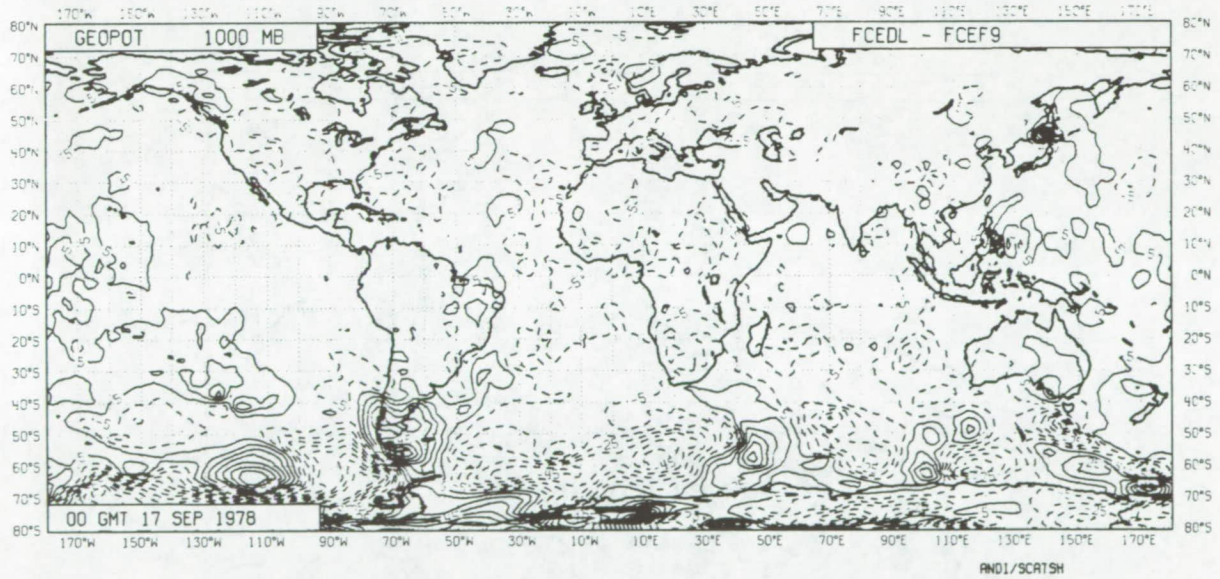

Fig. 4.11 Differences between AESASS and NOSASS forecasts from September 15, 00 UTC after 48 hours. The differences in the NH are small scale and generally of small amplitude. A small area where wind differences are up to 6 m/s exists near the Ark Royal storm.

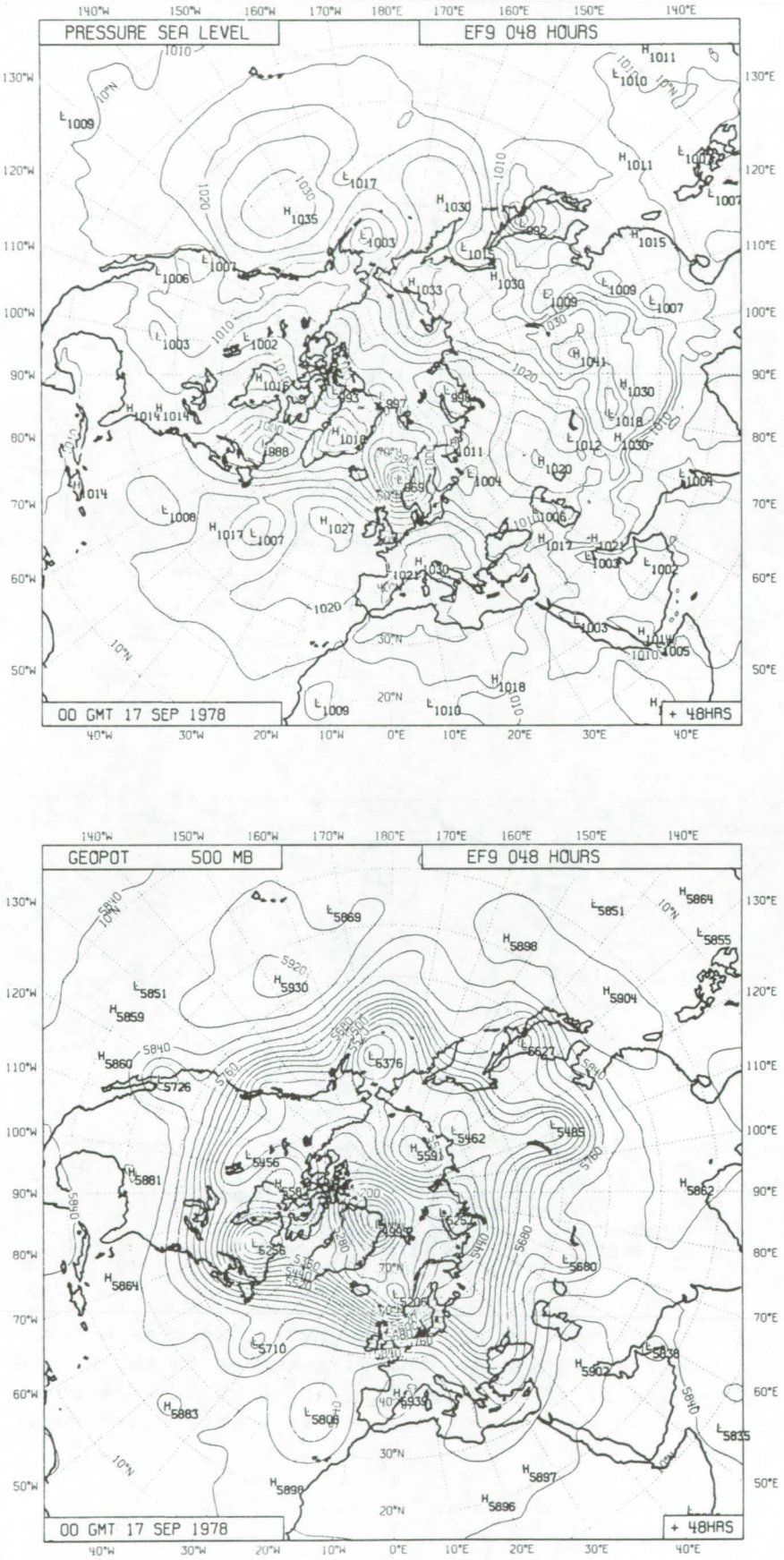

Fig. 4.12 Surface pressure and height of the 500 mb surface: forecast for 00 UTC on 17th Sept from the AESASS analysis of 00 UTC on 15th Sept.

5. DEALIASING

5.1 Dealiasing dual-pol data

a. Real dual-pol data

The algorithm which finds possible solutions for (v,ϕ) for given σ^o input, returns, in addition to possible values of (v,ϕ), a measure of the agreement between the selected values of (v,ϕ) and the measured σ^o. The solutions are then given a rank (1,2,3,4) according to this perceived agreement. For single pol data, the ranking contains little skill, except for two-alias solutions, when rank 1 does have some skill (Appendix B). The skill can be increased if the solutions are overdetermined. Some increase in determination is achieved by operating SASS in dual-pol model. It is therefore possible to test dealiasing algorithms on the dual-pol data in the period 6-20 September, but this data is of limited extent since the dual pol mode of operation was used only infrequently.

Three methods of dealiasing (all three in preliminary stages of development) are tested:

(1) SLICE (U.K. Met Office; Offiler)
(2) Median Filter (JPL; Schultz)
(3) UWP (Univ. of Wisconsin and JPL; Wylie, Hinton, Pihos)

The dealiasing algorithms may use the ranking information based on dual-pole information. The dealiasing algorithms override the ranking of the SOS to select a rank 2, 3 or 4 if this is more consistent with neighbouring solutions.

Table 5.1 gives a number of statistics on the skill of the de-aliasing algorithms for dual pol data extracted from the 2 week period 6-20 September. A number of interesting features are of note:

(1) The skill in the dual pol ranking is not high. (41%) (For single-pol this figure is ~ 26%). Note however that we are dealing with real data here, for which the true direction is not known. In these experiments truth means the direction (alias) chosen by the team of analysts (Appendix A).

(2) Overall, the dealiasing algorithms do improve the skill to 46%, 51%, 51% for Slice, Median, UWP respectively, but this increase is not very large.

Table 5.1

Automated ambiguity removal of actual dual-pole SASS data
for the 15-day data set

(Reprocessed and at 100 km Resolution)

COMPARISON TABLE OF COUNTS-PERCENT
FOR THE DIFFERENT METHODS

CASE NO	TOTAL COUNT	SLICE TO TRUTH	MED FILT TO TRUTH	U WSC TO TRUTH	SLICE TO MED	SLICE TO U WSC	MED FILT TO U WSC	RANK 1 TO TRUTH	RANK 1 OR 2 TO TRUTH
1	317	193	180	196	279	314	276	155	237
		60.9%	56.8%	61.8%	88.0%	99.1%	87.1%	48.9%	74.8%
2	320	182	179	165	141	216	161	139	212
		56.9	55.9	51.6	44.1	67.	50.3	43.4	66.3
3	87	4	4	4	81	87	81	17	36
		4.6	4.6	4.6	93.1	100	93.1	19.5	41.4
4	162	122	112	83	127	88	103	73	117
		75.3	69.1	51.2	78.4	54.3	63.6	45.1	72.2
5	250	150	135	103	173	179	149	118	188
		60.0	54.0	41.2	69.2	71.6	59.6	47.2	75.2
6	129	59	42	43	101	112	117	45	69
		45.7	32.6	33.3	78.3	86.8	90.7	34.9	53.5
7	252	87	86	90	204	200	202	93	168
		34.5	34.9	35.7	81.0	79.4	80.2	36.9	66.7
8	254	55	154	174	91	68	153	89	169
		21.7	60.6	68.5	35.8	26.8	60.2	35.0	86.5
9	177	86	133	156	118	99	148	107	142
		48.6	75.1	88.1	66.7	55.9	83.6	60.5	80.2
10	165	43	47	55	153	140	152	33	73
		26.1	28.5	33.3	92.7	84.8	92.1	20.0	44.2
ALL	2113	981	1074	1089	1468	1503	1542	869	1411
		46.4%	50.8%	50.6%	69.5%	71.1%	73.0%	41.4%	66.8%

Table 5.2

Automated ambiguity removal of simulated dual-pole SASS data
9 Revs over Pacific Ocean Basin on September 7, 1978

(50 km Resolution)

COMPARISON TABLE OF COUNTS-PERCENT
FOR THE DIFFERENT METHODS

CASE NO	TOTAL COUNT	SLICE TO TRUTH	MED FILT TO TRUTH	U WSC TO TRUTH	SLICE TO MED	SLICE TO U WSC	MED FILT TO U WSC	RANK 1 TO TRUTH	RANK 1 OR 2 TO TRUTH
1	537	202	324	213	394	317	329	186	319
		37.6%	60.3%	39.7%	73.4%	59.0%	61.3%	34.6%	59.4%
2	2650	2004	2007	1936	2394	2238	2284	1451	2044
		75.6	75.7	73.1	90.3	84.5	86.2	54.8	77.1
3	2249	1609	1578	1775	1715	1758	1840	1318	1896
		71.5	70.2	76.9	76.3	78.2	81.8	58.6	84.3
4	2885	2205	2113	2213	2306	2318	2341	1572	2269
		76.4	73.2	76.7	79.9	80.3	81.1	54.5	78.6
5	3327	2316	2382	2235	2777	2660	2838	1649	2661
		69.6	71.6	67.2	83.5	80.0	85.3	49.6	80.0
6	3307	2191	2134	2145	2640	2744	2708	1587	2492
		66.3	64.5	64.9	79.8	83.0	81.8	47.4	75.4
7	2522	1786	1908	1967	2013	1956	2048	1338	2058
		70.8	75.7	78.0	79.8	77.6	81.2	53.1	81.6
8	2127	1648	1613	1706	1827	1783	1767	1149	1733
		77.5	75.8	80.2	85.9	83.8	83.1	54.0	81.5
9	626	576	584	572	597	587	555	375	501
		92.0	90.1	91.4	95.4	90.6	88.7	59.9	80.0
ALL	20230	14537	14623	14784	16683	16341	16708	10605	15973
		71.9%	72.3%	73.0%	82.4%	80.0%	82.6%	52.4%	79.0%

(3) If the skill in the rank 1 solution is low, the dealiasing techniques can decrease it further. (See for example cases 3,7,8).

(4) Although the different algorithms often return similar solutions, there are examples where they behave very differently. For example case 9 illustrates a situation where the initial skill is quite high (60%) but Slice decreases it while the others lead to an improvement. Case 6 is an example of Slice leading to an improvement while Median and UWP do not.

b. Simulated dual-pol data

This study has been repeated with simulated data generated by flying the SASS simulator in dual-pol mode over the Seasat orbits over the Pacific on 7th September. The results are presented in Table 5.2.

For the simulated data, the skill of the rank 1 solution is higher (52%) than for the real dual pole data discussed above for which the skill was only 41%. In the case of simulated data, all the dealiasing methods improved the skill, to ~ 72%, and there were no occasions where the dealiasing methods decreased the skill. The length of the orbits is longer than those for Table 5.1. As is commonly the case, simulated data gives optimistic results compared with the real data of table 5.1. This optimism probably applies to the results of Section 5.2 also.

5.2 Dealiasing simulated data for 3 beam scatterometers

An alternative way of increasing determinism is to use a third antenna as is planned for ERS-1. Fig. 5.1 shows the possible (v, ϕ) solutions for each beam separately when a patch of ocean is viewed by 3 beams. If there is no noise then only one solution is possible. However, if there is noise (equivalent to moving the curves up or down), then the solution will not be unique. But one expects that some measure of the extent to which possible solutions fit the data would be meaningful, and that therefore the residual after the fit information should be used for more than just ranking the solutions.

Some preliminary tests for simulated data from the ERS-1 and NSCAT simulators have been made. Fig. 5.2 is a histogram of the angular error between the rank 1 solution and truth. Most solutions have an error less than ±20° of the true

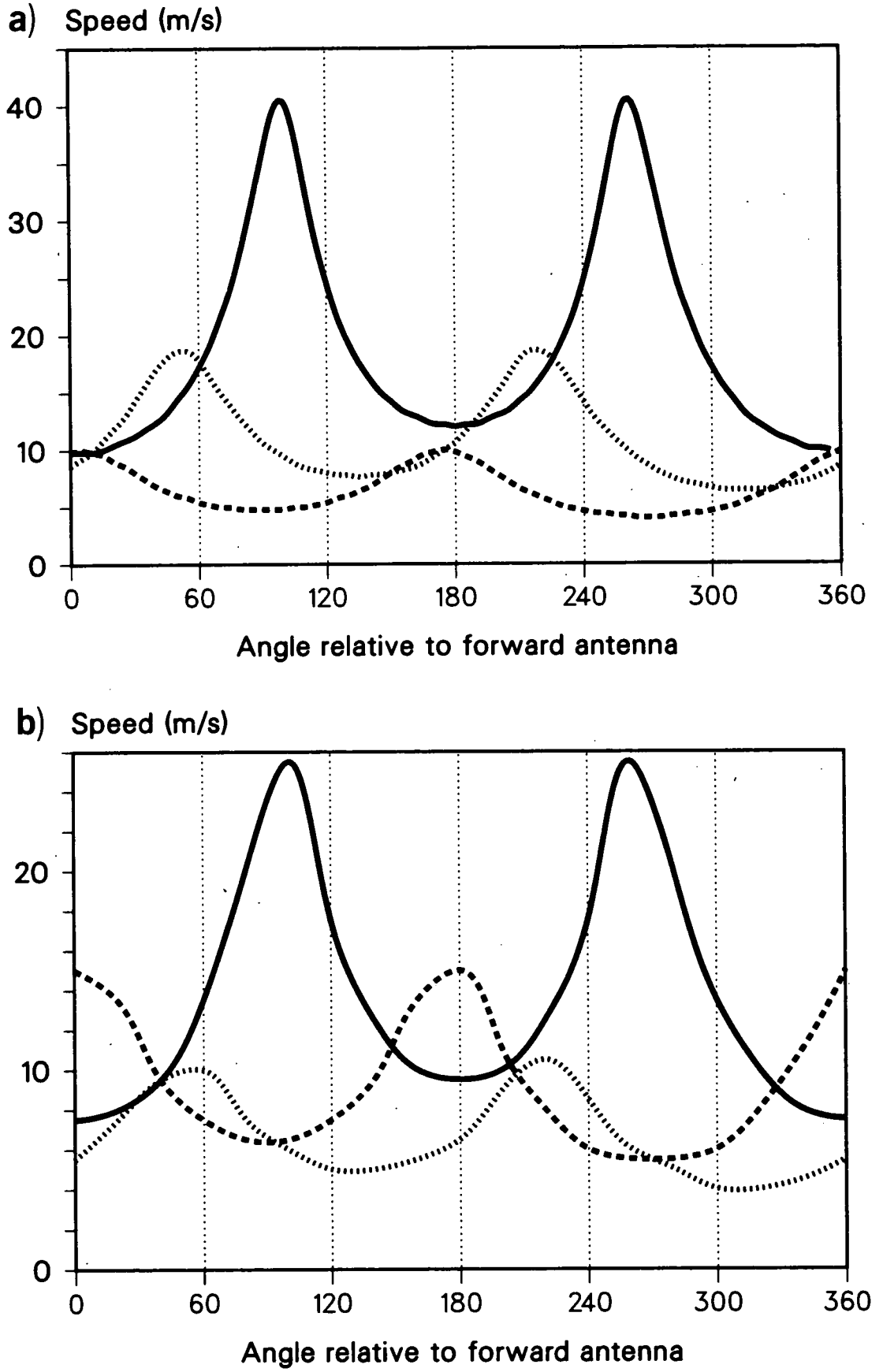

Fig. 5.1 Sketch of possible (v,ϕ) curves for a single value of σ^{o} from the forward beam (solid), rear beam (dashed) and central beam (dotted). For (a) wind direction almost up the beam 1, and (b) at 40° to beam 1. For simulated ERS-1 data.

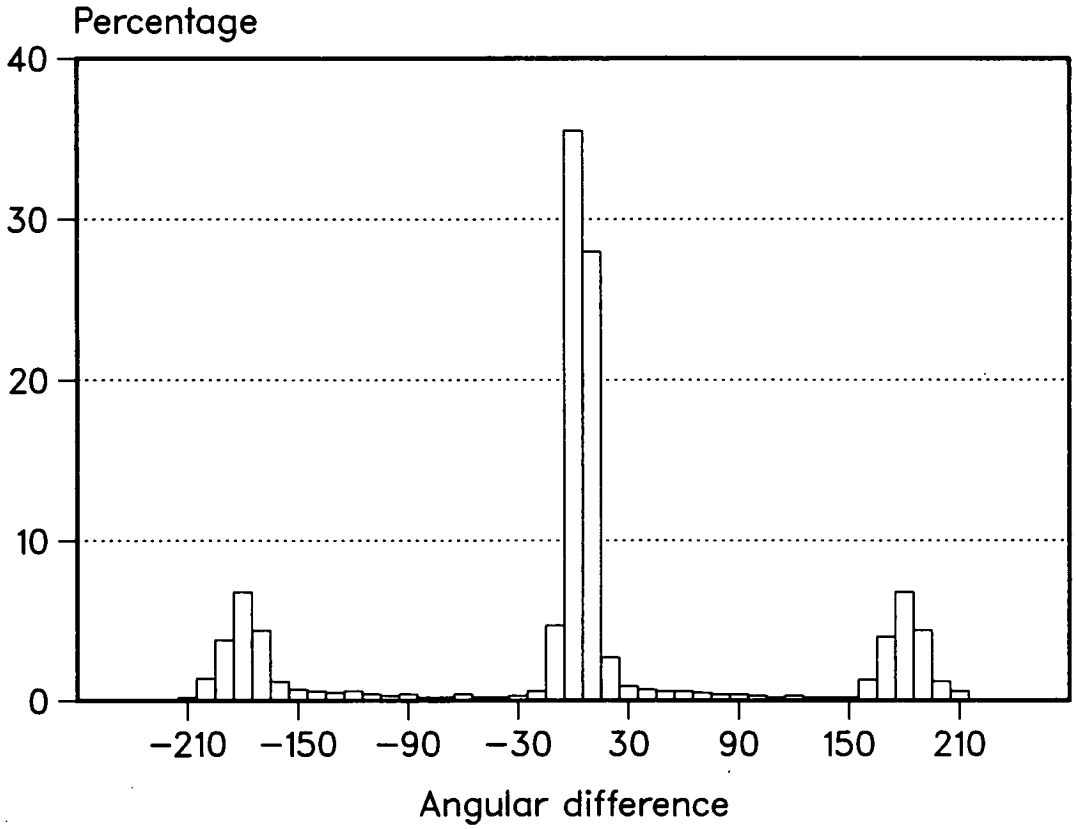

Fig. 5.2 Histogram of the number of solutions with a given angular error for simulated NSCAT data. Most solutions cluster around 0° ±20, but there is a significant number at 180° ±20 as well as intermediate angles.

direction, but there is a significant number of vectors which have errors clustered around ±180° and quite a few with angular errors in between. For reasons discussed earlier, although the bulk of solutions have errors less than 20°, those with greater errors could present problems when the data is passed to a high resolution assimilation system. If however one selects only data which is classified as having a high probability of being correct, then the angular fits improve. (Probability is related to the inverse of the residual).

a. The value of the probabilities

For 4 vector solutions, zero skill corresponds to probability of .25 for all solutions. If, from all 4-vectors one selects only those with rank 1 probability more than .2 above the rank 2 solutions, the histogram of Fig. 5.3a is obtained. Fig. 5.3b is for 3 vector solutions where the probability of rank 1 solution exceeds the rank 2 solution by more than .3, and Fig. 5.3c for 2 vector solutions where the rank 1 probability exceeds rank 2 probability by more than .4. In all 3 cases, there are very few occurrences of angular errors between 20° and 160°. Further the peaks centred on 180° error are much reduced though not eliminated completely.

These curves suggest that indeed a dealiasing scheme using this probability information could be beneficial: there is more skill in the probability than in the ranking. The number of high probability solutions for the 4, 3, 2 aliases above are respectively 41%, 36.5% and 30% of the possible, 4, 3, 2 aliases, so on average about 35-40% of the data would be chosen. This data could be used as anchor points for the dealiasing algorithm.

The criteria for choosing high probability solutions is arbitrary. The values used above of .2, .3, .4 for 4, 3,2 alias solutions were obtained from Fig. 5.4. This shows the percentage of solutions correct as a function of the probability difference between rank 1 and rank 2 solutions for (a) 4 aliases, (b) 3 aliases (c) 2 aliases. If one wants 80% of the chosen solutions to be correct than the choice of .2, .3, .4 follows. It would be possible to tighten the criteria to make for example 90% of the chosen solutions classified as high probability correct, at the cost of accepting initially fewer solutions.

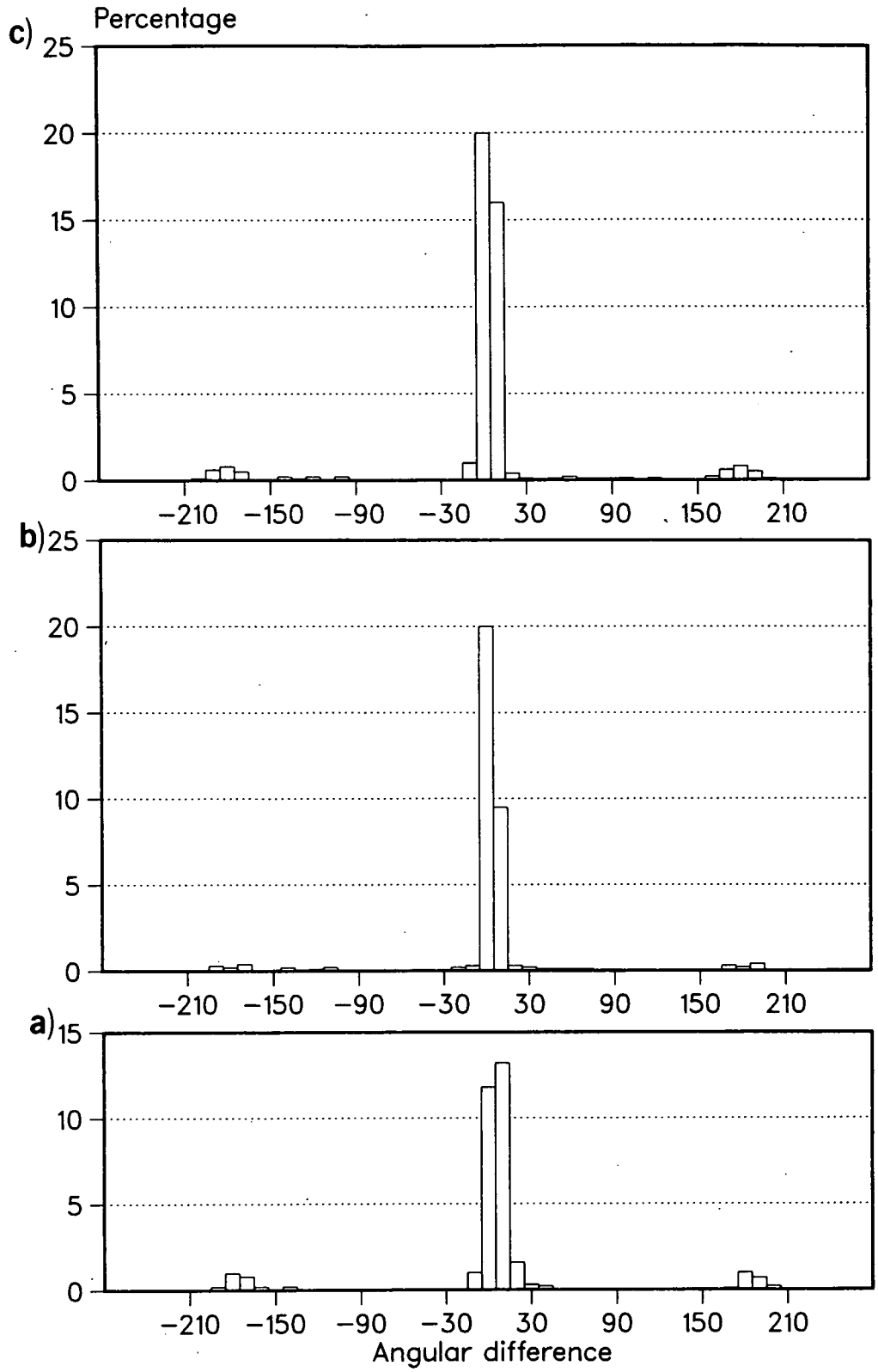

Fig. 5.3 a) As for 5.2 but only for 4 vectors for which the probability of the rank 1 solution exceeds rank 2 by more than .2. For simulated NSCAT data.

b) As for a, but only for 3 vectors for which the probability of the rank 1 solution exceeds rank 2 by more than .3.

c) As for a, but only for 2 vectors for which the probability of the rank 1 solution exceeds rank 2 by more than .4.

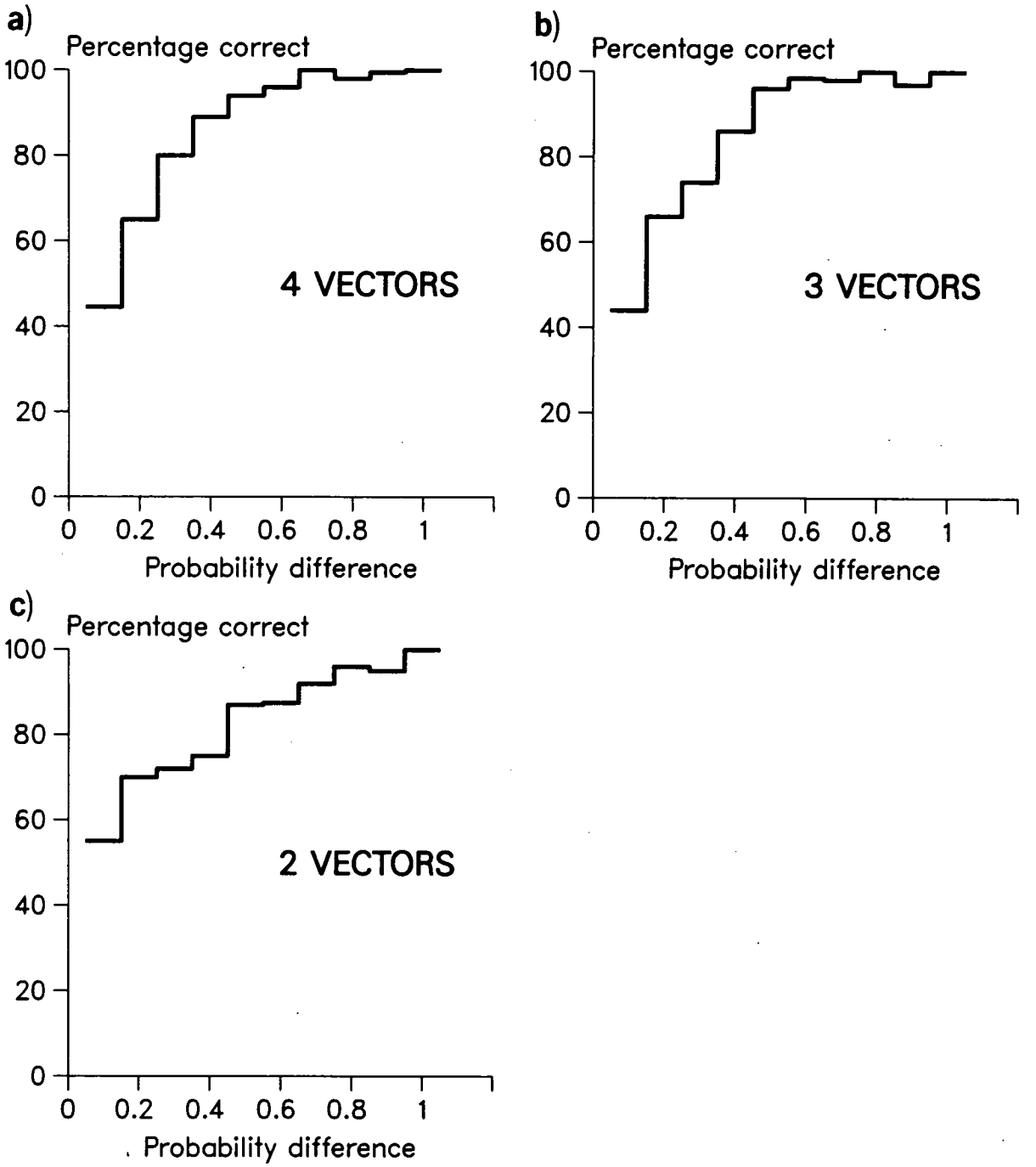

Fig. 5.4 Percentage of solutions which are correct plotted against the amount by which the rank 1 probability exceeds rank 2 probability. For simulated NSCAT data.
(a) 4 vectors
(b) 3 vectors
(c) 2 vectors

b. Tests on existing dealiasing algorithms

An algorithm incorporating the full use of probability has not yet been developed. We have however, tested the MEDIAN, UWP and SLICE dealiasing algorithms on the NROSS simulated data. The percentage of correct solutions produced by the 3 dealiasing algorithms is given in Table 5.3. The percentage of rank 1 solutions correct was ~ 69%, and this was increased to 90%, 86%, 88% respectively by the SLICE, MED and UWP algorithms. The size of the box over which neighbouring solutions are compared for consistency in SLICE is variable. Table 5.3 was obtained using 5x5 boxes. The accuracy of SLICE does depend on the size of this box. For a sample wind field, the skill of SLICE was 82%, 91%, 89% for 3x3, 5x5 and 7x7 boxes: hence the choice of 5x5 boxes. It is to be anticipated, however, that the optimum size of box will be a function of the scale of the meteorological features present.

Although the figures in Table 5.3 look very encouraging, all the dealiasing methods tested suffer from clustering of errors, where whole areas may be wrong. Fig. 5.5 illustrates the wrong solutions produced by the median filter.

Fig. 5.6 is a close up of a cluster of wrong solutions produced by the SLICE algorithm used on simulated NROSS data. Fig. 5.6 shows those solutions which are low probability - it accounts for most of the wrongly chosen vectors though there are also some 'high' probability solutions which are wrong (heavy shading). For the limited data sample examined here, it appears that the error clusters are primarily low probability solutions, and so there is some hope of reducing the clustering problem by using probability information.

A comparison of the different dealiasing techniques which do not use probability information, but only ranking, has also been performed using the ERS-1 simulator. The results are shown in Table 5.4. The same data as for Table 5.3 is used (there are now 18 revs. as, for NSCAT, the two swaths to either side of the space craft are considered as one rev., while for the simulated ERS-1 data, they are considered independent, since the scatterometer on ERS-1 will look to one side only). The percentage of rank 1 solutions correct is 59% and this is increased to 69%, 70% and 72% by the SLICE, MED and UWP algorithms.

Table 5.3

Automated ambiguity removal of simulated NSCAT data
9 Revs over Pacific Ocean Basin on September 7, 1978

(50 km Resolution)

COMPARISON TABLE OF COUNTS-PERCENT
FOR THE DIFFERENT METHODS

CASE NO	TOTAL COUNT	SLICE TO TRUTH	MED FILT TO TRUTH	U WSC TO TRUTH	SLICE TO MED	SLICE TO U WSC	MED FILT TO U WSC	RANK 1 TO TRUTH	RANK 1 OR 2 TO TRUTH
1	816	502	545	660	561	609	599	436	641
		61.5%	66.8%	80.9%	58.8%	74.6%	73.4%	53.4%	78.6%
2	4912	4464	4244	4304	4469	4434	4502	3320	4448
		90.9	86.4	87.6	91.0	90.3	91.7	67.8	90.6
3	4688	4290	4133	4271	4305	4256	4232	3451	4364
		91.3	88.0	90.9	91.8	90.6	90.1	73.5	92.9
4	5394	5068	4758	4853	4882	4936	4852	3838	4880
		94.0	88.2	90.0	90.5	91.5	90.0	71.1	90.1
5	64.68	5891	5528	5623	5899	5896	5722	4856	5988
		91.1	85.5	88.9	91.2	91.2	88.5	72.0	92.6
6	6454	5982	5699	5655	5884	5965	5701	4405	5782
		92.7	88.3	87.6	91.2	92.4	88.3	88.3	89.6
7	5531	4849	4768	4774	4897	4905	4825	3716	3982
		87.7	86.2	86.3	88.5	88.7	87.2	87.2	89.7
8	4538	3884	3739	4037	4108	3958	3850	2980	4065
		85.8	82.4	89.0	90.5	87.2	84.8	65.7	89.6
9	2486	2294	2211	2251	2252	2235	2243	1710	2282
		92.3	88.9	90.5	90.6	89.9	90.2	68.8	91.0
ALL	412970	37224	35626	36428	37257	37194	36526	28510	37372
		90.1%	86.3%	88.2%	90.2%	90.1%	88.4%	69.0%	90.5%

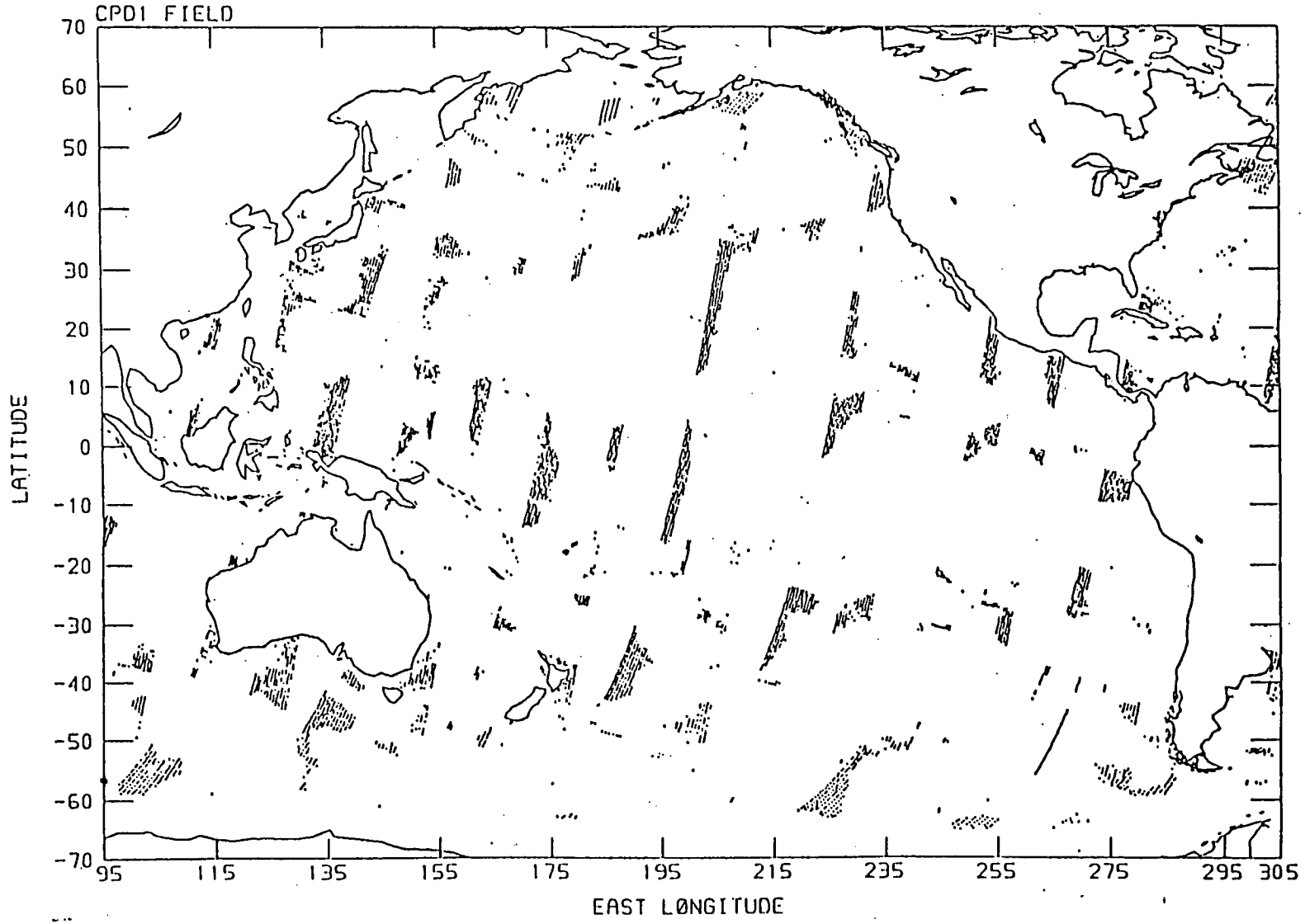

Fig. 5.5 Plot of wrong solutions chosen by median filter dealiasing algorithm, showing clustering of errors. For simulated NSCAT data.

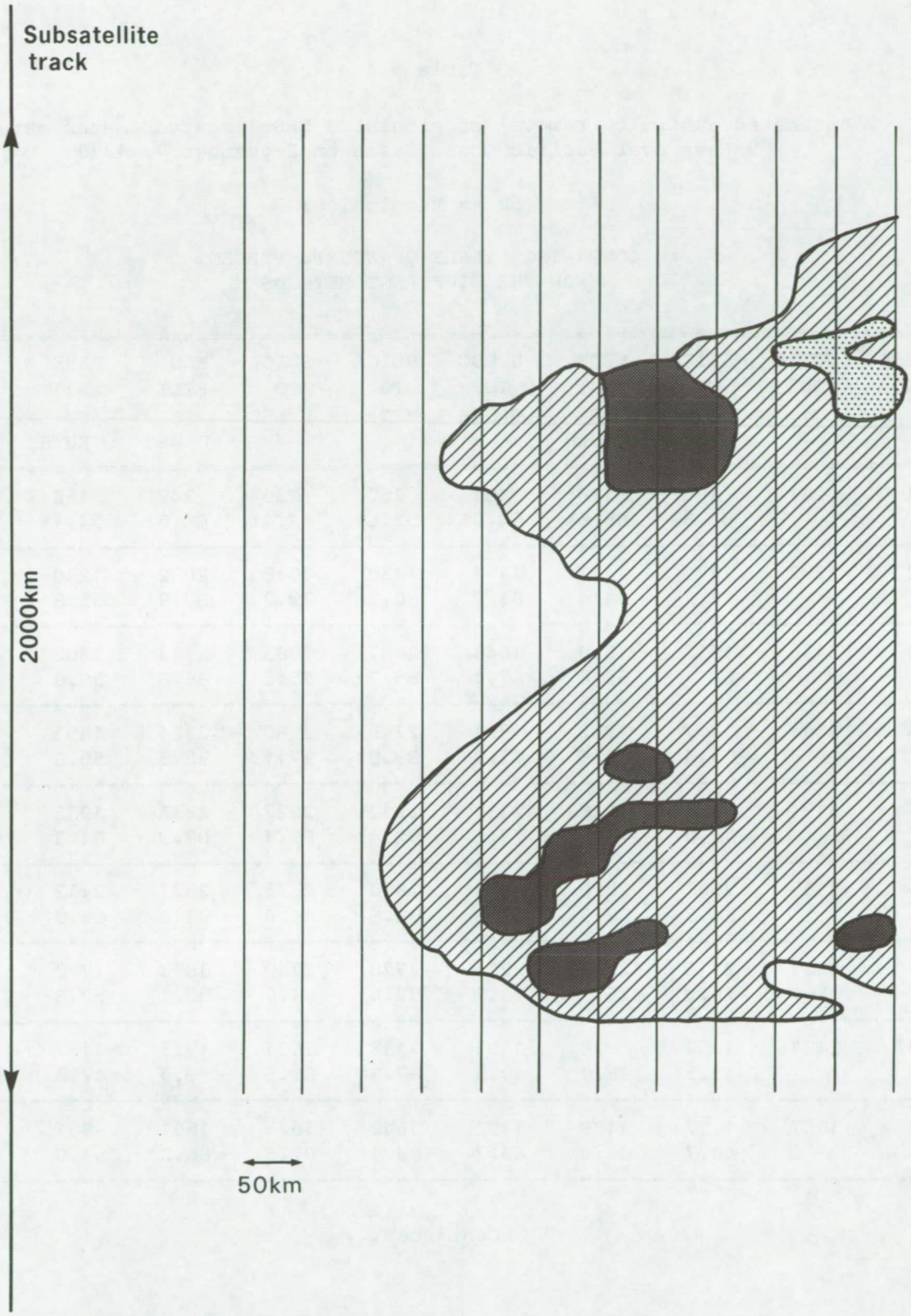

Fig. 5.6 Close-up of a cluster of errors, showing those solutions which are low probability (light shading). Of the points which are high probability (as defined in Fig. 5.4), some have only small angular errors (speckled) but others have larger angular errors (heavy shading). Vertical lines parallel to the subsatellite track indicate the central location of the retrieved winds. Where no shading is used, the dealiased solution is correct. Simulated NSCAT data has been used. Objective dealiasing was via the SLICE algorithm.

Table 5.4

Automated ambiguity removal of simulated ERS-1 scatterometer data
9 Revs over Pacific Ocean Basin on September 7, 1978

(50 km Resolution)

COMPARISON TABLE OF COUNTS-PERCENT
FOR THE DIFFERENT METHODS

CASE NO	TOTAL COUNT	SLICE TO TRUTH	MED FILT TO TRUTH	U WSC TO TRUTH	SLICE TO MED	SLICE TO U WSC	MED FILT TO U WSC	RANK 1 TO TRUTH	RANK 1 OR 2 TO TRUTH
1	283	180	194	181	265	236	249	153	224
		63.6%	68.6%	64.0%	93.6%	83.4%	88.0%	54.1%	79.2%
2	2293	1771	1477	1461	1839	1816	2082	1280	2029
		77.2	64.4	63.7	80.2	79.2	89.9	55.8	88.5
3	2435	1512	1520	1640	2087	2083	2113	1382	2090
		62.1	62.4	67.4	85.7	85.5	86.8	56.8	85.8
4	2504	1787	1942	1951	2249	2180	2324	1493	2239
		71.4	77.6	77.9	89.8	87.1	92.8	59.6	89.4
5	3151	2270	2228	2432	2912	2827	2833	1933	2746
		72.0	70.7	77.2	92.4	89.7	89.9	61.3	87.1
6	3155	2667	2596	2628	2920	2775	2877	2112	2929
		84.5	82.3	83.3	92.6	88.0	91.2	66.9	92.8
7	3021	2116	2298	2211	2778	2749	2873	1777	2639
		70.0	76.1	73.2	92.0	91.0	95.1	58.8	87.4
8	2421	1054	920	1193	2113	2021	1935	1157	2050
		43.5	38.0	49.3	87.3	83.5	79.9	47.8	84.7
9	1857	1127	1189	1182	1642	1626	1601	961	1616
		60.7	64.0	63.7	88.4	87.6	86.2	51.8	87.0

Continued...

Table 5.4 continued

Automated ambiguity removal of simulated ERS-1 scatterometer data
9 Revs over Pacific Ocean Basin on September 7, 1978

(50 km Resolution)

COMPARISON TABLE OF COUNTS-PERCENT
FOR THE DIFFERENT METHODS

CASE NO	TOTAL COUNT	SLICE TO TRUTH	MED FILT TO TRUTH	U WSC TO TRUTH	SLICE TO MED	SLICE TO U WSC	MED FILT TO U WSC	RANK 1 TO TRUTH	RANK 1 OR 2 TO TRUTH
10	533	459	437	463	503	517	499	366	472
		86.1	82.0	86.9	94.4	97.0	93.6	68.7	88.6
11	2619	2077	2150	2202	2408	2404	2428	2792	2356
		79.3	82.1	84.1	91.9	91.8	92.7	68.4	90.0
12	2263	1678	1744	1720	2144	2053	2112	1276	1926
		74.1	77.1	76.0	94.7	90.7	93.3	56.4	85.1
13	2890	2049	2141	2111	2639	2627	2627	1743	2513
		70.9	74.1	73.0	91.3	90.9	90.9	60.3	87.0
14	3317	1976	2076	2211	2936	2971	2902	1949	2976
		59.6	82.6	66.7	88.5	89.6	87.5	58.8	89.7
15	3299	2373	2387	2353	3095	2997	3030	1961	2945
		71.9	72.4	76.8	93.8	90.8	91.8	59.4	89.3
16	2510	1612	1724	1687	2134	2199	2118	1329	2217
		64.2	68.7	67.2	85.0	87.6	84.4	52.9	88.3
17	2109	1180	1328	1425	1664	1626	1852	1189	1895
		56.0	63.0	67.6	78.9	77.1	87.8	56.4	89.9
18	613	432	445	422	577	563	572	344	570
		70.5	72.6	69.8	91.1	91.8	93.3	56.1	93.0
ALL	412373	28320	28796	29655	36905	36270	37007	24197	38432
		68.6%	69.8%	71.9%	89.4%	87.9%	89.7%	58.6%	88.3%

A number of points are worthy of note:

(1) The Rank 1 solution for the ERS-1 simulator is correct 58% of the time. This is somewhat lower than the value used by Offiler (70%) for the first test sample of winds from an earlier version of the simulator, or for the NSCAT simulator (69%).

(2) Because the 1st rank skill is lower for ERS-1 the statistical improvement as a result of ambiguity removal is less in the case of simulated ERS-1 data than that of simulated NSCAT data. (For SLICE the skill is increased from 58% to 68% in the case of ERS-1 simulated data and from 69% to 90% in the case of simulated NSCAT data).

(3) As noted for the dual-pole data, objective dealiasing can lead to a reduction in skill below that of rank 1 if the skill in rank 1 is low e.g. rev 8 of Table 5.4.

5.3 Conclusion

For a single pol ., 2 beam scatterometer, there is no skill in the ranking, except for some special upwind cases (see Appendix B). Increasing skill can be obtained by making additional observations of σ^o which lead to an overdetermined system of equations for (v, ϕ). The dual polarisation mode of operation of SASS does achieve some overdeterminism and we found some skill in the rank 1 solution (correct 41% of the time). The dealiasing algorithms SLICE, MEDIAN and UWP can increase the skill, but examples were also shown where the skill was decreased. The dual pol mode provides less redundancy than the 3 beam single polarisation scatterometers for ERS-1 or NSCAT. The results of the dual pol study of real data are therefore likely to be worse than would be experienced for ERS-1 when 3 beams are operating.

When simulated data for ERS-1 are used, the rank 1 solution is correct ~58% of the time and all the dealiasing techniques lead to a statistical improvement in the skill (around 70%). Isolated examples of the skill being reduced as a result of automatic ambiguity removal also exist. The 3 schemes tested only use ranking information based on the closeness of fit of the possible solutions (aliases) to the measured σ^o. But this closeness of fit can be used to give a weight (or probability) to the ranks which is shown to be useful. It is also shown that high probability data can also be wrong.

Dealiasing algorithms suffer from the generic problem of returning clusters of wrong solutions. These may be mostly low probability solutions, but the exact circumstances which lead to the clusters has not been identified. The characteristics of objective ambiguity removal schemes have not been related to meteorological conditions. It does appear however that dealiasing schemes using probability information should do better than those which do not use the probability information. Finally, one should note that the results using the simulated dual pole data were considerably better than those using the real dual-pole data from SASS. It is to be anticipated therefore that the results using simulated ERS-1 data are likewise over optimistic - a frequent feature of simulated data.

6. SUMMARY AND DISCUSSION

The dealiased SASS data from AES/JPL/UCLA has been used in the data assimilation procedure at the ECMWF. The assimilation was done as if the scatterometer data had arrived in real time, just like all the other data. The files on which the diagnosis was based were created while all the data were disc-resident, so the structuring of the diagnostic files was a small extra cost. For anyone wanting to do additional validation or quality assessment, all the available data and assimilation fields are put together in a neat package.

Two assimilations were performed for the period 6-17 September 1978:

(1) a control (NOSASS) assimilation, in which scatterometer data was passed to the analysis, tested by the analysis, subjected to tests with the FG and other data but not allowed to influence the analysis.

(2) an active assimilation (AESASS) similar to (1) but in which SASS data did influence the analysis.

Use of any type of data in an analysis system is a two-way process. The data is presented to the analysis, in the expectation that it will improve the analysis and lead to a subsequent improvement in the forecast. But the global observational database and the analysis fields themselves can also be used to check the quality of a specific data type. Since more data is probably collected at a weather centre that anywhere else, it is easier to make such routine checks at an operational centre. Special validation checks by well calibrated ships such as used in campaigns like GOASEX or JASIN are also essential, but they cannot be carried out in all environmental conditions or very frequently. Collocations of ERS-1 data with other observing systems such as ship winds or a subset of selected high quality voluntary observing ships can be done routinely at an operational centre. Furthermore the first guess or analysis, which is an amalgam of all current and previous weather observations, can also be used to validate the ERS-1 scatterometer data. This checking relies on there being some redundancy between observation types. As the models and the analysis proceed to higher resolution, this redundancy decreases locally making it more important to continually verify data quality in a global or statistical way.

A substantial part of this contract has been devoted to looking at ways to quality control the data. A number of ways were illustrated:

(a) Collocation of SASS with Ship reports

Despite the limitations of the ship reports, this work has shown

(1) a low speed bias (SASS high with respect to ship at low speeds).
(2) a high speed bias (SASS low with respect to ships at high speeds).
(3) a possible sea surface temperature dependence to this bias.
(4) a dependence of retrieved wind direction on incidence angle.

The result (3) was anticipated many years ago, yet it took 8 years (Woiceshyn et al. 1986) to confirm both (1), (2) and (3). Several papers exist to the effect that SASS data agrees well with surface validation data at intermediate and high wind speeds. In this report, we do find that SASS and ship speeds are in reasonable agreement at intermediate speeds (4-10 m/s) but biases are present at high speeds. Our estimate for the size of this speed bias is much bigger than that of any previous validation. It is independent of whether ship speed is obtained by Beaufort or Anemometer. The scatter is high (Fig. 2.1f) and the statistics are not Gaussian at higher wind speeds, so that care is required in interpreting the results.

A large part of the scatter in Fig. 2.1f results from scatter in ship measurements. It is expected that this can be reduced by selecting high quality voluntary observing ships (VOS) and there are plans within WCRP (World Climate Research Programme) to identify such ships. Fig. 2.1f was based on two weeks of collocations. If only selected VOS were used then a longer time period would be required to accumulate sufficient statistics. The time period is likely to be even longer than for SASS, since presumably the 'errors' in ERS-1 will be more subtle than those for SASS. As shown in Section 3, a more rapid check on scatterometer data can be made by comparing with the forecast model. This folds errors or biases in the forecast model into the collocation, but the comparison can be made in almost real time (within a few hours). It is worth stressing again that neither the comparison with ship data nor with the model need attribute a cause to any discrepancy found.

We do not find that the angular fit of SASS data is as good as claimed by Lame and Born (17° rms). Over all angles and wind speeds we find an rms error of greater than 50°. Some of this could result from dealiasing. (For example the 17° rms is obtained by choosing that angle from the aliases closest to the comparison angle, and so is over optimistic). It is found (e.g. Figs. 2.4) that the angular accuracy is a function of the incidence angle. At inner incidence angles (Fig. 2.4) the wind vectors along the beams are never chosen whereas at outer incidence, wind vectors along the beams dominate. For large scale atmospheric structures, the analysis may be able to filter the noise in the wind directions. However, if as argued earlier, SASS and ERS-1 data may be beneficial at smaller scales, the opportunity for filtering decreases and these angular irregularities could be more serious. Some tests on how much of this noise is filtered by the analysis could be done, but time has not permitted these tests during this contract.

No attempt has been made to assess the influence of precipitation on the scatterometer wind speeds, although it has been suggested that this can increase or decrease the inferred speed. A correction has been made by NASA to data from the right side of the spacecraft.

(b) Statistical comparison of SASS data with the analysis and first guess fields

Histograms of the differences between model FG and initialised analyses were calculated. Gaussian distributions are indicative of well behaved systems. Ideally, therefore, these histograms should reveal a normal distribution of departures, with zero bias. A distribution with a long tail is indicative of problems. A high frequency of departures making up the tails may be associated with wrong data or with particular synoptic situations and times when the forecast or initialised analysis is poor. The presence of bias is indicative of more systematic errors, either in the data, in the use of the data in the analysis, or in the model. Examples of such histograms indicated that they were tighter after analysis than before, showing that the analysis was drawing to the data. There was a tropical (equatorward of 20°) bias in the zonal component of velocity, frequently nearly 2 m/s. The model speed was high compared with SASS, despite the fact that SASS is biased high at low wind speeds.

Contour plots of SASS speed v model FG and IN speeds showed that there were biases between model and SASS. At low speeds SASS was biased high relative to the model, but at intermediate and high speeds the model was biased high relative to SASS. The scatter in the contour plots when SASS was compared with the model was less than when SASS was compared with ship observations, giving greater weight to the result that SASS was biased low relative to the model at higher wind speeds.

Contour plots of SASS angle vs. model FG angle revealed clustering when angles were measured relative to azimuth, very similar to the behaviour noted when SASS was compared to ships. The dependence of clustering on incidence angle also agreed with results obtained from ships. Collocations between SASS and ship suggested that the speed dependent bias at high speed was worse for the outer incidence angles. Comparison with the model FG confirmed this dependence. But in neither case was the dependence suggested by Shroeder et al. confirmed for other incidence angles.

(c) Detailed synoptic comparisons

Some illustration of the agreement or otherwise of SASS with the 6 hour forecast or analysis were given. Illustrations included.

- A small scale cyclonic feature well represented by SASS data and qualitatively agreeing with the model. There were significant differences in speed however between SASS and model FG.

- the QEII storm. Again there was good qualitative agreement but substantial velocity differences.

- Sharp frontal feature, very well resolved by SASS, less well resolved by the FG or analysis.

- Many cases where the SASS winds changed abruptly by 90°, apparently in an unphysical way.

The forecast model which was used to produce a first guess for the analysis is by present standards high resolution (115 km). The analysis grid however is

less highly resolved (1.875 degrees) and this reduction in resolution coupled with the Optimum Interpolation method of combining data and model FG may act to filter small scale features in the data. This is probably desirable for most other observing systems since they have lower resolution than the SASS data (Wylie et al. 1985), but it may not be so good for good quality high resolution scatterometer data. However, if scatterometer data suffers from angular irregularities such as noted in Section 2.2 or 4.2.3, or speed biases such as noted in 2.1.1, then it will not be possible to weight heavily the scatterometer data in the analysis procedure. The presence of such defects implies that maximum impact cannot be expected from the data.

Differences in the 1000 mb wind between the NOSASS and AESASS analyses are typically up to 10 m/s in the NH and tropics and to 20 m/s in the SH. The scale of the changes tend to be small scale in the NH. In the tropics changes of ~5 m/s are small scale, but larger scale changes of smaller magnitude (2 m/s) are common. Both large and small scale changes are noted in the SH implying that although VTPR data could determine much of the larger scale patterns in the SH it can not set it all, and SASS has a role to play. It does not follow that scatterometer data from ERS-1 would have the same impact however. In 1978, there were no drifting buoys in the SH. Today, as part of TOGA, there are about a hundred. These buoys do not resolve small scale features but presumably do see the large scale. It is therefore likely that scatterometers, buoys and infrared satellite sensors would have redundancy at the large scale. A scatterometer is the only instrument capable of resolving very small scales (50 km). The expectation is, that as far as forecasting is concerned, the impact of scatterometery may be greatest between synoptic scale and mesoscale.

At present neither the EC forecast model nor analysis can make best use of the data. A scatterometer provides measurements of the surface wind: single level boundary layer data. Any single-level data type poses particular problems for analysis systems, but single-level data from the boundary layer is especially difficult to use. Substantial effort is required to determine how to get maximum information from this data type.

(d) Forecast studies

A series of forecasts was run from the NOSASS and AESASS analyses. Forecasts from the two analyses tend to be very similar for the first few days, in the NH, as gauged by surface pressure. Changes, again small scale of ~5-10 m/s, are evident in the NH low-level wind field which could be important in wave forecast models but this has yet to be confirmed. In the SH, the differences in the forecasts can be large (~ 20-30 mb within 1 day).

An earlier study (Duffy and Atlas, 1986) had suggested that at ~100 km resolution, use of SASS data could improve forecast skill (for the QEII storm). The work of this report suggests that this is over optimistic. Improvements in model formulation and analysis procedures used in our study over that used by Duffy and Atlas (1986) mean that our forecast without SASS data is better than the Duffy and Atlas forecast with SASS data, and that SASS data has little impact on our forecast. None-the-less, our forecast still failed to capture the rapid development of this intense, medium scale storm, and it is possible that scatterometer data, properly used in a higher resolution model (50 km) would have a beneficial impact. One should note that some satellite derived quantities e.g. temperatures and cloud level winds have been available for 15 years, yet there are still questions on how best to use that data. Many aspects of the assimilation system will need refinement to make best use of ERS-1 data - removal of redundant interpolations (the analysis grid here was an N48 grid, 1.875 degrees, rather than one suitable for the T106 model), higher resolution structure functions in the analysis algorithm, improved quality control and de-aliasing algorithms, better relative weighting of scatterometer data, etc. One should therefore not interpret the lack of impact of SASS too pessimistically - rather to note that at present we do not know how best to use it. And there exist occasions when the present system fails to analyse or forecast intense medium scale systems over the oceans. Fig. 6.1 gives an example for 00 UTC on 30th December 1986. There are a number of island wind reports suggesting a strong tropical storm. Yet the analysis fails to recognise this fact and produces only a weak system. The reason is that wind information from island stations was not used, as it is frequently unrepresentative of the large scale flow and only pressure information is used. So this system is barely observed. A scatterometer must surely help to analyse such a system.

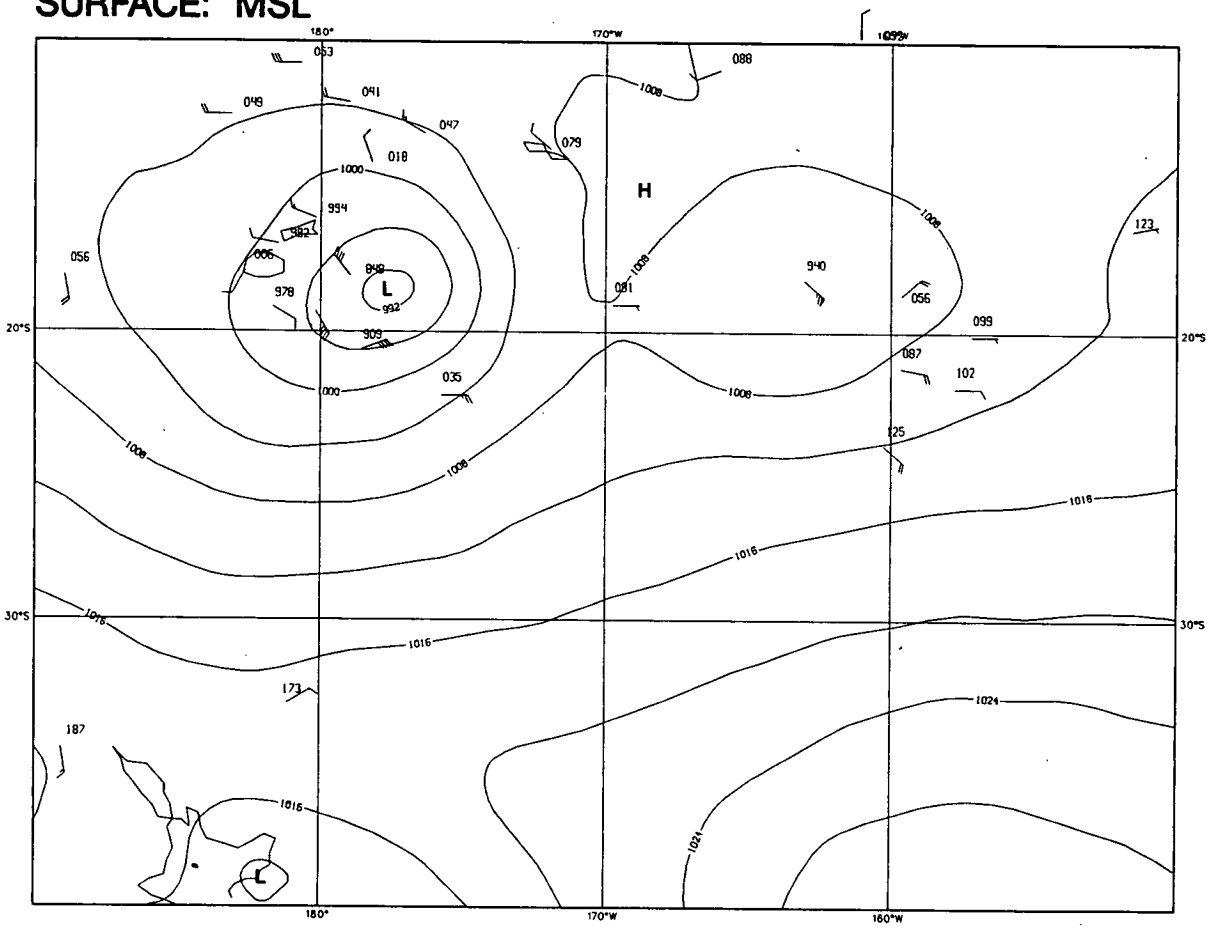

Fig. 6.1 Plot of the wind and pressure observations for a poorly analysed tropical system. The island wind data was not used in the analysis, which is consequently anaemic. A scatterometer must help analysis of such a feature.

This study represents only a start. A number of questions remain. How to use single-level data is an area of active research. In this study we have not addressed this question in depth. Any analysis system is in a continuous state of change with improvements to either the analysis procedure or the model used to produce the FG.

(e) Ambiguity removal

Removal of ambiguities from different types of scatterometer data was examined. For short periods, SASS was operated in dual pol mode (c 10% of the time). During the dual pol mode of operation, the skill in the rank 1 solution is increased from 25% to approximately 41% and dealiasing algorithms such as SLICE, Median filter or UWP all managed to increase the skill somewhat. But the increase was not large ~7%. The dual pol mode of operation is thought to produce less redundancy in the retrieval than would a 3 beam scatterometer such as ERS-1 so this may be considered as a worst case for normal ERS-1 operation. When simulated dual pol data were used, the skill in the rank 1 solution increased to 52% and the ambiguity removal algorithms increased that by approximately 20%. These results suggest however that using simulated data gives over-optimistic results.

Simulated ERS-1 data was also used. This gives the results that the rank-1 was correct 59% of the time and the ambiguity removal schemes increased this by approximately 10%. Simulated NSCAT data was used to illustrate the clustering of errors exhibited by present dealiasing algorithms. These use only ranking information, but residual after the fit information can be used to give a probability to the data. Most of the wrong solutions in the clusters were low probability, suggesting that automated ambiguity removal procedures should use more probability information than is currently the case.

7. RECOMMENDATIONS

The present study has demonstrated the ability of a modern data assimilation system to perform an extensive and penetrating quality assessment and validation of wind scatterometer data. The following set of recommendations are based on the results of the study.

1. Global utilisation of the wind data from ERS-1 requires that they be made available to operational centres in real time. Meteorological assimilation is so expensive that there is little realistic possibility of assimilating several years of ERS-1 wind data other than in real time. Global assimilation requires that effective quality assessment and validation be done on a global basis.

2. Global quality assessment and validation of the low-bit rate ERS-1 wind data will be greatly assisted by comparisons with all other data types, and with the output of the most sophisticated assimilation and forecasting systems. Because of the massive volumes of data involved, this is most efficiently done in real time, when the global databases are disc-resident. Once the data goes off-line to tape, the data processing problems of merging and re-structuring files are prohibitively expensive. Data processing for quality assessment and validation of ERS-1 data must be done, as far as possible, in real time. The results of the real-time quality assessment can be made available, in conveniently structured form, for off-line use. A customised database of this sort would be a powerful stimulus to many investigations, especially in the area of quality assessment and validation.

3. There will be two types of real-time users of ERS-1 scatterometer data - centres for whom the ESA de-aliased winds are sufficient, and larger centres who wish to do a more comprehensive processing of the ERS-1 wind data before use, and who can provide real-time global quality assessment and validation. The latter centres require more information in real time. The present study identified serious errors in the SASS data which have been un-detected for a decade. The sources of the errors could have been identified in near real time. Near real-time validation of the whole chain of steps in the ERS-1

wind-retrieval is possible if the following data is provided in real time to operational centres:

* The normalised radar cross-sections (σo) and the noise statistics (Kp).

* Information on azimuth, angle of incidence, etc.

* All the ambiguous winds with their ranking.

* The ESA-derived wind

(The last two items are derivable from the first two with the necessary software and modest processing power). The availability of this ERS-1 data with the real time meteorological data would enable comprehensive global near real-time research on quality assurance and validation of all aspects of the ERS-1 wind retrieval (model function, de-aliasing, etc.) for the lifetime of ERS-1.

Comparison of ERS-1 data with ships may require several days of data to build up reliable statistics. A more rapid check can be made with the model first guess or analysis. For these latter comparisons a single 6-hour period can give sufficient collocations that the scatterometer data can be essentially checked every 6 hours and so monitored in quasi real time. Collocations with a selected high quality subset of the voluntary observing ships can also be made at the cost of needing a longer period to build up reliable statistics.

4. Some of the results of this study suggested that the radar back scatter may depend on non local processes such as swell. If so, the retrieval of the wind vector can best be done using output from an accurate wave forecasting model. This area merits further investigation.

5. The users of the ESA-derived de-aliased winds must be provided with some idea of the meteorological characteristics of the errors in the data. The present study has shown that when current de-aliasing techniques go wrong, the erroneous winds occur in clusters. If the clusters occur in weak wind situations, such as in the middle of a high pressure area, then the errors are of little consequence. If they occur in strong wind situations, then the consequences can be serious. Studies are needed to provide real-time users with reliable information on the likely error characteristics of ERS-1 winds.

6. The results of the study demonstrate that there is more information in the probabilities of the ambiguous wind solutions than there is in the simple ranking of the solutions. Further research is needed to explore the possibility of basing de-aliasing algorithms on such ideas.

7. Further work is needed on the problems of using single level data, such as ERS-1 wind data, in meteorological assimilation, so as to maximise the utilisation of the data.

Acknowledgements

We are grateful to Dr. S. Peteherych of AES Canada, Prof. M. Wurtele of UCLA, Mr. G. Cunningham of JPL and Dr. D.H. Boggs of dB Systems for considerable assistance in the form of data, advice and discussions. Many colleagues at ECMWF, particularly Mr. J. Pailleux, Dr. P. Lönnberg, Ms. J. Haseler, Mr. D. Vasiljevic, Mr. P. Unden, Mr. F. Delsol, Mr. E. Hellsten, Dr. P. Janssen and Mr. G.A. Kelly were generous with their time and experience. The support of Dr. L. Marelli, Dr. M. Fea, Dr. W. Wijmans and particularly Dr. E. Oriol, all of ESRIN, is gratefully acknowledged. Finally, sincere thanks are due to Mrs M. Simpson and Mrs J. Williams for their excellent work on the text and figures. The research described in this report was performed in part by the Jet Propulsion Laboratory, California Institute of Technology, under contract with the National Aeronautics and Space Administration.

References

Anthes, R.A., Y.-H. Kuo, and J.R. Gyakum, 1983: "Numerical simulations of a case of explosive marine cyclogenesis," Mon.Wea.Rev., 111, 1174-1188.

Arakawa, A., and V. Lamb, 1977: "Computational design of the basic dynamical processes of the UCLA general circulation model," in Methods in Computational Physics, Vol. 17, Academic Press, Inc., New York.

Atlas, D., R.C. Beal, R.A. Brown, P. DeMey, R.K. Moore, C.G. Rapley, and C.T. Swift, 1986: "Problems and future directions in remove sensing of the oceans and the troposphere: a workshop report," J.Geophys.Res., 91, 2525-2548.

Atlas, R., W.E. Baker, E. Kalnay, M. Halem, P. Woiceshyn and S. Peteherych, 1984: "The impact of scatterometer wind data on global weather forecasting," Proceedings of the URSI Commission F Symposium and Workshop, Shoresh, Israel, May 14-23, 1984, NASA Conf. Publ. CP-2303, 567-573.

Aune, R.M. and T.T. Warner, 1983: "Impact of SEASAT wind data on a statistically initialized numerical model," paper presented at the Sixth Conf. on Numerical Weather Prediction, Amer. Meteorol. Soc., Omaha, Nebr.

Baker, W.E., R. Atlas, E. Kalnay, M. Halem, P.M. Woiceshyn, S. Peteherych, and D. Edelmann, 1984: "Large-scale analysis and forecasting experiments with wind data from SEASAT A scatterometer," J. Geophys, Res., 89, 4927-4936.

Bergman, K.H., 1979: "Multivariate analysis of temperatures and winds using optimal interpolation," Mon.Weather Rev., 107, 1423-1444.

Brown, R.A., 1983: "On a satellite scatterometer as an anemometer," J.Geophy. Res., 88, 1663-1673.

Donelan, M.A., and W.J. Pierson, 1986: A two-way Bragg-Scattering model for microwave backscatter from wind generated waves. IGARSS-86.

Donelan, M. A. and W.J. Pierson, 1986: "Radar-scattering and equilibrium ranges in wind-generated waves - with application to scatterometry," accepted for publication in J. Geophys. Res.

Duncan, J.R., W.C. Keller and J.W. Wright, 1974: Fetch and wind speed dependence of Doppler Spectra Radio Science 9, 809-819.

Duffy, D.G., R. Atlas, T. Rosmond, E. Barker, and R. Rosenberg, 1984: "The impact of SEASAT scatterometer winds on the Navy's operational model," J. Geophys. Res., 89, 7238-7244.

Duffy, D.G., and R. Atlas, 1986: "The impact of SEASAT-A scatterometer data on the numerical prediction of the Queen Elizabeth II storm," J. Geophys. Res., 91, 2241-2248.

Eliassen, A., 1954: Provisional report on calculation of spatial covariance and autocorrelation of the pressure field. Inst. Weather and Climate Res.,Aca.Sci. Oslo, Rept. No. 5.

Ernst, J.A., 1981: Scatterometer-derived winds over the QE-II storm. In "Oceanography from Space". J. Gower Ed. Plenum, 978 pp.

Gandin, L.S., 1963: Objective analysis of meteorological fields. Translated from Russian by Israeli Program for Scientific Translations, 242pp.

Gustafsson, N., 1981: "A review of methods for objective analysis", in Dynamic Meteorology: Data Assimilation Methods, ed. L. Bengtsson, M. Ghill, and E. Kallen, Springer-Verlag, New York, 17-76.

Gyakum, J.R., 1983: "On the evolution of the QE II Storm. I: Synoptic Aspects," Mon.Wea.Rev., 111, 1137-1155.

Harlan, J. Jr., and J.J. O'Brien, 1986: Assimilation of Scatterometer Winds Into Surface Pressure Fields Using a Variational Method. Journal of Geophysical Research, 91, 7816-7836.

Hawkins, J.D. and P.G. Black, 1983: "SEASAT scatterometer detection of gale force winds near tropical cyclones," J. Geophys. Res., 88, 1674-1682.

Hollingsworth, A., and P. Lönnberg, 1986: The statistical structure of short-range forecast errors as determined from radiosonde data. Part I: the wind field. Tellus 38A, 111-136.

Hollingsworth, A., D.B. Shaw, P. Lönnberg, L. Illari, K. Arpe and A. Simmons, 1986: Monitoring of observation and analysis quality by a data assimilation system. Mon.Wea.Rev., 114, 861-879.

Hollingsworth A., 1987: Objective Analysis for Numerical Weather Prediction. J.Met.Soc.Jap., (in press).

Jones, W.L., L.C. Schroeder, D.H. Boggs, E.M. Bracalente, R.A. Brown, G. J. Dome, W.J. Pierson an F.J. Wentz, 1982: "The SEASAT-A satellite scatterometer: the geophysical evaluation of remotely sensed wind vectors over the ocean," J. Geophy. Res., 87, 3297-3317.

Lame, D.B., and G.H. Born, 1982: "SEASAT measurement system evaluation: achievements and limitations," J. Geophys. Res., 87, 3175-3178, 1982.

Levy, G., and R.A. Brown, 1986: "A simple objective scheme for scatterometer data," J. Geophys. Res., 91, 5153-5158.

Liu, W.T., 1984: "The effects of the variations in sea surface temperature and the atmospheric stability in the estimation of average wind speed by SEASAT-SASS," J. Phys. Ocean., 14, 392-401.

Lleonart, G.T., and D.R. Blackman, 1980: The spectral characteristics of wind-generated capillary waves. J.Fluid.Mech., 97, 455-479.

Lönnberg, P., and A. Hollingsworth, 1986: The statistical structure of short-range forecast errors as determined from radiosonde data. Part II; The covariance of height and wind errors. Tellus, 38A, 137-161.

Lönnberg, P., and D. Shaw, 1985: Data selection and quality control in the ECMWF analysis system. ECMWF Workshop on the Use and Quality Control of Meteorological Observations, 6-9 November 1984.

Lorenc, A.C., 1981: A global three-dimensional multivariate statistical interpolation scheme. Mon.Wea.Rev., 109, 701-721.

Offiler, D., 1987: ESA Contract No. XXX

Orlanski, I., and J.J. Katzfey, 1987: Sensitivity of model simulations for a coastal cyclone. To appear in Mon.Wea.Rev.

Peterherych, S., P.M. Woiceshyn, W. Appleby, L. Chu, J. Spagnol, and J.E. Overland, 1981: "High resolution marine meteorological analysis utilizing SEASAT data," in Oceanography from Space, ed. J.F.R. Gower, Marine Science, Vol. 13, Plenum Press, N.Y., pp. 581-586.

Peterherych, S., P.M. Woiceshyn, W. Appleby, L. Chu, J. Spagnol, and J.E. Overland, 1981: "Applications of SEASAT scatterometer wind measurements for operational weather forecasting," in Final Report - An Evaluation of the Utility of Seasat Data to Ocean Industries, Vol. III, ed. Hubert, W., B.P. Miller and D. Montgomery, JPL Int. Doc. 622-225, Jet Propulsion Laboratory, Pasadena, California.

Pierson, W.T., 1981: Winds over the ocean measured by scatterometer. In Oceanography from Space. J. Gower Ed., Plenum, 978 pp.

Pierson, W.J., and M.A. Donelan, 1986: Verification results for a two-scale model of microwave backscatter from the sea surface. IGARSS-86.

Schroeder, L.C., D.H. Boggs, G.J. Dome, I.M. Halberstam, W.L. Jones, W.J. Pierson and F.J. Wentz, 1982: "The relationship between wind vector and normalized radar cross section used to derive SEASAT-A satellite scatterometer winds," J. Geophys. Res., 87, 3318-3336.

Shaw, D.B., P. Lönnberg, A. Hollingsworth and P. Unden, 1987: The 1984/85 revisions of the ECMWF assimilation system. Quart.J.Roy.Meteor.Soc. 113, 551-567.

Stewart, R.H., 1985: Methods of satellite oceanography. Univ. of California Press, 360 pp.

Valenzuela, G.R., M.B. Laing and J.C. Daley, 1971: "Ocean spectra for the high-frequency waves as determined from airborne radar measurements," J.Marine Res., 29, 69-84.

Wentz, F.J., S. Peteherych, L.A. Thomas, 1984: A model function for ocean radar cross sections at 14.6 GHz. J.Geophysical Res. 3689-3705.

Woiceshyn, P.M., M.G. Wurtele, D.H. Boggs, G.F. Cunningham, M. Ghil, 1987: Global Meteorological Research with Scatterometer Wind Data. J.P.L. Doc. No. D-4570 Available from Jet Propulsion Lab. Pasadena, California, 91109.

Woiceshyn, P.M., M.G. Wurtele, D.H. Boggs, L.F. McGoldrick, and S. Peteherych, 1986: "The necessity for a new parameterisation of an empirical model for wind/ocean scatterometry," J. Geophys. Res., 91, 2273-2288.

Wurtele, M.G., P.M. Woiceshyn, S. Peteherych, M. Borowski and W.S. Appleby, 1982: "Wind direction alias removal studies of SEASAT scatterometer-derived wind fields," J. Geophys. Res., 87, 3365-3377.

Wylie, D.P., B.B. Hinton, M.R. Howland, and R.J. Lord, 1985: "Autocorrelation of wind observations," Mon.Wea.Rev., 113, 849-857.

Yu, T.-W., and R.D. McPherson, 1984: "Global data assimilation experiments with scatterometer winds from SEASAT-A," Mon.Wea.Rev., 112, 368-376.

APPENDIX A

The data sets used

SASS data with the aliases present can not be readily used in an analysis system. It is necessary to remove the ambiguities. One possibility is to chose the SASS direction closest to the first guess, but it was felt that this is undesirable, as the main information of the data is then reduced to just speed. Instead, for the purposes of this study we chose to use data with unique wind vectors. A global record of 100 km resolution data (about 400,000 measurements) was produced manually by meteorological analysts from the JPL, UCLA, and AES Canada in a manner consistent with meteorological principles, with satellite imagery and with some surface reports. The period dealiased is 6-20 September.

The dealiased data is available in one of two forms

(1) a short dealiased record. This contains only the speed and direction of the chosen alias together with its latitude and direction.

(2) A more comprehensive record, containing not only the speed and direction of all aliases together with a flag to indicate the chosen alias, but also the incidence angle and azimuthal directions of the pointing antenna, and residual-after-the-fit-information from the SOS algorithm.

In the beginning, the short record was used both for collocation with ships and for assimilation into the analysis. Later, it was found that some of the additional information from the comprehensive record was desirable so a recollocation with ships was started. Assimilation is a computationally expensive exercise. It was therefore not possible to reassimilate data for an extended period from the comprehensive data set. One day has been reprocessed, however, incorporating incidence and azimuthal information. The observational data other than SASS data were extracted from the so-called "FGGE Build-up year Dataset" created at NMC Washington. It includes ships reporting in delayed mode.

In the Southern Hemisphere where data is normally scarce, the Australian Bureau of Meteorology produces pseudo observations (manually derived

observations from a subjective analysis). No such observations are used in this study. Fig. A1 shows typical coverage for one (6 hour) observation period. The SASS data is passed to the analysis in DRIBU format, and thus shows in Fig. A1 as DRIBU's. Note there are very few Australian observations, although the coverage over Southern Africa and South America is good. Over the Southern ocean, observations are largely confined to SATEM's and SASS with only a few island observations. There are no drifting buoys.

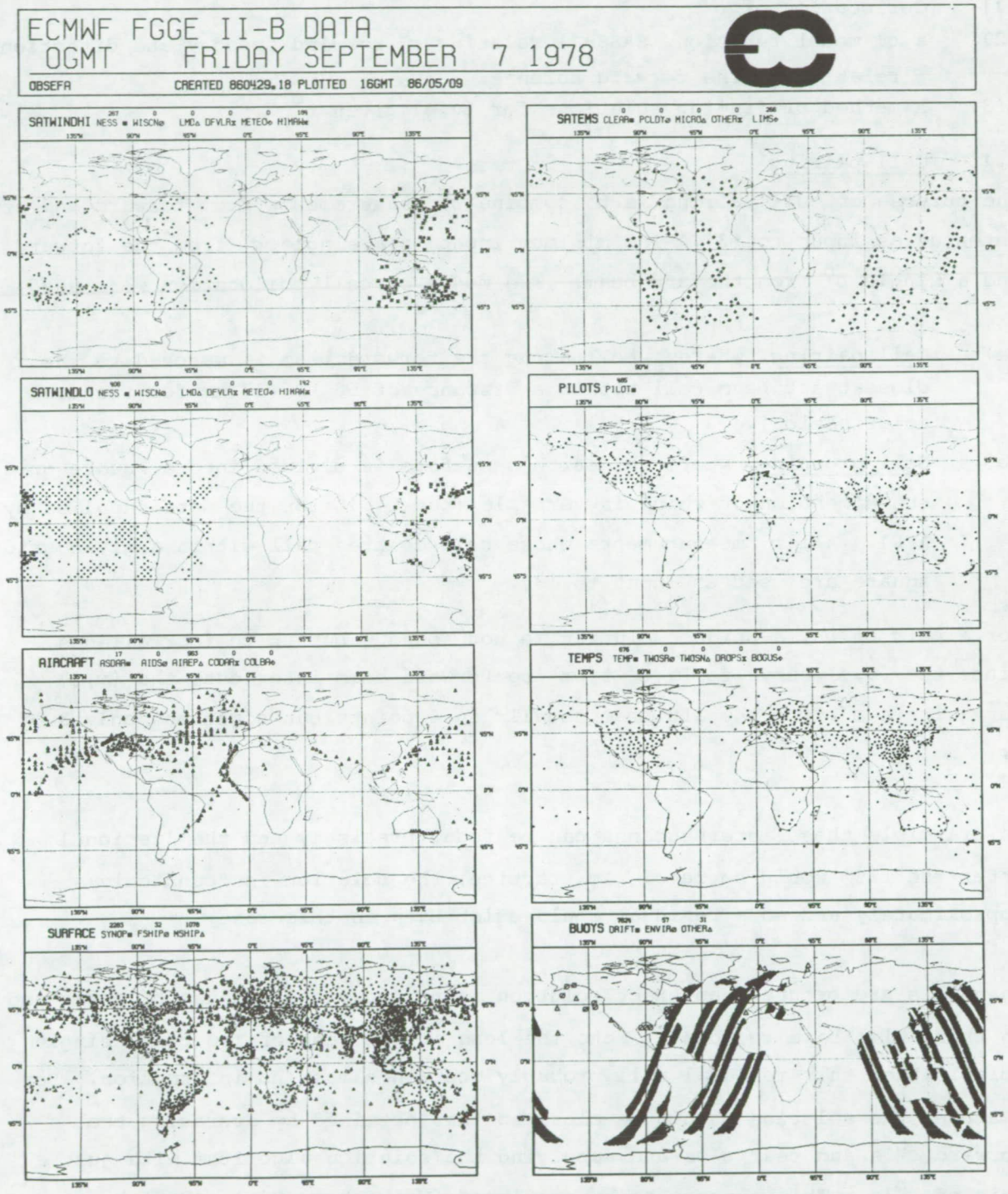

Fig. A1 Data coverage at 00 GMT ± 3 hours on Sept 7 1978. The left hand column from the top shows the availability of upper level cloud track winds (SATWINDHI), lower level cloud track winds (SATWINDLO), Aircraft, and surface observations (SHIPS and SYNOP stations). The right hand column from the top shows VTPR temperature soundings (SATEM), pilot balloons (PILOT), rawinsondes (TEMPS) and finally, drifting buoys and SASS data (BUOY).

APPENDIX B - The Sum of Squares Algorithm (SOS)

Retrieving wind vectors from radar backscatter involves three processes:

(1) Collocation of σ^o

(2) a σ^o model function (SASS-1) relating σ^o to wind speed v and direction ϕ relative to the forward antenna.

(3) A method of finding solutions for (v,ϕ) given $\sigma^{o's}$.

B.1 Cell pairing

The purpose of cell pairing is to combine σ^o measurements from forward and aft antennas as input to (3). The minimum input is a single σ^o from the forward and a single σ^o from the aft beam. Two modes of cell collocation were used.

(a) Cell pairing, where a cell along the forward beam is matched to the closest aft beam cell within a distance of 50 km (37 km for the dual polarisation).

(b) Cell grouping, where the earth's surface is divided into a square grid, the dimension of which is variable (but is 1° for the data supplied by AES). All σ^o measurements whose cell centres fall within a given grid square are used as input to (3).

For a pair of σ^o, a unique solution is not found - but up to four aliases, since the (v,ϕ) curve for a σ^o from the forward beam intersects the (v,ϕ) curve for a σ^o from the aft beam usually in 4 points but sometimes only 3 or 2.

In principle these intersections can be found precisely and the 'residual after the fit' would be zero. In practice, the solution is found only approximately and so a residual could exist even in this case.

When $\sigma^{o's}$ are grouped, an exact solution is not possible because of noise and so there will be a residual. None the less in the case of two beam, single polarisation this residual will probably contain almost no information. For example, the solution should be close to that obtained by averaging the forward σ^o's and rear σ^o's and supplying the solution algorithm with just a pair of σ^o's. This appears to be confirmed (Woiceshyn et al. 1986) by the table B.1 except for the 2-vector case*.

*For upwind directions (see Fig. 5.1) the solution in the absence of noise would be essentially unique. SOS somehow returns 2 aliases, but one would expect skill in the rank 1 in upwind cases (see Tables B1 and B3). This would not follow for winds blowing down the beam direction because of the upwind downwind differences.

Table B.1
Table of Percentage Correct Solutions from SASS data
(September 6-20)

	Alias R_1	Solution R_2	Rank R_3	R_4
All 4 vectors	26.6	26.8	23.9	22.8
All 3 vectors	33.4	28.9	37.7	
All 2 vectors	79	21.		

The cell grouping in principle makes the problem overdetermined since one will have more σ^{os} than unknowns but in practice, as the averaging argument indicates, does not, since the data is almost redundant except to reduce the noise. True skill however can be expected if the solution is overdetermined.

B.2 Dual polarisation

If the same area is viewed by both V pole and H pol , then some additional information is provided and some skill in ranking can be expected. Woiceshyn et al have shown that this is indeed the case, but the skill increase is not very great as is shown in table B.2.

Table B.2
Table of Percentage Correct Solutions from SASS - Dual Pol : data

	R_1	R_2	R_3	R_4
All 4 vectors	34.5	28.4	20.2	17
All vectors	40.5	27.7	19.3	12.5

SASS did operate approximately 10% of the time in dual-pol mode during the period 6-20 September, and almost all the time for a few days in July but only the dual pole data in the 6-20 September is considered in this report (Section 5).

Table B.3
Statistics for choices made by analysts of SASS directions
for the 15-day dealiased data set

Percentage of time for which the upwind solution (i.e. the wind solution for which a component of the wind was directed towards the sub-track of the satellite) of the 2-vector class of ambiguities that was chosen by the analyst as the true wind direction

Antenna Selection Mode	======> INCIDENCE ANGLE DECREASING ======> Cell Number							
	1	2	3	4	5	6	7	ALL
1	50.0%	69.6%	79.5%	89.7%	94.1%	87.6%	55.7%	82.3%
2	-	-	-	-	-	-	-	-
3	53.2	75.9	80.5	89.8	91.2	88.4	53.0	81.1
4	-	81.8	85.4	90.8	95.5	84.6	55.5	82.5
5	100.0	93.8	91.1	91.4	93.4	83.8	72.1	86.5
6	-	66.7	80.0	100.0	92.9	94.4	75.0	90.0
7	64.4	81.0	87.4	95.8	91.5	81.3	55.9	85.3
8	-	0	77.8	92.9	82.4	96.4	92.0	86.6
ALL	61.9%	74.9%	80.1%	90.0%	93.6%	87.1%	56.8%	82.4%

Notes:
Mode 1 = vertical polarization both sides
Mode 2 = horizontal polarization both sides
Mode 3 = dual-pol left side only
Mode 4 = dual-pol right side only
Mode 5 = double-density - vertical pol left side only
Mode 6 = double density - vertical pol right side only
Mode 7 = double density - horizontal pol left side only
Mode 8 = double density - horizontal pol right side only

Cell No. 1 is at the outside edge of the swath and cell no. 7 is the closest to Nadir.

B.3 The Sum of Squares (SOS) algorithm

The method used to find solutions (v,ϕ) for given $\sigma^{o's}$ is to minimise

$$SOS = \sum_{i=1}^{n} \frac{[\log \sigma_i^o - F(\theta,\chi_i,\varepsilon,v)]^2}{\delta_i^2}$$

where δ_i is the expected standard deviation between the σ^o measurement and the model function.

The model function F is a tabulated form of

$$F = G(\theta,\chi,\varepsilon) + H(\theta,\chi,\varepsilon) \log V$$

where G and H are tabulated for incidence angles θ from 0° to 70° in 2° intervals, and for χ in 10° steps from 0° to 180°. For a given data group SOS is calculated for 72 wind directions ranging from 0° to 355° in 5° step.

A coarse search for wind direction is implemented at 5° intervals in α ($\chi=\phi-\alpha$) to identify local minima, which are at even multiples of 5° (Jones et al 1982). A finer search at 1° follows.

Woiceshyn et al., 1987, have noted that 5° granulation can be identified in histograms of the dealiased wind direction, suggesting deficiencies in the way the SOS minima are found.